To My Parents

THE LINEAR GROWTH RATES OF PENTAERYTHRITOL CRYSTALS

by

SIKANDAR REHMATULLAH

(M.Sc.)

A Thesis submitted for the Degree of Doctor of Philosophy in the Department of Chemical Engineering, University of Aston in Birmingham, England.

March 1973

ACKNOWLEDGEMENTS

The author wishes to express his sincere thanks to the following:

Dr. D. E. Creasy for his advice, encouragement, and supervision throughout the course of the research and during the preparation of the thesis.

Miss Lorraine Terry for checking the manuscripts.

Professor G. V. Jeffreys, and the University of Aston for providing a research grant and research facilities.

Dr. J. D. Jenkins for his frequent help.

The technical staff of the Chemical Engineering Department for fabricating the equipment.

The glass blowing section of the Physics Department for fabricating the glass cells.

ABSTRACT

The linear growth rates of the (101) faces of single crystals of Pentaerythritol (Pe) in aqueous solutions have been measured as a function of temperature (10-50^{o}C), and concentration difference (0.25×10^{-2} - 2.60×10^{-2} KgPe/Kg Solution) under stagnant conditions in a batch cell. The effect on growth rate of the two main by-product impurities of Pe manufacture, di-Pe and a Formal, and several other impurities has been determined over a range of working conditions.

It was found that the growth rate of the pure material varied with time and also from crystal to crystal. Due to the purification method used in preparing the solutions an impurity (X) was removed which resulted in these growth rates being at least two orders of magnitude greater than those previously reported. The pure material growth rate was kinetically controlled having a parabolic law over most of the range of conditions studied with an activation energy of 8.47 Kcal/mol.

The effect of di-Pe was generally that it caused a slight reduction in the growth rate except at certain critical concentrations where the effect was an increase by up to a factor of two.

The effect of the Formal was that it drastically reduced the crystal growth rate virtually to zero, when in concentrations greater than the order of 0.001 mass fraction.

Of the other added impurities, only Formaldehyde, Sodium hydroxide, and 1,1,1,trimethylolethane had significant effects in reducing the growth rate. In the absence of (X) and Formal, Pe crystals were found to exhibit (110) and (001) faces in addition to the usually

reported (101) faces. The phenomenon of secondary nucleation appears to be related to the magnitude of the crystal growth rate under the conditions investigated.

It appears that (X) may be 1,1,1,trimethylolethane or similar compound.

LIST OF FIGURES

LIST OF TABLES

TABLE OF CONTENTS

Page

CHAPTER 6 continued

CHAPTER 1

INTRODUCTION

The use of Pentaerythritol in the manufacture of resins and drying oils for surface coating materials has gained considerable importance in the last two decades. Although an enormous volume of literature exists on the chemistry and the preparation of Pentaerythritol, very little work appears to have been done on the determination of its crystallisation characteristics. The formation of by-products in the manufacturing process is likely to offer difficulties in its crystallisation. Thus Rogers[84] found that the presence of a Formal, a disputed compound, reduced the growth rate of the commercial material. Although he later succeeded in removing this and other by-product impurities by the hydrolysis of Pentaerythritol with hydrochloric acid, and observed a second order dependence of the growth rate on supersaturation, his material was still suspected to contain trace concentrations of an unknown impurity (X). The presence of (X) was suspected to reduce the growth rate of Pentaerythritol by several orders of magnitude. It forms a part of this work therefore, to identify and extract the impurity (X) from the commercial Pentaerythritol. Another aim is to measure the linear growth rates of Pentaerythritol as a function of temperature and concentration difference, and also to determine the effects of several impurities on the growth rate of the pure compound.

The measurement of linear growth rate in a batch cell would eliminate the problems of attrition encountered by Rogers and the maintenance of a constant concentration difference would allow the determination of growth rate as a function of time. It would also enable the close observation of the change in crystal habit due to the presence of certain impurities. Since the growth of the crystals appears to be kinetically controlled, the use of a batch cell does not seem unreasonable.

CHAPTER 2

SURVEY OF LITERATURE ON CRYSTALLISATION

2.1 Introduction

It is generally considered that the growth of crystals from solution involves two phenomena occurring in series: the transport of the solute from the bulk supersaturated solution to the crystal surface, and the incorporation of the solute into the crystal lattice, called surface integration. The second process can be divided into several stages: they consist of the adsorption of the particles onto the surface, migration over the surface, and finally, incorporation into the crystal lattice. Each of these processes is influenced to a greater or lesser extent by the parameters such as temperature, rate of stirring of the solution, the presence of impurities, the degree of supersaturation of the solution, and the solution viscosity. The most important single factor is probably supersaturation since, if it is altered considerably, not only the controlling mechanism but the growth mechanism itself may change.

The complex dependence of the growth rate of crystals on various factors has resulted in the development of a large number of theories. Any acceptable theory of crystal growth should account for the strong tendency of the crystal faces to be simple polyhedra. It should also account for the apparent flatness of the faces, yet provide an explanation for the step-like imperfections so frequently observed on growth surfaces. Finally, it should explain the effect of the parameters on the growth rate that is found experimentally.

In the next sub-section (2.2) much of the work which has contributed to the understanding of growth in the absence of impurities will be reviewed. Then, based upon the general concepts developed, the influence of impurities upon the growth process will be reviewed (sub-section 2.5).

2.2 Theories of Crystal Growth without Impurity

2.2.1 Introduction

All the theories dealing with the growth of crystals from pure solutions (hypothetical) can be broadly divided into three main groups. These are: the earlier growth theories which gave no consideration to the structure sensitiveness of the growth rate; theories which regard the structure of crystals to be a perfectly ordered array of atoms or molecules, and finally those which assumed the existence of microscopic imperfections on all real crystals to be indispensable for growth.

2.2.2 The Earlier Theories

2.2.2.1 Thermodynamic Theories of Crystal Growth

The early theories, put forward to account for the growth process, regarded crystallisation as being controlled only by thermodynamic restraints. Gibbs[1] made the first significant contribution by introducing the concept of surface free energy. His idea was extended by Curie[2] and Wulff[3] who proposed that for a crystal in equilibrium with its surroundings at constant temperature and pressure, its total surface free energy is a minimum for a given volume, i.e.

$$\sum_{i=1}^{n} A_i \sigma_i = \text{minimum} \qquad (1)$$

where A_i = Surface Area of the ith face (m^2)

σ_i = Surface Free Energy per unit area of the ith face. ($ergs/m^2$)

They suggested that the perpendicular distance from the point of origin of a crystal to a face is proportional to the free energy of that face. Curie's theory was further developed by Marc and Ritzel[4] who introduced the concept that solution pressure accounted for the different solubilities of different faces of a crystal. Curie's theory has not found wide acceptance for two reasons: firstly, numerous workers have shown that the surface energy is not the controlling factor in determining crystal habit with the exception of very small crystals[5], and secondly, Curie's theory is unable to explain the dependence of the growth rate of crystals on the super-saturation, stirring, and many other parameters. However, these parameters were considered in theories which were developed concurrently with the Thermodynamic Theories and which are considered next.

2.2.2.2 Diffusion Theories of Crystal Growth

The theories of diffusion controlled growth were first put forward by Noyes and Whitney[6], and Nernst[7], and later modified by Berthoud[8] and Valeton[9]. The main criterion of all these theories was the assumption that there existed a stagnant boundary layer at the surface of a crystal. In order that the crystal should grow, the solute has to diffuse through this layer. An apparent error of the theory was the assumption that the liquid in contact with the crystal was saturated whereas Miers[10] found it to

be supersaturated. Also, the thickness of such a boundary layer has been found to be virtually zero in vigorously stirred solutions[11]. These theories came before the chemical engineering concept of process resistances in series and hence to overcome these objections Berthoud and Valeton suggested that there might be some "Surface Integration" resistance which had to be overcome in addition to that of diffusion. Thus in the absence of the diffusion resistance one would expect surface integration resistance to be controlling the growth process. Crystal faces of different types would then be characterised by different rates of growth at the same supersaturation because of having different surface integration resistance.

This modified diffusion theory is in agreement with many experimental observations in that the growth rate has been found to increase continuously with (i) increasing supersaturation and (ii) increasing agitation up to the limiting value at which surface integration takes over control[12]. However, the modified theory is still unable to explain all the phenomena observed during crystal growth such as the layer by layer growth of crystals and the presence of defects. In view of the objections to this diffusion theory, other theories have been developed which consider the crystal growth as a process taking place in discrete steps on perfect crystal faces.

2.2.3 Growth Theories for Perfect Crystals

Molecular events occurring at the surface of crystals play a very important role in determining the growth rate of the faces and hence the resulting habit of the crystal. Recognition of this possibility led to the next set of theories.

2.2.3.1 Two-Dimensional Growth Theories

In the late 1920's, Kossel[13] and Stranski[14] laid the important groundwork for two-dimensional nucleation (TDN) theories by considering the growth of perfect crystals to take place by propagation of a distinct layer of molecules across the crystal face. By carefully analysing the energy of attachment and detachment of molecules at various surface configurations for a cubic face of an ionic NaCℓ type crystal, they concluded that molecules would attach easily to lattice steps on the crystal surface and even more easily to an incomplete row on the edge of a step, i.e. a step-kink. Kossel expressed the energy of attachment as being made up of three distinct components:

$$F = F' + F'' + F''' \qquad (2)$$

where F' and F" are tangential to the growth directions and F'" is at right angle to the growth direction. Thus, when a molecule is attached to a smooth surface, there will be a high probability of its desorption back into the solution before it can reach a step.

They reasoned that once a crystal has started growing, the step advances across the face and fills that particular layer. For crystal growth to continue a new step must be formed. To accomplish this, a two-dimensional nucleus has to be formed. As soon as this nucleus is formed, growth can proceed as before until a new step is required. It has been estimated that a supersaturation (defined as $X = \Delta c_{/c^*}$) not less than 0.25 to 0.50 must exist for such a nucleation to take place[15]. From the thermodynamic considerations

Frank[15] states that there must be a concentration of kinks, other than zero, at any finite temperature along any step. The formation of two-dimensional nuclei is assumed to take place by the repetitive collision of molecules and will be treated in the next set of theories. The Kossel-Stranski theory requires the formation of only one nucleus for every new crystal layer to be added and is called Mononuclear-Two Dimensional Nucleation or MNTDN theory. The theory assumes that the growth rate of a crystal face is controlled solely by the rate of formation of a two-dimensional nucleus and that once one is formed the subsequent lateral growth is very rapid. From thermodynamic considerations, the size of such a nucleus is given by:

$$\rho_c = \sigma V_c / RT \ln(X+1) \cong \sigma V_c / RTX \quad \text{for small } X \tag{3}$$

where V_c = Molar Volume of Solute (m^3/mol)

σ = Interfacial Free Energy (ergs/m^2)

R = Gas Constant (ergs/mol K)

T = Absolute Temperature (K)

X = Supersaturation = $S-1=\Delta c_{/c^*}$ (-)

ρ_c = Radius of a critical size nucleus (m)

The rate of formation of such a nucleus has been given by Ohara[16] as

$$I = C_1[\ln(1+X)]^{\frac{1}{2}} \exp.[-C_2/T^2 \ln(1+X)] \tag{4}$$

where $C_2 = \pi h Vm \sigma^2 / R^2$ (5)

and C_1 is mainly a function of speed of migration of molecules across the crystal surface.

h = Height of a monomolecular step (m)

V_m = Volume of a solute molecule (m^3/molecule)

Equation (4) indicates the strong dependence of I on X. Although the steps initiated by the formation of two-dimensional nuclei are not straight, as ρ increases much beyond ρ_c, the effect of curvature may be neglected. Since the linear growth rate of a crystal face is given by

$$g = A\, I\, h \tag{6}$$

$$\therefore \quad g = A\, h\, C_1[\ln(1+X)]^{\frac{1}{2}} \exp.[-C_2/T^2 \ln(1+X)] \tag{7}$$

Hence at constant supersaturation

$$g \propto A \propto L^2 \tag{8}$$

i.e. faces with large surface area will have higher growth rates than those with smaller surface area. There is some disagreement in the literature on this point: some investigators have reported that growth rate does increase with crystal surface area[17], while others reject it on the grounds that the rate of advance of a layer across a crystal surface could not be rapid enough to make the possibility of simultaneous formation of more than one nucleus unlikely. Equation (7) predicts appreciable growth only if X is considerably greater than unity, which is contrary to the frequent experimental observation that growth occurs at very low supersaturation.

Another class of two-dimensional nucleation theory assumes that the rate of formation of two-dimensional nuclei is very rapid relative

to their lateral growth on the crystal faces. Such a theory requires the formation of nuclei only to complete a layer and is called the Polynuclear Two-Dimensional Nucleation (PNTDN) theory. Various growth rate expressions based on different simplifying assumptions have been presented. A modified form of these is given by Ohara[16] as:

$$g = \pi \rho_c^2 h I \tag{9}$$

$$= \{C_3/T^2[\ln(1+X)]^{3/2}\} \exp[-C_2/T^2\ln(1+X)] \tag{10}$$

where C_3 is a function of the speed migration of molecules, their surface concentration and the surface energy.

Although the area dependency of g has disappeared here, it appears possible for it to pass through a maximum with increasing X (due to the inverse relation of X with ρ_c) a phenomenon which has not yet been observed experimentally[16].

Between the two extreme cases mentioned above there are numerous intermediate models. According to these, both the rate of formation of two dimensional nuclei and the rate of lateral growth are finite and competitive. The models, however, differ in the dependence of g on various system parameters. The common assumptions of these models are that during the growth or spreading of nuclei, they may be considered to slip over the surface so that there is no intergrowth, and that the spreading velocity is constant[16].

During the growth of cubic crystals of NaCl, Yamamoto[18] observed that very thin layers sprouted from the corners of a cube to the middle of the face. At low supersaturations, the new layers developed at the corners only after the previous layers had been completed, whereas at higher supersaturations the new layers were occasionally found to start immediately after the previous ones had commenced, i.e. MNTDN control at low supersaturation and PNTDN control at higher supersaturation. Sheftal's[19] discussion of crystal growth processes also tends to suggest that MNTDN takes place preferentially at lower supersaturations, whereas at higher supersaturations PNTDN takes over perhaps due to non-uniform distribution of solute on the crystal surface.

In the past, the formation of layers at corners and edges has usually been regarded as a sign of growth involving TDN. Petrov[20] suggests that this is not sufficient proof for the non-existence of any other mechanism. Thus, the above characteristic is frequently due to the special properties of the diffusion field near a crystal in the case of the dislocation growth mechanism, to be discussed in the section (2.2.4).

Hence, although there are several instances where this mechanism of crystal growth appears to have been confirmed experimentally[21], the theory of TDN fails to give a satisfactory explanation of the bulk of the experimental data. It predicts both a higher resistance to growth than that which is actually observed and also a different surface structure from that which is actually observed. Thus, the

examination of the surface structure of a growing crystal usually reveals a large number of macroscopic steps moving rather slowly and not the molecularly smooth surface resulting from the rapid spread of a two-dimensional nucleus. The probability of formation of a two-dimensional nucleus will be treated in the next section.

2.2.3.2 Adsorption Layer Theories of Growth

During the period when Kossel and Stranski were developing their theories of TDN, Volmer[22] formulated a theory based on the assumption that there is an adsorbed layer of molecular dimensions on the crystal surface. He proposed that the particles arriving at the surface of a crystal lose only a part of their energy. The remaining energy enables them freedom of movement and thus they migrate over the surface of the crystal like molecules in a two-dimensional gas. Due to desorption, a state of equilibrium would be established between the adsorption layer and the solution. Frequent collision between molecules in the adsorbed layer would result in two-dimensional nuclei. These nuclei grow by further collision to form a new layer. The growth of the crystal is then governed by the rate of capture of particles from the adsorbed layer.

Brandes[23], making similar assumptions to Volmer, considered the surface free energy to have little influence on crystal growth. He considered that the work of formation of the two-dimensional nuclei was the controlling factor for crystal growth, since the growth of the nucleus to complete the layer was very rapid compared with the nucleus formation.

Like the TDN theory, the adsorption theory also gained wide experimental support especially in explaining such results where planar growth of crystal faces has been observed despite different

solute flux on different parts of the crystal faces[24-25]. However, the treatment suggests that growth and dissolution are reciprocal, but this reciprocity is in general not observed.

The classical theories for the growth of a perfect crystal considered so far predict that the crystal should become bounded by atomically smooth closed-packed faces. These faces should then grow by the spread of successive layers created by a two-dimensional process. The critical supersaturation necessary for the formation of such two-dimensional nuclei (below which no growth should occur) was far higher than that encountered in actual practice. Frank[26] therefore suggested that such a disagreement between theory and practice was due to the presence of a type of surface defect called a "Screw Dislocation" on a crystal face which provided it with a self-perpetuating step and hence catalysed the growth. The role of a screw dislocation in the growth of a crystal will be considered in the next section.

2.2.4 Growth Theories of Imperfect Crystals

2.2.4.1 Introduction

Frank[26] suggested that no visible crystal can exhibit a completely perfect face and the growth rate is strongly influenced by the presence of structural irregularities. According to Frenkel[27] the surface roughness of the crystal was only due to thermal fluctuations but Burton, Cabrera and Frank[15] have established that the defects in a real crystal are much larger than those which could be caused by such fluctuations. Based on the

existence of a screw dislocation the characteristics of which are considered next, Frank developed a theory for the growth of a crystal from its vapour which was extended to growth from solution by Bennema[28].

2.2.4.2 Screw Dislocation and its Role in Crystal Growth

A screw dislocation is an extended defect in a crystal surface in which the Burgers vector is parallel to the dislocation line. Since the Burgers circuit can be continuously displaced along the dislocation line without changing its Burgers vector a screw dislocation once started cannot terminate within a crystal. A screw dislocation gives rise to "Growth Spirals" which may be either clockwise or anti-clockwise. Frank[26] has suggested that the dislocation density is of the order of 10^8 per cm^2 on a crystal face.

A screw dislocation emerging on the face of a crystal provides it with a self-perpetuating step. Frank[16] suggested that such a step can be eliminated only by its migration towards the edge of the face or by encountering another dislocation of opposite sense. The growth of a crystal face containing a screw dislocation proceeds by the continuous adsorption of solute molecules on the crystal surface followed by their surface diffusion to the steps and finally their incorporation into kinks in the steps; thus the step advances. Hence the presence of a screw dislocation eliminates the necessity for the formation of a two-dimensional nucleus for the continuation of growth.

2.2.4.3 The Growth Rate due to a Single Screw Dislocation

If a step created by a single screw dislocation is initially straight, and if it moves forward at a constant linear velocity, it must twist into a spiral. Frank[15] formulated the following equation for the rate of advance of a curved step:

$$v_\rho = v_\infty(1 - \rho_c/\rho) \tag{11}$$

where ρ = radius of curvature of advancing step (m)

ρ_c = radius of curvature of a critical nucleus (m)

v_∞ = rate of advance of a straight step (m/s)

v_ρ = rate of advance of a curved step (with curvature $1/\rho$) (m/s)

With the continuation of growth, the radius of curvature of the step at the centre continuously decreases until it becomes comparable to ρ_c at which point the rate of advance of the step becomes considerably reduced.

With the reduction in the velocity of the curved step relative to a straight one a steady state configuration of the growth spiral may be obtained in which the apparent angular velocity (ω) of the spiral is constant (irrespective of the distance from the centre). If the rate of advance of the curved step is independent of its orientation, the growth spiral will form a cone with continuously curved steps. If, however, the step velocity is dependent upon the orientation then the dislocation forms a pyramid with straight sides.

The number of revolutions of a spiral per second is given by $\omega/_{2\pi}$ and is defined as the "Activity of Dislocation". Since each revolution of the spiral raises it by one step height, the linear growth rate of the face is given by

$$g = \omega h/2\pi \tag{12}$$

where ω is the apparent angular velocity of the spiral.

In order to determine the value of ω, Frank[15] represented the spiral by the equation

$$\theta = f(r) + \omega t \tag{13}$$

where θ and r are the polar coordinates of the spiral whose origin is at the dislocation centre and t is the time. That is to say, the spiral is of the form $\theta = f(r)$. From geometric considerations the radius of curvature of the step, ρ, is given by[15]:

$$\rho = (1 + r^2\theta'^2)^{3/2} /(2\theta' + r^2\theta'^3 + r\theta'') \tag{14}$$

where θ' and θ'' are the derivatives of θ with respect to r at constant time. Also the velocity normal to spiral at any desired point, r, is

$$v(r) = \omega r/(1 + r^2\theta'^2)^{\frac{1}{2}} \tag{15}$$

The equation (13) must satisfy the equations (11), (14) and (15) and the solution for g interms of v_∞ suggested by Frank was an Archimedian spiral as a simple approximation for the sequence of equidistance steps and not too close to the origin, i.e.

$$r = 2\rho_c\theta > 0 \tag{16}$$

By allowing r to become infinite in equation (15),

$$\omega = v_\infty/2\rho_c \tag{17}$$

The distance between radially successive steps of the spiral, y_o, can be obtained from equation (16) simply by increasing θ by 2π. Therefore,

$$y_o = 4 \pi \rho_c \tag{18}$$

The numerical analysis of Ohara[16] gives

$$\omega = 0.33 \quad v_\infty/\rho_c \tag{19}$$

and

$$y_o = 19 \quad \rho_c \tag{20}$$

Frank et.al.[15] considered the interaction between dislocations and between groups of dislocations and came to the conclusion that their net effect is to increase the growth rate of a face by between x 1 and x 10 that due to a single dislocation when the dislocations are of the same sign and are at a distance less than $2\pi\rho_c$.

2.2.4.4 Kinks in a Step

Frenkel[27] and Burton, Cabrera and Frank[26] studied the structure of the monomolecular step and calculated the number of kinks per unit length of the step. According to Frankel the number of kinks (which may be positive or negative) is proportional to

$$\exp.(-W/KT) \tag{21}$$

where W is the energy required to form a kink and K is the Boltzman constant. They assumed that the mean distance between the kinks, x_o,

$$x_o \propto \frac{1}{2} h \exp(W/KT) \tag{22}$$

Since typical values for W/KT range from 2 to 6, x_o varies between h and 10h.

2.2.4.5 Growth at Dislocations with Bulk Diffusion Resistance

Frank et.al.[15] suggested that the controlling resistance to the growth of crystals was offered by a stagnant boundary layer surrounding the crystal. A screw dislocation was first assumed on the crystal surface which would continuously generate steps which were essentially straight ($\rho \to \infty$) and a mutual distance y_o apart. Under this condition

$$g = v_\infty h/y_o \tag{23}$$

By assuming a complicated three-dimensional geometric shape for the diffusion field boundary and negligible motion of molecular sinks they showed that:

$$g = \{Dc^* V_m h RT X^2 / 2x_o \sigma V_c [1 + 2\pi h(\delta - y_o)/x_o y_o + (2h/x_o) \ln(y_o/x_o)]\} \tag{24}$$

where c^* = saturation concentration (Kg solute/Kg solution)

x_o = distance between kinks (m)

δ = Thickness of stagnant boundary layer (m)

D = Diffusivity (m^2/s)

i) For low supersaturations the third term in the bracket of equation (24) becomes dominant and the growth rate becomes parabolic with respect to supersaturation

i.e. $$g = (Dc^* V_m RT/4\sigma V_c \ln y_o/x_o) X^2 \tag{25}$$

ii) For high supersaturations, the second term in the bracket becomes most important and the growth rate becomes linear with respect to supersaturation.

i.e. $$g = (Dc^* V_m/\delta) X \tag{26}$$

The theory predicts that the transition from a parabolic to a linear relationship will occur when $y_o < 2x_s$, which they estimated would occur when X = 0.001. Bennema[28] suggests a rather lower value.

In the above treatment it was assumed that the spacing between steps, y_o, remains constant over the crystal surface. This assumption is not valid in view of the bunching of steps observed in many cases[5]. The diffusion field about each step would then vary. Furthermore, y_o is obtained by the use of the equation (11) which assumes that the step edges are exposed to bulk supersaturation. However, the supersaturation at the curved steps is much less than that, because of the supersaturation decrease over the diffusion path through the stagnant boundary layer to the step. Thus Beck[29] suggests that the predicted growth rates should be viewed as the maximum possible growth rates. However, the BCF bulk diffusion model still predicts the correct order of magnitude and has been supported by many experimental observations[30].

Chernov[31] made a simplifying assumption that the distance between two successive kinks is small enough to consider a step as a line sink of the mass flux which reduces the problem to a two-dimensional one. He came to the same conclusions as Frank et.al. for the dependence of the linear growth rate of a crystal upon supersaturation, i.e. a parabolic relationship at low supersaturation and a linear one at higher supersaturation. However, unlike Frank, Chernov's model predicts that the extrapolation of the linear law will cut the X coordinate at some positive value and will not pass through the origin.

An increase in crystal/solution relative velocity should continuously decrease the resistance of the stagnant boundary layer in the above treatments and the growth rate should increase. Although this has been found to be true in many cases[30], instances of growth rates becoming independent of crystal/solution relative velocity[12,30] and of maxima in growth rate have also been reported[32]. Under these conditions the aforementioned treatments do not seem applicable. This led to the development of another model, the Surface Diffusion Model of crystal growth.

2.2.4.6 Growth at Dislocations with Surface Diffusion Resistance

Based on Volmer's concept[22] of the existence of an adsorbed layer of molecules over the surface of a crystal, Frank[15] developed a surface diffusion model (SDM) for the growth of crystals from vapours. Here he assumed that the main resistance to the growth of a crystal is the diffusion of the adsorbed molecules over the surface prior to their attachment at a step. By further assuming that $x_s \gg x_o$ Frank showed that the rate of advance of a step across the crystal surface was independent of its orientation. He obtained the following equation for the linear growth rate of a crystal from its vapour:

$$g = \beta V_m n_o f \exp.(-W_o/KT)(X^2/X_1) \tanh (X_1/X) \qquad (27)$$

where $X_1 = (2\pi\rho_c/x_s)X$

$$= 2\pi \gamma h/KTx_s \qquad (28)$$

$$\beta = (1+x_s\tau/h\tau_s)^{-1} \qquad (29)$$

τ = Time of relaxation necessary to re-establish equilibrium near the step (s)

x_s = Mean displacement of adsorbed molecules (m)

τ_s = Mean life of an adsorbed molecule before being evaporated into vapour (s)

γ = Edge energy of the nucleus per molecule (ergs/molecule)

n_o = Concentration of adsorbed molecules on the surface (molecules/m^2)

W_o = Energy of evaporation (ergs/m^2)

K = Boltzman constant (ergs/molecule K)

f = A frequency factor $(s)^{-1}$

For low supersaturation; ($X \ll X_1$) a parabolic law is obtained

$$g = \beta V_m \, no \, f \exp(-W_o/KT) \, X^2/X_1 \tag{30}$$

For high supersaturation ($X \gg X_1$) a linear law is obtained

$$g = \beta V_m \, no \, f \exp(-W_o/KT) X \tag{31}$$

Bennema[33] adapted the SDM of BCF for growth from vapour to growth from solution and showed that

$$g = C \, X^2/X_1 \tanh X_1/X \tag{32}$$

where C is a function of the surface diffusion properties of the solute molecules and the probability of their adsorption at kink-sites and X_1 is a function of the interactions of the growth spirals. Equation (32) again simplifies to the parabolic law i.e.,

$$g = C \, X^2/X_1 \tag{33}$$

and linear law, i.e.

$$g = C \, X \tag{34}$$

at low and high concentration respectively.

The SDM suffers from a serious defect: the spacing between the steps (y_o) is dictated only by the curvature at the centre of the spiral which is based on the bulk supersaturation. The actual supersaturation, which fixes ρ_c and hence y_o, is smaller and under these conditions the calculated values of g will be the largest. Thus Beck[29] has suggested that the growth rate might have a relationship to the supersaturation somewhere between the first and the second power. Liu,et.al.[34] showed that the data obtained by Cartier et.al.[31] from the crystallisation of anhydrous citric acid satisfied Frank's SDM with a dependence of the growth rate on supersaturation of approximately 1.6 .

Despite these criticisms the BCF surface diffusion model has gained wide experimental and theoretical support in the last few years and more and more workers tend to rely on this model to give a satisfactory explanation of their g vs. X curves. The growth rate measurement of $NaClO_3$ by Bennema[28] and that of several other materials[33] support the model. The above model also explains the many features of the fine structure of crystals during growth. However, deviations from predicted g vs. X dependence are not uncommon at high supersaturations[35,36]. Thus, in the case of $CaSO_4$, the growth of crystals at low X followed the expected parabolic law but, at high X, the exponent was greater than two rather than less and was sometimes as high as 13[35]. In order to explain these deviations from BCF model many workers have suggested the co-existence of two different growth models and formulated what is described in the literature as "Compound Growth Models".

2.2.4.7 Compound Growth Models

It has become increasingly common in the last few years to use what might be called compound growth models[36-39]. The purpose of invoking such models is to explain the deviations of experimental data from a chosen theoretical model. Thus Bennema et.al.[38] observed a deviation from linearity in the g vs. X curves of K-alum at $X \gtrsim 0.01$ and attributed this to the onset of two-dimensional nucleation. He proposed that both a PNTDN and dislocation growth occurred simultaneously, the overall rate being equal to the sum of the growth rates arising from the component models. Since the highest supersaturations that Bennema measured were only 0.012, the data supporting this compound mechanism was not nearly as complete as those showing the linear relationship at $X < 0.01$.

Botsaris and Denk[39], combined the MNTDN and the dislocation models to explain their data obtained from the crystallisation of K-alum.

Lefever[40] suggests that such a compound model can be explained by the existence of high solute concentrations near the crystal edges as has been observed by several workers[24,41]. Under conditions of low growth rate the supersaturation is insufficient to cause TDN so long as screw dislocation growth continues. Under conditions of high growth rate, the difference in surface concentration between the edges and the centre increases. Eventually the supersaturation at the corners becomes sufficient to cause TDN there.

Liu, et.al.[34] have shown quite convincingly that the data obtained from Botsaris and Denk's work fit the BCF correlation as accurately as the compound model. Ohara[16] analysed mathematically the existing modern theories of crystal growth and severely criticizes the use of several conflicting assumptions necessary to postulate compound models.

Levina and Belyustin [36], faced with the similar problems of obtaining growth surge at high supersaturation, have suggested that it is due to the disintegration of the macroscopic steps into microscopic steps which have been considered by Frank[5] to move at higher velocities than macroscopic ones. They assumed that such a distintegration took place because of the formation of TDN on the edges of the macroscopic steps. The existence and the formation of macroscopic steps on growing crystals has been explained in terms of the "Kinematic Theory of Crystal Growth" by Frank[5],and Cabrera and Vermilyea[42]. Working independently, both Frank and Cabrera et.al. came to the identical conclusion that the formation of macroscopic steps in the absence of impurities can be explained by assuming that the velocity of a step at a point depends only on the density of the steps in the vicinity of that point.

The theory suggests that the formation and break of macroscopic steps from and into microscopic steps is a continuous process and it affects the growth rate accordingly. Thus, during the growth rate measurement of β-methylnaphthalene from alcoholic solutions, continuous transformation from thicker to thinner steps and the reverse was observed with changes in supersaturation[43]. At low

supersaturation thicker steps were found to predominate; with increase in supersaturation most of the steps observed were thinner while at still higher supersaturation the number of thicker steps increased again. The growth rate also changed accordingly: at the lower supersaturation it followed a linear law, then the exponent increased rapidly (i.e. a growth surge was observed), and finally at still higher supersaturations changed back to linear dependence.

The kinematic theory was originally developed to deal with the growth of crystals before a steady state is achieved and the stability of growth to minor perturbations in the absence of an impurity. However it is doubtful whether pure conditions ever exist in practice and in particular in growth from solution where the solvent itself can act as an impurity.

2.2.5 Conclusions

Of all the growth theories considered in this work, the surface diffusion model of BCF appears to be the most satisfactory in the light of the majority of the crystallisation data. It explains the finite resistance to growth observed where bulk diffusion is shown to be of no importance. It also explains the frequently observed growth rates at very low supersaturations where the TDN theory predicts the complete absence of any growth. It also seems to allow an explanation of many features of the fine structure of crystals during growth.

The dependence of g on X appears to be first order for the Diffusion theories, first to second order for the BDM and SDM of BCF and for the BDM of Chernov whereas higher orders are predicted for MNTDN, PNTDN and BSM. The effect of crystal/solution relative velocity is significant for the BDM of BCF, that of Chernov and for the diffusion model. The size of the crystal seed could have an important role for the diffusion model, and for the BDM of BCF and that of Chernov in the growth of crystals in suspension. The MNTDN theory predicts that the growth rate is dependent on the area of the crystal face.

2.2.6 Interpretation of Growth Rate Results in Terms of Classical Growth Mechanisms

1. Diffusion Controlled Growth: If the surface resistance to growth were negligible, then the rate of crystal growth would be determined by the rate of diffusion of solute through a stagnant layer of solution adjacent to the crystal surface. Since the supersaturation at the surface would be zero,

$$g = MX \tag{35}$$

and

$$\ln g = \ln M + \ln X \tag{36}$$

where M = a constant for given conditions of agitation, dependent on the diffusion layer thickness and the solute diffusivity.

Thus for a diffusion controlled growth mechanism, a plot of ln g vs. ln X should give a straight line with a slope of unity, as shown by the line AB in the figure (1a). An estimate of the thickness of the diffusion layer could also be made for comparison with those of known diffusion controlled processes.

2. Two-Dimensional Nucleation Mechanism of Growth: According to the equation (7) the TDN concept of growth predicts a linear relationship between ln g and 1/ln (X+1) with a slope proportional to the crystal/solution interfacial free energy. Equation (7) also predicts a curve of the form MP in the figure (1a) between ln g and ln X. It can be seen that below a certain supersaturation (0.25 - 0.50) the equation (7) predicts no measurable growth rates. However, a curve like MP could possibly also be obtained despite being dislocation controlled growth because of strong solvent adsorption on a crystal face leading to a solvent screen. Also the presence of heterogeneous impurities could result in growth rates higher than indicated by the curve MP despite being TDN controlled growth. Thus the qualitative observations of surface are also essential for analysing growth rate results in terms of this model of growth.

3. Growth from Dislocation: The theory of growth from dislocations predicts that growth rates should be proportional to the second power of supersaturation for "low" supersaturation levels (i.e. a slope of 2 on a plot of ln g vs. ln X as shown by the curve CD in the figure (1a) and proportional to the first power of supersaturation for "high" supersaturation levels (shown by the curve DE). The transition from second order to first order occurs over a supersaturation range of about a factor of 10 which therefore suggests that growth rate data should be obtained over a very wide range of supersaturation.
Since both, the BDM and SDM predict identical g vs. X curves, additional considerations based on other data are required (as for example the effect of the rate of flow of solution passing the crystal surface).

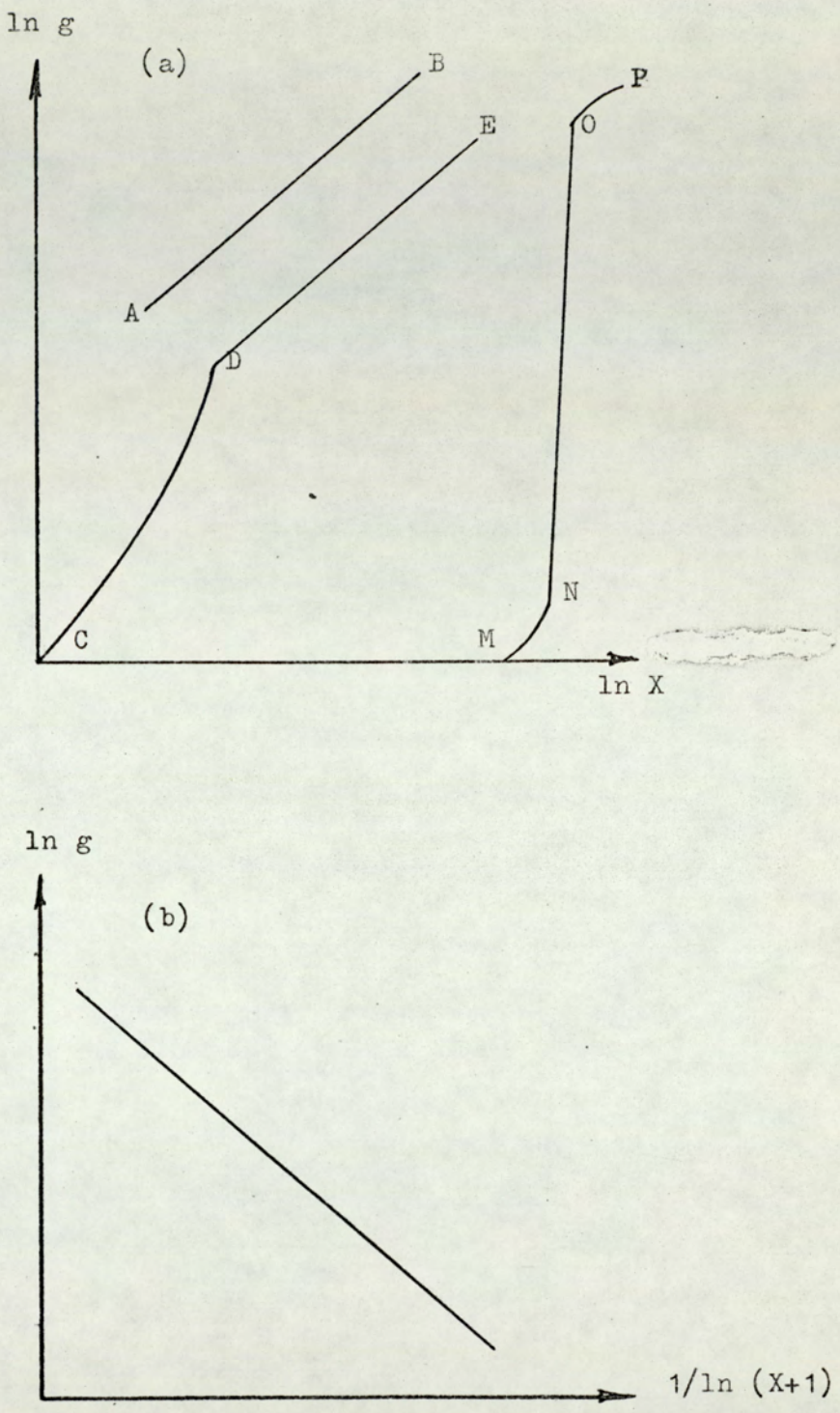

Fig. 1 Theoretical dependence of the growth rate of a crystal

a) AB Bulk diffusion controlled growth
CDE Dislocation controlled growth
MNOP Surface nucleation controlled growth

b) Linear dependence for TDN.

2.3 Secondary Nucleation

2.3.1 Introduction

It is quite clear from the various theories discussed in the previous section that the growth rate of a crystal is a function of the supersaturation in the bulk of the medium. The maintenance of a constant supersaturation is an essential requirement, therefore, for the accurate measurement of the linear growth rate of a single crystal. The growth of a crystal in the presence of a few other crystals (due to the phenomenon of secondary nucleation) would severely impair the constant supersaturation conditions in a batch cell where the amount of mother solution could be very small. In a flow cell, the problem can be solved by flushing out and by dissolving all such secondary nuclei by raising the solution's temperature. In a batch cell, however, the problem is more acute and demands the prevention of the formation of these nuclei. This could be achieved only if an insight into the mechanism of secondary nucleation is available.

Secondary nucleation is defined as the nucleation that occurs in the presence of seed crystals of the material being crystallised. The secondary nucleation can occur not only in contact with the main crystal but also at some distance away from it. This kind of nucleation has just begun to receive attention because it is now relatively clear that the nucleation which occurs in the suspension of crystals encountered in industrial crystallisers is predominantly secondary nucleation. In contrast with homogeneous nucleation, secondary nucleation exhibits relatively low order dependence on supersaturation since it also occurs at considerably lower super-

saturation than homogeneous nucleation. This process has not been sufficiently studied nor is it currently under control.

Strickland-Constable[44] has outlined some of the ways in which secondary nucleation could occur. These may be summarised as follows:

a) Initial Breeding: A crystal introduced into a supersaturated solution directly from its environment can generate a number of new crystals. This is called initial breeding and is brought about due to stray crystallites which are already present on the crystal surface. It usually occurs when the crystal is first introduced into the solution and no further crystals appear after the first batch.

b) Polycrystalline Breeding: This kind of nuclei breeding occurs when a single crystal (cured of initial breeding) develops into a polycrystalline mass when allowed to grow in a supersaturated solution. The latter eventually breaks into small fragments, which in turn generate new crystals.

c) Needle Breeding: This type of breeding occurs when the supersaturation of the solution exceeds the limit at which the growth becomes dendritic. Such a growth is mechanically weak and its bonds with the parent crystal are easily broken. Fracture of these results in the formation of many small crystals.

d) Collision Breeding: It occurs at supersaturation below that required for needle breeding and takes place when the crystal is free to collide with any solid surface, either with other crystals or parts of the apparatus. Inertia considerations suggest that this kind of secondary nucleation is only significant when the crystal size exceeds 100 microns.

In order to identify the origin of the secondary nucleation, the above mentioned different kinds of breeding phenomena can be broadly divided into two classes:

(i) Contact Nucleation or Collision Breeding.

(ii) Non-Contact Nucleation (This includes the first three types).

2.3.2 Contact Nucleation

The phenomenon of contact nucleation has received considerable attention lately. Strickland-Constable,et al.[45] investigated this phenomenon in great detail and found that the rate of contact nucleation was an increasing function of the supersaturation. They suggested that it was a microattrition process in which the secondary nuclei came directly from the seed crystals. Based on this result Strickland-Constable formulated a "Survival Theory" according to which the fragments produced by the contact of seed crystals would be in the same size range as the critical nucleus. Only that fraction of the so produced nuclei would survive which were greater than the critical nucleus. All others would dissolve. The survival theory is also supported by the contact nucleation of $NaClO_3$[46,47]. Direct evidence of the survival theory, however, comes from the work of Denk and Botsaris[48] who utilized the enantiomorphic properties of $NaClO_3$ crystals to investigate the origin of secondary nuclei from contact nucleation. Precured crystals of $NaClO_3$ were immersed in a super-saturated solution and were either tapped with a metal rod or allowed to slide about the bottom of a crystallisation flask. They found that almost all the product crystals had the same structure as the seed crystal at all supersaturations and liquid velocities, and that the number of product crystals was a function of the contact energy and

supersaturation but independent of liquid velocities. They suggested that the dependency of the number of secondary nuclei on the supersaturation arises for two reasons - because the supersaturation influences the number of fragments originally produced as well as the percentage of these fragments that survive. The effect of the supersaturation on the initial generation of fragments could be due to the general observation of various surface irregularities at high supersaturations. Fraction of these fragments which survive would depend on the size of the critical nucleus and thus depend upon supersaturation. They suggested that the dependence of the surviving product crystals on supersaturation could be represented by an S-shaped curve. The existence of such a curve has actually been established by Garabedian and Strickland-Constable[46].

2.3.3 Non-Contact Nucleation

As to the origin of secondary nucleation in the non-contact situation practically no literature has been found. The only significant work appears to be that of Denk and Botsaris[49].

Initially cured crystals of $NaClO_3$ were immersed in pure supersaturated solutions under stagnant and flow conditions. In some stagnant solutions trace quantities of a soluble impurity (Borax) was also added. The enantiomorphic properties of $NaClO_3$ were used to determine whether the secondary nuclei came from the parent seed or the solution. From the results so obtained they concluded that non-contact secondary nucleation may be caused by more than one mechanism depending upon supersaturation, liquid velocity, and impurity concentration. They

suggested that the secondary nuclei can come from the parent seed crystal by one of 3 possible mechanisms:

(i) the growth and detachment of irregularities such as dendrites on the surface of the seed crystal. These dendrites can detach themselves from the main crystal either because of "Dendrite Coarsening" or because of the liquid shear forces resulting from the flow of the solution past the crystal. The seed crystals obtained under these conditions all have the same structure as the parent seed. The former mechanism has been suggested to be the predominant mode of detachment of dendrites in stagnant solution. Or

(ii) because of an impurity concentration gradient in the boundary layer resulting from the uptake of the impurities by the growing seed crystals. This can be explained in terms of the "Impurity Concentration Gradient" (ICG) Nucleation Model initially formulated by Botsaris et.al[50]. The model says that if trace amounts of a dissolved impurity suppress the rate or prevent the formation of secondary nuclei and if the impurity is incorporated into the growing crystal, secondary nucleation could occur in the boundary layer near the crystal surface. This will happen possibly due to the low impurity concentration near the crystal surface due to an impurity conventration gradient in a layer surrounding the crystal. In their work this mechanism was considered to be operative where the presence of an impurity increased the super-saturation requirements for spontaneous nucleation. Under these conditions an equal number of both forms of $NaClO_3$ crystals were obtained. Or[49]

(iii) because of the presence of seed crystals leading to a possible ordering of water molecules near the crystal surface which in turn lead to a high local supersaturation. The increase in local super-

saturation could result from the difference in the solubility of crystallising species in the ordered water structure and that in the bulk of the solution. They suggested that the local rise in supersaturation could become high enough to induce spontaneous nucleation. Equal proportions of both forms of $NaClO_3$ crystals would then be formed. They further suggested that under some conditions, such as at low supersaturations, this mode of secondary nucleation could occur along with the dendritic model such that 80% of the total crystals are formed by the former techniques. A total of 60% of the product crystals would then be expected to have the same structure as the parent seed crystal, as was in fact obtained. Similar work was performed by Belyustin and Rogacheva[52] on the secondary nucleation of $MgSO_4.7H_2O$. They suggested that the secondary nuclei did not come from the seed crystal. Since the filtration of the solutions retarded both seeded and unseeded nucleation, they proposed that secondary nucleation was caused by suspended heterogeneous matter coming in contact with the seed crystal, becoming activated and converted into crystal nuclei. However, this mechanism cannot explain the observed increase in the proportion of the right-handed $MgSO_4.7H_2O$ crystals in the presence of a right-handed seed crystal or a left-handed quartz crystal in their experiments. Besides, they did not consider the effect of the presence of impurities NaOH and Boric acid on the nucleation mechanism.

Suggestions have been made that the catalytic effect of an impurity results in secondary nucleation. This has been explained as being due to a decrease in the free energy of the formation of a nucleus on a crystal surface due to the reduction in contact angle between the crystal and the nucleus. However, this hypothesis has gained little

experimental support. In fact the presence of impurities has been found to prevent supersaturation from building up to the level required for homogeneous nucleation. The presence of trace quantities of dissolved impurities (like surface active agents) has been found to raise the supersaturation required for homogeneous nucleation.

2.3.4 Conclusion

Considerable evidence has arisen in the recent years to suggest that the phenomenon of secondary nucleation requires the existence of seed crystals in supersaturated solutions. In the case of contact nucleation the formation of secondary nuclei has been repeatedly emphasised to be a microattrition process and the rate of nucleation to depend upon the contact energy and supersaturation. In the case of non-contact nucleation however, the relatively little amount of experimental data leaves the mechanism open to question and requires closer examination.

2.4 The Rythmicity of Crystal Growth

2.4.1 Introduction

It has been observed by many workers that visibly flawed crystals grow two or three times as fast as the clear flawless ones, but it seems to have been rather generally assumed that crystals free from obvious flaws would grow at the same rate. Yet several cases have been reported in current literature where the growth rate of a face has been found to vary greatly with time under fixed external conditions like supersaturation and temperature. The reasons for this are far from clear, as shown by the great variety of

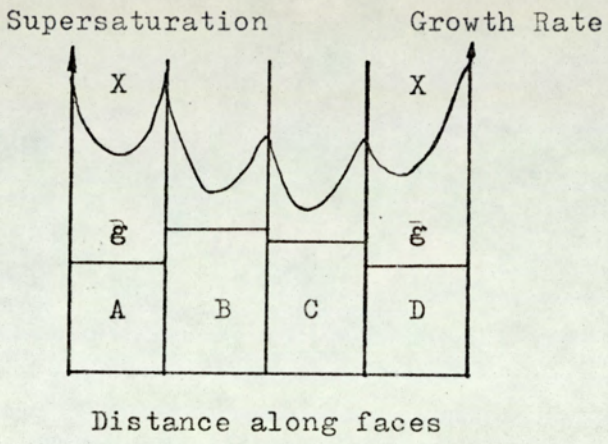

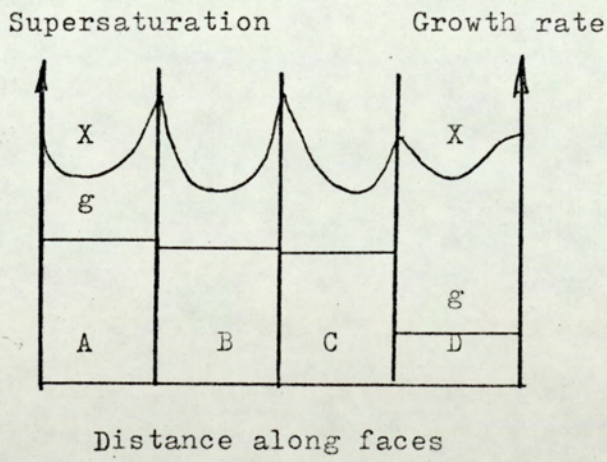

Fig. 2 Supersaturation along faces and growth rates of faces of Sodium Chlorate crystals
(Ref. 24 , p. 134)

hypotheses [15,19,53,54,55]. All the available information is scattered and no single paper even touches upon the various reasons that have been put forward for the wide variation of the growth rate of a crystal face under fixed (hypothetical) external conditions. An attempt has, therefore, been made to collect such papers which offer different explanations for this observed rythmicity in crystal growth.

2.4.2 Experimental Evidence and Discussion

It appears that a fluctuation in growth rate could occur by one or more of the following effects combined together. These are:

a) The surface imperfections on the crystal face.
b) The statistical fluctuation of supersaturation and temperature on the crystal face.
c) The change of control mechanism of crystallisation.
d) The formation of inclusions within the crystal.
e) The incorporation of impurities in crystal growth.

Since more than one of these could be acting at the same time, a sharp division appears to be difficult and a general discussion of their effects will be given in the following section.

Experiments by Bunn[24], Humphreys-Owen[41], and Berg[25] showed for the first time that the growth of a crystal is interruptable and can even be suspended under fixed external conditions. These researchers grew crystals of $NaClO_3$ in a thin film of aqueous solution between optically-plane glass plates. Growth was constrained to the four faces in the plane of the film. The growth rate, concentrations,

and concentration gradients were measured simultaneously. The concentration being deduced by means of interference fringes formed in the solution surrounding the crystal. It was found that the concentration along the surface of a growing crystal was not constant, but was lowest at its centre, rising on each side to its corners as shown in figure 2. The component of the concentration gradient normal to the face was also not uniform over the face; it was highest at the centre of the face decreasing towards the corners. The crystallographically equivalent faces were found to grow at different rates and some stopped growing completely though there was plenty of solute available. Indeed it was found that the most slowly growing faces were in contact with the most strongly supersaturated solutions. Berg[25] attributed such a difference to the presence of local traces of impurities. However, the way in which such impurities can enhance the growth of three identical faces while retarding that of the fourth one at the same time could not be explained. Bunn[24], on the other hand, considers such a non-uniformity in growth to be due to the nature of the surface structure in the initial stages and the changes occurring in it during the growth. He suggests that crystal faces which did not grow at all initially were perhaps more perfect than those which grew at a finite speed. The variation in growth was regarded as an indication of the importance of the diffusive flow of the solute to the growing crystal. Faces adjacent to a less perfect face grew faster than the other identical faces. Concentration gradients on these faces were also greater than those on faces away from the less perfect face.

Buckley[56] has pointed out that a rapidly growing face

tends to impoverish the solution on adjacent faces and slows then down. Conversely, faces adjacent to a retarded face tend to grow faster than otherwise.

Frank[57] suggests that sudden changes in growth rate are to be expected due to the sudden rearrangement of dislocations which may occur even under very low stress. He also showed that an active step connecting a pair of dislocations could be temporarily halted or even broken down if it faced another step connecting another pair of dislocations in its way[26].

In terms of the spiral-growth mechanism of Frank[15], the growth rate of a crystal is proportional to the number of imperfections present on it and the different degrees of imperfections will produce different individual growth rates. As to the effect of random distribution of dislocations, Frank demonstrated that their most favourable interaction would be to increase the number of steps generated by a small factor of probably less then two, over that of a single screw dislocation. However, Burton et.al.[15] have argued that the growth rate of a crystal face could be affected if there were several screw dislocations at a distance less than $2\pi\rho_c$ apart. Thus they indicated the possibility of an increase in growth rate if the dislocations were of the same sign, and a decrease in growth if they were of opposite sign due to their mutual interaction leading to reinforcement in the former case and annihilation in the latter.

Strickland-Constable et.al.[58,59] grew crystals of Salol and Benzophenon at low supercooling from their melts in narrow capillary

tubes. They observed that the growth rate gradually decreased with time when the crystals entered the narrow capillary tubes until finally they stopped growing. The growth, however, recommenced if the crystal's surface was touched with a spike or if the crystals emerged from the capillary tubes. In fact when the crystals were allowed to emerge into the melt at the bottom end of the tube, the rate almost immediately regained the original value of a free growing crystal. At first it was suggested that perhaps the growth was inhibited due to hinderance offered by the walls of the capillary tubes to the nucleation of new layers at the crystal edges[59]. In a later paper[60], however, Strickland-Constable et.al. contradicted this by arguing that such an explanation would demand an immediate once for all retardation on first entering the capillary. Instead they suggested that the fall in growth rate was due to a reduction in dislocation density, as the dislocations present on the crystal surface would gradually grow out to the walls and no further dislocations would be introduced. To explain such a dependence of growth on dislocation density, however, he had to assume that there were 170 dislocation lines present at a distance less than $2\pi\rho_c$ apart on a free growing crystal of Salol. This is because the variation in growth was observed to be over a range of 170/1 as the crystal grew in the capillary.

The growth rate of a crystal by screw dislocation mechanism is dependent upon the height of growth steps, which is an uncontrollable parameter[61]. Thus Lemmlein and Dukova[62] found that the step velocity of p-Toluidine crystals growing from the vapour phase

increased rapidly as the height of the steps decreased. They concluded that this was due to the fact that smaller steps require less solute to move a certain distance than the larger steps. This explanation does not seem reasonable as a system of smaller steps of fixed height needs precisely the same amount of solute to move a given distance as one step of the same total height. Bunn and Emmette[63], therefore, suggested that perhaps it is due to a decrease in surface energy with an increase in step height.

An excellent account of how the presence of dislocations determines the growth rate of a crystal and the control mechanism has recently been given by Mussard and Goldsztaub[53]. The growth rate of $NaClO_3$ crystals was measured under a classical microscope while the concentration currents surrounding the crystal were photographed using a Baker Interference microscope. It was noticed that certain faces grew at a very low speed and had practically no dislocations while other crystallographically similar faces grew at a substantially higher rate and had a significant number of dislocations on them. The concentration gradients were also found to be greater in the case of the latter faces. An increase in supersaturation was found to generate screw dislocations on the slow growing (blocked) faces and concentration gradients were also observed to be set up in the solution surrounding the blocked faces. The growth rate of these blocked faces was found to increase with supersaturation more rapidly than for the unblocked faces until the two growths were the same. Thus Mussard and Goldsztaub suggested that at low supersaturation, faces with a sufficient number of screw dislocations will grow at a substantial rate

and their growth will be controlled by screw dislocation mechanism. More perfect faces will, however, have to rely upon the formation of two-dimensional nuclei at low supersaturation and therefore will have smaller growth rate. Similar conclusions have been arrived at by others[54, 64].

In Frank's scheme for the formation of growth spirals by two screw dislocations differing in sign, it was assumed that the point of emergence of dislocations remained fixed during crystal growth. However, Dakova and Lemmelein[65] found that during the growth of p-Toluidine from the vapour phase screw dislocations of equal and opposite Burgers vectors would occasionally be located near one another. As growth proceeded, these growth centres slowly approached one another and fused. Fusion resulted in mutual annihilation of the dislocations and cessation of growth. No new spiral layers were then formed once the fusion occurred. They also suggested that the interaction between screw dislocations depends upon their separation distance compared with the distance between turns of the spiral that they form. Thus a separation in excess of twice the distance between the turns of the spiral would lead to little or no interaction and the growth might be unaffected.

From the foregoing discussion it is tempting to conclude that at least the growth rate of a perfect crystal will not vary with time. However, Sheftal'[19] has shown clearly how a periodicity could also occur when the growing crystal has smooth surfaces and the growth is surface nucleation controlled.

Thus, it seems that a periodicity in growth rate is obtainable when either of the two molecular kinetic mechanisms is operative. However, the scale of oscillation of growth rate has been suggested to decrease when the surface nucleation control is operative or when it takes over from the dislocation control[20]. An increase in supersaturation or growth rate has been found to decrease the scale of oscillation of the growth rate of a crystal face with time[29], diminish the difference between the growth rates of similar crystallographic faces[54,66], and reduce the size distribution in the growth of many crystals together[64]. Two mechanisms have been put forward to explain such a dependence:

Either

1) At low supersaturation, dislocation is the growth controlling phenomenon and therefore the growth rate is very sensitive to surface imperfections. At higher supersaturations, screw dislocation becomes less important in the overall growth process (perhaps surface nucleation takes over) and thus the growth rate becomes much less sensitive to the surface imperfections.

Or

2) An increase in supersaturation or growth rate diminishes the difference between the surface imperfections of identical crystallographic faces and that between different crystals.

The presence of an impurity in the solution has also been suggested to lead to fluctuation in growth rates. Thus Sheftal'[19], states that the statistical fluctuation in supersaturation and temperature on the surfaces of a crystal can lead to a rythmic inclusion of impurities in the crystal. This, in turn, can lead to

higher magnitudes of fluctuations in growth rates. Ovsienko et.al.[54] have also considered the periodicity in growth rate of a crystal to be due to the changes in its structure due to a possible adsorption of impurities. Thus, they suggest that the capture of impurity atoms or insoluble particles, capable of producing dislocations, may lead to an increase in growth rate. Alternatively, an increase in growth rate may also be produced by a reduction in the work of formation of two-dimensional nuclei on the active sites formed by the re-entrant angles between a crystal face and the surface of the insoluble impurity particles. The fall in growth rate with time may be caused by the poisoning of the growth sites by the adsorbed impurity atoms[31].

An increase in impurity concentration has been suggested to reduce the scale of oscillation in growth rate with time. White and Wright[64] have reported that in a well-stirred crystalliser crystals of Sucrose, initially all of one size and growing under the same conditions show variation in growth rate. This produces an increase in product size distribution. The magnitude of size distribution decreases with increasing impurity concentration. They suggest that an increase in impurity concentration requires an increase in supersaturation of the solute to maintain a given growth rate, which gives a more even distribution of growth centres among crystals and thus gives a smaller size distribution. Alternatively, impurities were thought to interfere with the dislocation mechanism and cause the surface imperfections to become less important.

Many other workers have also considered the presence of the impurity atoms to be the possible cause of the instability in growth

rates[16,25,39,67,68]. Thus, Ohara[16] has shown mathematically how the presence of strongly adsorbed impurities can lead to an instability in growth rate thereby yielding two different growth rates for a single set of experimental conditions (section 2.5.3).

The formation of inclusions is sometimes regarded as an indication of the rythmic character of the crystal growth process and has been found to be succeeded by an abrupt increase in growth rate[55]. One explanation given for the formation of inclusions in general is that an area of the crystal face ceases to grow, whilst the neighbouring areas continue to grow; this may result in the formation of channels where the growth has ceased. After a certain period has elapsed the channel is covered over by the lateral growth of a layer, thereby enclosing the trapped mother liquor. Sheftal'[19] has suggested that this process is rythmic in character and on the surface of the growing crystals periodic intermediate layers of the mother liquor may occur.

Petrov[69] considers that in the growth of crystals from solution, the solvent itself can act as an impurity and provoke a periodicity in growth rate by forming inclusions. During the crystallisation of KNO_3 from solution he observed that the growth rates varied over wide ranges and sometimes ceased for periods up to 30 minutes at considerable supersaturation. Occasionally he also observed the formation of thick layers at the edges and the corners of crystal faces which finally resulted in the formation of inclusions in the middle of the faces. An abrupt increase of growth rate was then noted. He explained the observed periodicity in growth rate in terms of the thickness of a layer of solvent adsorbed on the

crystal faces; local variations in this layer affecting the growth rate. Thus the absence of growth was taken to be an indication of a complete blockage of the solute access to the crystal face by the solvent. The solvent layer was regarded as highly mobile and most effective in blocking at the centre of the crystal face. At the corners and edges however, the layer was considered to be weak and its rupture would lead to higher growth rates at these sites.

The formation of inclusions at the centre of a crystal face has also been observed by Denbigh and White[70]. Analysis of their data showed that inclusion formation occurred at high supersaturation and a certain crystal size. Trevius[55] suggested that this was perhaps due to an increased diffusional resistance of the medium to such a value that the face begins to grow non-uniformly. Thus the formation of inclusions has also been found to occur with an oscillation in supersaturation[71].

From the above discussion it appears that crystal growth is an interruptable and variable process itself on the atomic scale. On one hand small fluctuations of growth conditions on the crystal surface may accumulate and result in much larger order fluctuations thereby causing a variation of growth rate with time. On the other hand, the growth of the crystal surface itself may upset the equilibrium growth conditions and result in larger fluctuations. Such a state of growth in which g depends on time has been described by Cabrera and Coleman[72] as a transient state. The effect of a transient state on the $g(X)$ curves has not been envisaged by any of the growth

models proposed so far. Even the most widely accepted SDM of BCF deals only with the steady state conditions. Cabrera and Coleman believe that a steady state corresponding to BCF is difficult to achieve experimentally. They propose that such an ideal state might only arise after a sufficiently long time of growth under constant external conditions.

2.5 Theories of Crystal Growth with Impurity

2.5.1 Introduction

Impurities are known to affect the growth rates of crystal faces as already mentioned in the previous section. Their usual effect is to retard the growth rate although in a few cases acceleration of growth rate has also been reported[29,73,74,75,76]. Different index faces have been found to be affected differently by the same impurities thus leading to a modification of crystal habit. Many theories have been put forward to explain the way impurities may alter growth rates. However, no single theory has been found which accounts for all the features observed nor the mechanisms involved in the growth of crystals in the presence of impurities. A common feature of the most widely accepted theories is the belief that to alter the growth rate on a crystal face, an impurity must be adsorbed to some extent on that face and this has given rise to the postulation of two possible mechanisms.

2.5.2 Impurity Adsorption at the Growth Steps

Sears[74] proposed a mechanism to explain the retardation of the growth rate of Lithium Fluoride in the presence of Ferric Fluoride by assuming that the impurity was adsorbed at the active

sites along the growth steps (or kinks) and thus poisoned them.

Sears suggested that the impurity does not necessarily have to be incorporated into the crystal. Thus there exists a competition between impurity units and the growth units to occupy the active sites on a step. The growth rate of the crystal is then controlled by the number of sites on the step which are not occupied by the impurity. Sears emphasised that for an impurity poison to be effective it must form a monolayer on the step otherwise the rate of step motion would be insensitive to the concentration of the impurity in the solution. This treatment explains the frequently noted rapid decrease in the growth rate of a species for a small increase in impurity concentration depending on the shape of the adsorption isotherm.

The impurity probably acts by increasing the interfacial free energy of the solute/crystal. This in turn, at constant super-saturation and temperature, will decrease the nucleation rate for the two-dimensional nucleation theories and increase the step spacing for the dislocation theories. Thus a retardation in growth rate will be inevitable.

Smythe[12] determined and compared the relative growth rates of eight principal pairs of faces of Sucrose crystals grown from pure solutions and from solutions containing various impurities. He found that C_6 type of Oligo-saccharides strongly inhibited the growth of certain faces of Sucrose crystals whereas other Oligosaccharides had comparatively very little effect. This was explained as due to

stereospecific adsorption of these impurities at kinks-sites on the steps of growing Sucrose crystal surfaces.

2.5.3 Impurity Adsorption between Growth Steps

Cabrera and Vermilyea[42] assumed that the impurity adsorption takes place on the plane region between the steps. On this basis they put forward a mechanism which involves the assumption that when a step encounters a pair of adsorbed immobile impurities it must force its way between them with its growth front being effectively pinned at the impurities. Consequently, the step must become curved, and its velocity correspondingly reduced according to the equation

$$v_\rho = v_\infty (1 - \rho_c/\rho) \qquad (11)$$

where ρ now refers to the radius of curvature of the step passing between the impurities and is a function of either the distance between the impurities, ρ_x, or the density of impurity molecules adsorbed on the surface. If $\rho_x \leqslant 2\rho_c$ the curvature of the step becomes so large that the step movement completely ceases. However, Cabrera and Vermilyea considering the density of impurity molecules, rearranged the equation (11) to the form:

$$v_i = v_\infty (1 - 2\rho_c d^{1/2})^{1/2} \qquad (37)$$

where v_∞ = Step velocity in the absence of impurity (m/s)

v_i = Step velocity in the presence of impurity i (m/s)

d = Density of adsorption of impurities (molecules/m^3)

Cabrera and Vermilyea assumed that once a step had gone past an impurity unit the latter is virtually buried inside the growing crystal and offers no further impediment to growth.

Using different approximations Ohara[16] estimated four different values of v_i as follows:

$$v_i = v_\infty(1 - 2\rho_c d^{\frac{1}{2}})^{\frac{1}{2}} \tag{37}$$

$$v_i = v_\infty\{1 - [2(3)^{\frac{1}{2}}]^{\frac{1}{2}}\ \rho_c(d)^{\frac{1}{2}}\}^{\frac{1}{2}} \tag{38}$$

$$v_i = v_\infty[1 - (\ln 2)\rho_c(d)^{\frac{1}{2}}] \tag{39}$$

$$v_i = v_\infty\{1 - [2\ (3)^{\frac{1}{2}}]^{\frac{1}{2}}\ (\ln 2)\rho_c(d)^{\frac{1}{2}}\} \tag{40}$$

Assuming a constant impurity flux of J_i from the bulk of the solution to the crystal surface, he obtained

$$d = J_i/\nu_i \tag{41}$$

where ν_i is the flow rate of steps with impurities and is given by:

$$\nu_i = v_i/y_o \tag{42}$$

The flow rate of steps without impurity can similarly be given by

$$\nu_o = v_\infty/y_o \tag{43}$$

Thus, the ratio of the two flow rates, u, is given by

$$u = (\nu_i/\nu_o)^{\frac{1}{2}} = (v_i/v_\infty)^{\frac{1}{2}} \tag{44}$$

Substituting the equations (41), (42), (43) and (44) into any of the equations (37 - 40) following corresponding equations are obtained:

$$u^5 - u + [2\rho_c(J_i/\nu_o)^{\frac{1}{2}}] = 0 \tag{45}$$

$$u^5 - u + \{[2(3)^{\frac{1}{2}}]^{\frac{1}{2}}\ \rho_c(J_i/\nu_o)^{\frac{1}{2}}\} = 0 \tag{46}$$

$$u^3 - u + [(\ln 2)\rho_c(J_i/\nu_o)^{\frac{1}{2}}] = 0 \tag{47}$$

$$u^3 - u + \{[2(3)^{\frac{1}{2}}]^{\frac{1}{2}}(\ln 2)\rho_c(J_i/\nu_o)^{\frac{1}{2}}\} = 0 \tag{48}$$

The equations (45 - 48) have one negative real root, since all the left hand sides are positive when u = 0. There may be zero or one or two positive roots for all. The condition to have at least one positive root for the equations (45 - 48) was obtained by Ohara as:

$$v_\infty/y_o \geq 12 \sim 15\ \rho_c^2\ J_i \tag{49}$$

Thus an important corrolary of the equations (45 - 48) states that for each impurity concentration there is a certain critical supersaturation, X_c, below which no growth should occur. Thus for any system for which there is an impurity flux J_i to the surface, the growth rate without impurity has to exceed an average value of $14\ \rho_c^2\ h\ J_i$ in order for any finite growth to occur when the impurity is present. By substituting equation (49) into the equation (25), Ohara obtained the following values for X_c:

For $X_c \ll 1$,

(i) For very small X_c

$$X_c = \left[\frac{14h\sigma^2 V_m^2 J_i}{C_6 k^2 T^3}\right]^{\frac{1}{4}} \tag{50}$$

(ii) For X_c larger than in (i) but still $\ll 1$

$$X_c = \left[\frac{14h\sigma^2 V_m^2 J_i}{C_6 C_7 k^2 T^2}\right]^{\frac{1}{3}} \tag{51}$$

where $C_6 = 2\ D_s c_s^*\ K\ \beta\ \gamma_o/19\ x_s\sigma$ (52)

and $C_7 = 19\sigma\ V_m/2\ k x_s$ (53)

D_s = Diffusivity coefficient on the crystal surface (m^2/s)

c_s^* = Equilibrium solute concentration on the crystal surface (molecules/m^2)

γ_o = Kink retardation factor

If, further, J_i, is mass transfer controlled, then above a certain agitation rate no growth will be possible. This is because of the increasing values of X_c with increase in flow rate. When $X_c = X$ for a given J_i, the equality holds for the equation (49) and this suggests that there is no growth and there is one positive root to one of the equations of Equations (45 - 48), however, if $X_c < X$ then there are two positive roots for all of the equations (45 - 48). Ohara[16] suggests that this might lead to an instability for the growth rate since there can be two different growth rates for a single set of experimental conditions: X, T and J_i.

The existence of X_c for a particular value of an impurity concentration, c_i, has been claimed for the growth of adipic acid crystals in the presence of anionic impurity[29] and for the growth of lead nitrate crystals in the presence of methylene blue[77].

The effect of impurities on the movement of steps on the surface of a growing crystal has been observed under a microscope by Dunning et.al.[78]. They found that Raffinose and Stachyose, which markedly affected the rate of advance (and also the shape) of the steps were greatly adsorbed and incorporated into the crystal. They found that the retarding effect of these two impurities, out of 18 impurities tried, was greater on the faster moving faces than on the

slower moving ones. They suggested that the tendency to stronger adsorption and consequently higher retardation effect of the two, was due to the greater ability to form stronger Fructose-Fructose bonds on the surface.

Chernov[31] attempted to explain the effects of impurities in terms of comparable step heights. He suggested that an impurity slows down the advance of elementary steps whose heights are comparable with those of adsorbed impurity molecules, and that this effect became less noticeable as the height of the advancing effect increased. The influence of impurities on the linear growth rate must therefore depend particularly on the mean step height.

Chernov stated that when adsorbed impurities have a short life time on the crystal surface, the impurity poisoning of the active sites becomes important and it is then practically impossible to incorporate new particles in the poisoned kinks. He suggests that assuming that the kinks are uniformly distributed on the surface and that the growth rate, g, is proportional to the number of active sites free of impurities, Bliznakov's derivation of the dependence of g on impurity concentration c_i is applicable. The equation is as follows:-

$$g_\theta = g_o - (g_o - g_m)\theta \qquad (54)$$

where g_o = linear growth rate in pure solution

g_θ = linear growth rate with a surface coverage of impurity θ

g_m = linear growth rate with a maximum coverage

θ = Fraction of the active sites occupied by impurities in Langmuir's adsorption isotherm.

Mullin[79] has shown how Bliznakov obtained an equation of the form:

$$\frac{1}{1-\mu} = \frac{B}{1-\mu_m}\,\frac{1}{c_i} \tag{55}$$

where $\mu = g_\theta/g_o$, and $\mu_m = g_m/g_o$, B is the Langmuir's constant and c_i is the impurity concentration. A plot of $(1-\mu)^{-1}$ versus c_i has been suggested to be a straight line.

2.5.4 The Time-Dependent Adsorption of Impurities

A more general treatment of the impurity effect has been given by Frank[5]. The impurities are assumed to be strongly adsorbed on the crystal surface and are immobile. The adsorption of impurities is regarded as a time-dependent process. This time dependency is the result of a feed back mechanism between the rate of crystal growth and the concentration of impurity on the crystal surface. The faster the growth rate, the shorter the time any given surface is exposed to impurities, because in this case the crystal surfaces will presumably be covered over faster by the layers. At steady state, the rate of growth and the surface concentration of the impurity would be fixed. If, however, the system was perturbed in some way so that the growth rate was suddenly decreased, this would increase the exposure time and increase the surface concentration of the impurity. This would lead to a further decrease in growth rate and the whole cycle would be repeated until equilibrium adsorption of the impurity was built up. This could explain the formation of bunches of many molecular steps observed in the growth of several crystals where the velocity of a step is continuously decreased due to the adsorption of an

impurity. This process continues until steps moving behind the retarded step catch up with the slowed step and eventually a macromolecular step of continuously increasing step size is formed. An increase in impurity concentration in the bulk solution would cause the equilibrium concentration of the impurity on all steps to be reached rapidly and the tendency to form bunches would be eliminated. The above mentioned trend might also occur in the opposite direction, i.e. a random increase in growth rate would decrease the exposure time and decrease the impurity concentration at the surface, leading to a further increase in growth rate. Even if this were not so, the increase in growth rate or supersaturation would raise the impurity concentration required for the bunching of steps and the final stoppage of growth.

2.5.5 The Growth Enhancement Due to an Adsorbed Impurity

Occasionally an impurity has been found to increase the growth rate of crystallising material. Thus Beck[29] observed that the growth rate of (110) face of Adipic Acid crystals was more than doubled in the presence of small quantities of anionic impurities in comparable conditions. At lower supersaturation and higher impurity concentration however, the growth rate was reduced. He suggested that the enhancement of growth was due to the increased rate of step generation caused by the impurity adsorption near the dislocation centre. Such an adsorption has been suggested by Burton, Cabrera and Frank[5] to reduce the edge energy of the step spreading across the crystal surface thereby reducing ρ_c and consequently increasing the dislocation activity or the rate of step generation. At lower

supersaturation and/or higher impurity concentration the retarding action of the impurity on the velocity of steps would become comparatively higher and thus the growth rate of the crystal would reduce. A similar enhancement in growth was also noted for the growth of (100) face of Sodium Triphosphate in the presence of an anionic impurity[73]. In this case the growth rate first increased with impurity concentration and then became independent of it at a supersaturation of 0.60 (figure 3). At a supersaturation of 0.80 the growth rate increased to a maximum and then decreased sharply with increasing concentration of the impurity. Besides these, substances like Glucose, Sulphates and Mangenous sulphates have also been found to increase the growth rate of Sucrose crystals[75] although in this case, the effect of these materials on the solubility of Sucrose was not taken into account. Apart from the above mentioned work, Sears[74] and Khamaskii[76] have also reported similar enhancing effects of impurities.

2.5.6 Conclusions

In general all the mechanism proposed have suggested that to alter the growth rate of a crystal an impurity must adsorb on the surface. The reduction or enhancement in growth rate has been suggested to be either due to a change in the edge energy of a nucleus or that of a step or else due to an alteration of the step velocity. The existence of a critical impurity concentration at which a sharp decrease in growth rate is to be expected has been suggested. This critical impurity concentration is altered by the solution super-saturation.

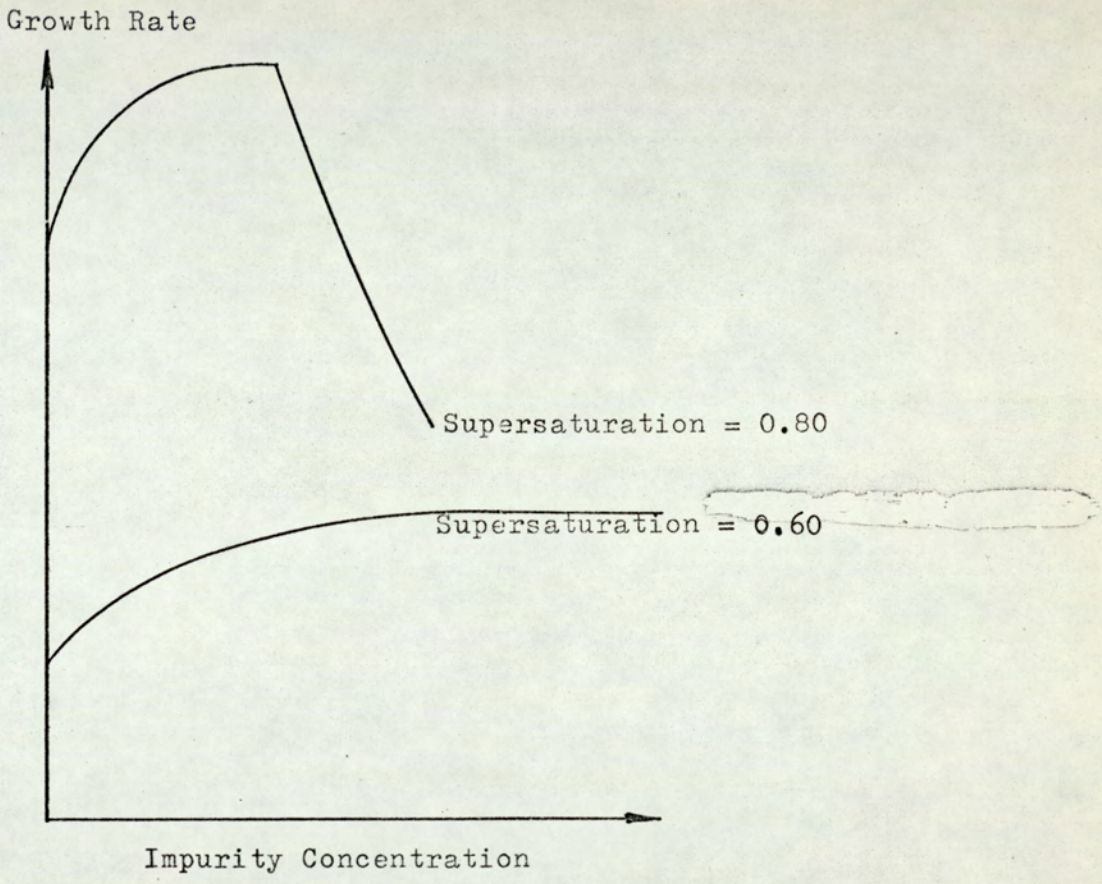

Fig. 3 Growth rate of (100) face of Sodium triphosphate hexahydrate as a function of Dodecylbenzene sulphonate .(Ref 73)

CHAPTER 3

PREVIOUS WORK DONE ON PENTAERYTHRITOL

3.1 Crystal Morphology and Habit

There has been much controversy over the structure of Pentaerythritol crystals in the past, but now it is agreed to be settled as being a 2nd order (hol) tetragonal bipyramid (class 4/mmm)[80]. Figure 4 shows a sketch of a tetragonal bipyramid in the 2nd order (hol) orientation where the Miller indices of the main faces and also of the minor ones, which sometimes appear, are clearly marked. Wyckoff[81] has recorded the values of the unit cell axes as $a_o = 6.083 \pm 0.002^oA$ and $c_o = 8.726 \pm 0.002^oA$ which gives the equivalent axes ratio of $c_o/a_o = 1.4345$. The a-b axes lie in a pronounced cleavage plane. Wyckoff also states that there is a phase change at 179.5^oC above which the unit cell becomes cubic and tetramolecular with $a_o = 8.963^oA$.

Wells[82] states that crystals of Pentaerythritol grown slowly from aqueous solutions are normally tetragonal bipyramids bounded by (101) faces. Rapid cooling of aqueous solutions, however, was found to yield thin square plates with predominant (001) faces. Similar results were obtained when Pentaerythritol was crystallised from β-ethoxyethanol. Frevel[83] also noted similar results during crystallisation from aqueous solutions. Octagonal and hexagonal shaped tabular crystals can be obtained from the Pentaerythritol habit by slicing at suitable angles. Rogers[84] noted the

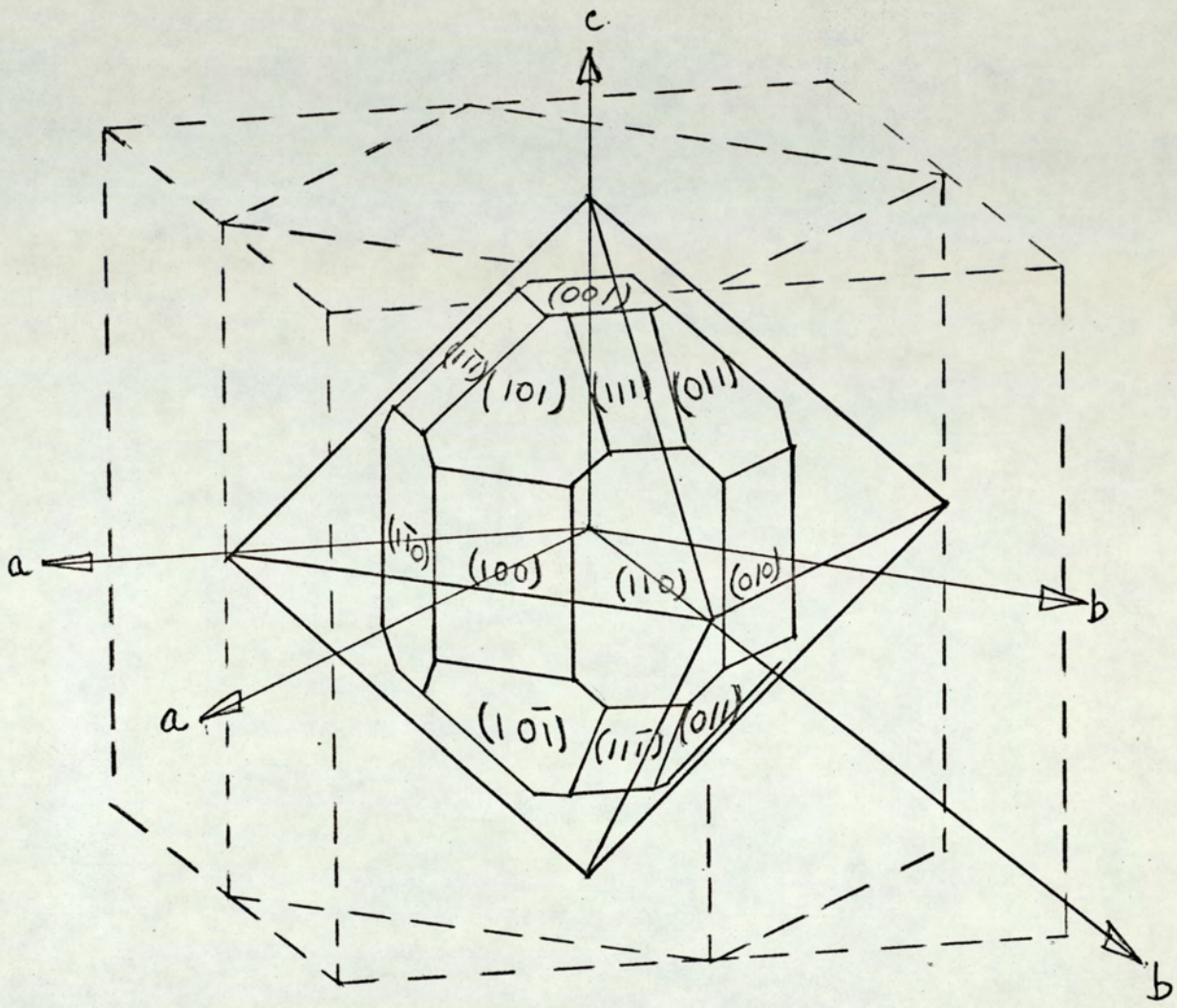

Fig. 4 Pentaerythritol crystal shape and structure
Tetragonal bipyramid (class 4 / mmm)
2 nd order (hol), c_o/a_o = 1.4345
(psudo-cubic) 1st order (hkl), c_o/a_o = 1.0145
$T < 179.5\ ^{0}C$

occasional occurrence of (001) faces when crystals were grown from Pentaerythritol purified from ethers by hydrolysis with hydrochloric acid. Such crystals were transparent and often had a slightly rectangular, as opposed to square, base. Thomas and Evans[85] also obtained two main forms of crystal on the slow evaporation of aqueous solutions of Pentaerythritol; well developed platelets with predominant (001) faces and rather small octahedra bounded by (101) type planes. They state that the molecules are arranged in H-bonded layers parallel to (001) and, whereas the CH_2 group protrudes above the OH at (001) faces, both CH_2 and OH occur in (101) faces in roughly equal amounts. He derived this conclusion from the measurement of the electrical conductivity over the two faces. The law of reticular densities suggest that (111) and (100) faces are very unlikely to appear (Table 1). Thus the crystallographic faces (111) and (100) observed by several authors[86,87] may be due to the numbering based on the 1st order orientation.

3.2 Physical Properties

Berlow et.al.[88] collected together the work published on the properties of Pentaerythritol up to 1958 and no references have been found up to this period which are not reported by them. Pentaerythritol is an odourless, white, crystalline compound which is non hygoscopic, practically non-volatile, and stable in air. The entropy of transition from a tetragonal to cubic structure is 22.8 e.u., its entropy of fusion is 3.2 e.u. The variously reported refractive indices for Na_D light are 1.556 parallel to C-axis and 1.515 perpendicular to C-axis[88]. The refractive index of aqueous Pentaerythritol solutions has also

been determined by Rogers et.al.[89] and the data was correlated by the following equation:

$$n_D = 1.3340 + 1.336 \times 10^{-1} x_1 + 2.406 \times 10^{-2} x_1^2 - 5.670 \times 10^{-5} T - 1.127 \times 10^{-6} T^2 \quad (56)$$

with a standard deviation of $\pm 9 \times 10^{-5}$ refractive index units where x_1 is the concentration of Pentaerythritol (mass fraction) and T is the temperature (^oC). For $x_1 > 0.08$ the above equation simplifies to

$$n_D = 1.3340 + 1.410 \times 10^{-3} x_1 - 5.670 \times 10^{-5} T - 1.127 \times 10^{-6} T^2 \quad (57)$$

with a standard deviation of $\pm 1.70 \times 10^{-5}$.

The variously reported melting points have been recorded by Berlow et.al.[88] as ranging from 256^oC to 265.5^oC. They state that Pentaerythritol exhibits a polymorphic transformation variously reported between 180^oC and 192^oC at which point a morphological change from tetragonal to cubic structure takes place.

Wyler and Warnett[90] report that Pentaerythritol forms a eutectic with 35% di-Pe melting at 190^oC. Rogers[84], however, observed a eutectic formation with 40% di-Pe at 185.5^oC. The discrepancy between the two results could have been due to the presence of 4% formal in the di-Pe source, "Dipentek", in Roger's results.

The theoretical density has been determined by Llewellyn[91] to be 1396 Kg/m^3. Rogers et.al.[89] found that for a given

temperature the density of Pentaerythritol solution had a linear dependence upon composition when measured as mass fraction. Over the temperature range considered the correlation lines between density and composition were reasonably parallel giving the following correlation:

$$H = 1.0024 + 0.2573\ x_1 - 1.3004 \times 10^{-4} T - 3.1692 \times 10^{-6} T^2 \qquad (58)$$

where H is the solution density Kg/m^3 and T, the temperature ^oC.

Pentaerythritol is moderately soluble in cold water and freely soluble in hot water. The solubility data have been reported by Cook[92], Kuznetsova and Gavrilova[86], and Rogers et.al.[89]. The empirical correlation of Rogers et.al. is

$$\log_{10} x_1 = 2.980 - 1242/T \qquad (59)$$

with a standard deviation of ± 2.6%; where x_1 is the concentration of Pentaerythritol (mass fraction) and T is the absolute temperature,K. From the data they determined the heat of the solution to be 6.1 K cal/mol at 30°C and 7.3 K cal/mol at 75°C. The solubility of Pentaerythritol in alcohols and organic solvent is very small[88].

The vapour pressure of Pentaerythritol has been found to range from 2.12×10^{-5} cm.Hg at 106.4°C to 52.4×10^{-5} cm Hg at 135.1°C and there is some discrepancy between the two published correlations [93,94]. The diffusion coefficients of Pentaerythritol in water at 20°C is 0.573 at a normality of 0.4 and 0.589 at a normality of 0.2.

3.3 Chemical Analysis

A number of analytical procedures have appeared in the

literature[88] from time to time, but only a few of them have proved to be sufficiently accurate and convenient for the analysis of Pe. The earlier methods like the acetylation method for hydroxyl groups have long been known to be nonspecific as applied to Pentaerythritol analysis. The low vapour pressure and the high melting point makes direct gas chromatography impossible. Although the volatile derivatives such as acetate esters have been chromatographed, the method is time consuming and not sensitive enough to detect any components with a higher molecular weight. An improved chromatographic method initially suggested by Suchanec[95], has been successfully used by Simons[96]. The method is based on the formation of volatile silane ethers of solid hydroxy-containing compounds (Pe, its homologous and acetals). Paper chromatographic methods have also been developed but they detected mainly the presence of reaction products and did not help in their quantitative estimation.

3.4 Purification of Pentaerythritol

It has been found extremely difficult, if not impossible, to obtain pure Pentaerythritol by recrystallising the commercial product from distilled water. Thus, Kuznetsova and Gavrilova[86] could raise the melting point of the commercial Pentaerythritol only up to 200°C (compared with 260°C reported in the literature) even after 25 successive recrystallisations from water and purification with activated charcoal each time. Impurities, mainly di-Pe and an un-identified compound Formal, have been considered responsible for this difficulty.

Several techniques have been employed to remove these impurities from the commercial Pentaerythritol, the most successful one has been to reflux the aqueous solutions of Pentaerythritol with hydrochloric acid to hydrolyse the poly ethers back to Pentaerythritol and Formaldehyde. A GC analysis of the TMS derivative of the Pe product recrystallised from water showed no impurities to be detectable. However, the presence of trace quantities of an unknown contaminent was still suspected and was considered to be the cause of crystallisation difficulties in Roger's work[84]. It was thought to be some kind of oil or grease from the glands of the processing equipment.

Rogers made several attempts to extract this impurity from the hydrolysed material with Toluene, Benzene, acid washed Kiesulghur, and molecular sieve (13X). Attempts were also made to counteract the impurity with detergents like Nonidet P-40 and Teepol and to nullify the growth inhibition effect with hydrochloric acid. Very little success was achieved by any one of these techniques although some improvement in growth rate occurred after the treatment with the molecular sieve and with AnalaR Benzene, the former being more successful than the latter. After six extractions with molecular sieve the amount of impurity was estimated to drop from 0.26% (2600 ppm) to 0.0329 ppm. The complete removal of the impurity could not be achieved, although the threshold of its effect on crystal growth rate must have been approached since very strange growth rate curves were obtained.

3.5 Crystal Growth Rate

Despite the use of inch size Pentaerythritol crystals as X-ray monochromators for many years very little work has been published on the crystallisation of Pentaerythritol. No quantitative data has been found although the difficulties in growing large crystals have been emphasized[86,87,91].

The growth rate of Pentaerythritol crystals being too low to make use of the single crystal technique, Rogers[84] measured the growth rate by following the change in refractive index of a suspension of stirred crystals over a temperature range of 30 to 75° C. The growth rates were calculated by assuming McCabe's Δ law to be applicable to Pentaerythritol crystals. The growth rates were also determined by the measurement of crystal mass increase in fluidized beds but these were very difficult to control.

The results obtained from the fluidized bed were in agreement with those obtained from stirred cells but were several orders of magnitude lower than those calculated for mass transfer control from Nielson's correlation[80]. The growth mechanism was suggested to be surface integration controlled. The growth rates were found to range from about 10^{-8} cm/min to 10^{-3} cm/min and were correlated with supersaturation by the equation:

$$g = k X^{b} \qquad (60)$$

where k is a constant.

The value of b varied with the amount of impurity and temperature, but was found to have an average value of ca.2. The activation

energy of the commercial material (containing mainly di-Pe and Formal) was found to be 21.6 Kcal/mol.[80]. A detailed analysis of Rogers' results is not justified as it is apparent that on many occasions nucleation occurred in the system.

Using the various techniques developed in the present work, Bankier[97] attempted the direct measurement of crystal growth rates by microscopic observation of crystals nucleated epitaxially on a tin substrate. He found growth rates to be ca.4 x 10^{-4} cm/min at a Δc of 1.00 x 10^{-2} (Kg Pe/Kg Solution) and a temperature of $30^{o}C$. However, some doubt exists as to which face the growth rate data referred.

CHAPTER 4

PREPARATION AND PURIFICATION OF Pentaerythritol

4.1 Introduction

Rogers[84] suggested that the unknown impurity (X) was probably oil or grease rather than a by-product of Pe formation reactions. The impurity was resistent to HCL purification process which breaks down the other main by-product impurities. Owing to the difficulty in extracting (X) an attempt was made to prepare Pe from purified reagents and thus eliminate (X) at source.

4.2 Preparation

Considerable time and effort was put into an attempt to prepare Pe in 0.5 Kg batches. Unfortunately all these attempts ended in failure. This suggested that the synthesis reactions of Pe from formaldehyde and acetaldehyde in the presence of an alkali are not as simple and straightforward as described in the literature. It also explained the necessity of such a wide publication on this aspect of Pe chemistry and the disagreement between individual publications. In particular it appears that Pe product reacts with the excess formaldehyde to form a syrup which does not easily break down. Since the preparation of Pe did not form the main aim of this project, it was decided after a period of 5 months to postpone this work for someone else to use as a separate project. Wacks[98] later investigated the reaction mechanism in greater detail. At

present, the work is still being continued as a separate project to be tackled in its own right.

4.3 Purification

Effort was therefore directed to the extraction of (X) from Pe by using molecular sieves as suggested by Rogers. The requirement of large quantities of Pe necessitated the use of a continuously operated column. The 2m long column was operated at room temperature to obtain improved adsorption (Rogers' technique employed batch process at 40°C) and the undersaturated solution was passed through the column at a flow rate of 4 cm^3/min. The product solution was found to contain suspension of turbid particles which passed through even 0.45 μm filter. Even the use of different batches and different grades of molecular sieve did not prevent the appearance of turbidity in product solutions. The initial washing of the sieve with distilled water also failed in overcoming the problem. Astonishingly the column operation at 40°C gave a clear solution. However, no improvement in crystal growth rate was obtained from the product Pe which therefore implied that presumably (X) had not been reduced below its threshold.

The purification of Pe by Ozone treatment and acid hydrolysis suggest that the sequence of the procedure used is very important[99]. Therefore, although Kuznetsova and Gavrilova[86] found little improvement in the crystal quality of Pe even after 25 extractions with charcoal, this might have been due to the charcoal becoming preferentially saturated with di-Pe. and Formal and leaving (X) in solution. It was therefore decided to perform a charcoal

purification after acid hydrolysis.

The results were spectacular. Although at first there were fresh problems associated with secondary nucleation, there was a very large improvement in growth rate. Several types of charcoal were tried and repeated extractions and crystal growth tests were then performed to obtain the most suitable working conditions. The standard procedure adopted to obtain the bulk of results has been described in section (4.3.2).

It was tentatively assumed that the improvement in growth rate was due to the removal of (X) by the charcoal and not by the addition of a counteracting impurity from charcoal. This point was checked by back extracting charcoal used to remove the impurity and using the washings to make solutions for single crystal growth tests. The growth rate in these tests was considerably reduced (exp.32-35, tables 2 and 3). The nature of this impurity is considered later.

4.3.1 Hydrolysis Procedure

Sufficient commercial Pe was dissolved in 10% (w/v) HCL to form a saturated solution at its boiling point. The solution was refluxed for 1 hour, cooled to about $0^{o}C$, filtered and washed with ice cold water. The procedure was repeated and the resulting Pe recrystallised twice from distilled water. The product was then washed with successive quantities of ice cold water and dried in an oven at about 90 to $100^{o}C$ for 2 - 3 days. A GC analysis of the dried material indicated the presence of not more than 0.05% di-Pe and the same of Formal.

4.3.2 Extraction Procedure

10% (mass fraction) of hydrolysed Pe was stirred with 1% (mass fraction) of activated charcoal (Norit SX1) at 40°C for 2 hours. The contents were filtered hot (T ≃ 70 - 80°C) through 100 μm filter paper. The procedure was repeated twice with the clear filtrate so obtained. After the third extraction, the filtrate from 100 μm filter was passed through 14 μm and 0.1μm membrane filters to remove the charcoal particles above 0.1 μm. The product crystals obtained from the evaporation of the final filtrate were recrystallised from distilled water at room temperature, washed with ice cold water and dried in an oven for 2 - 3 days at ≃ 90 - 100°C.

No attempt was made to extract (X) in a continuous column of charcoal due to the anticipated difficulties of maintaining a constant temperature, shorter residence time, and the pressure requirement to cause the flow of solution through the column.

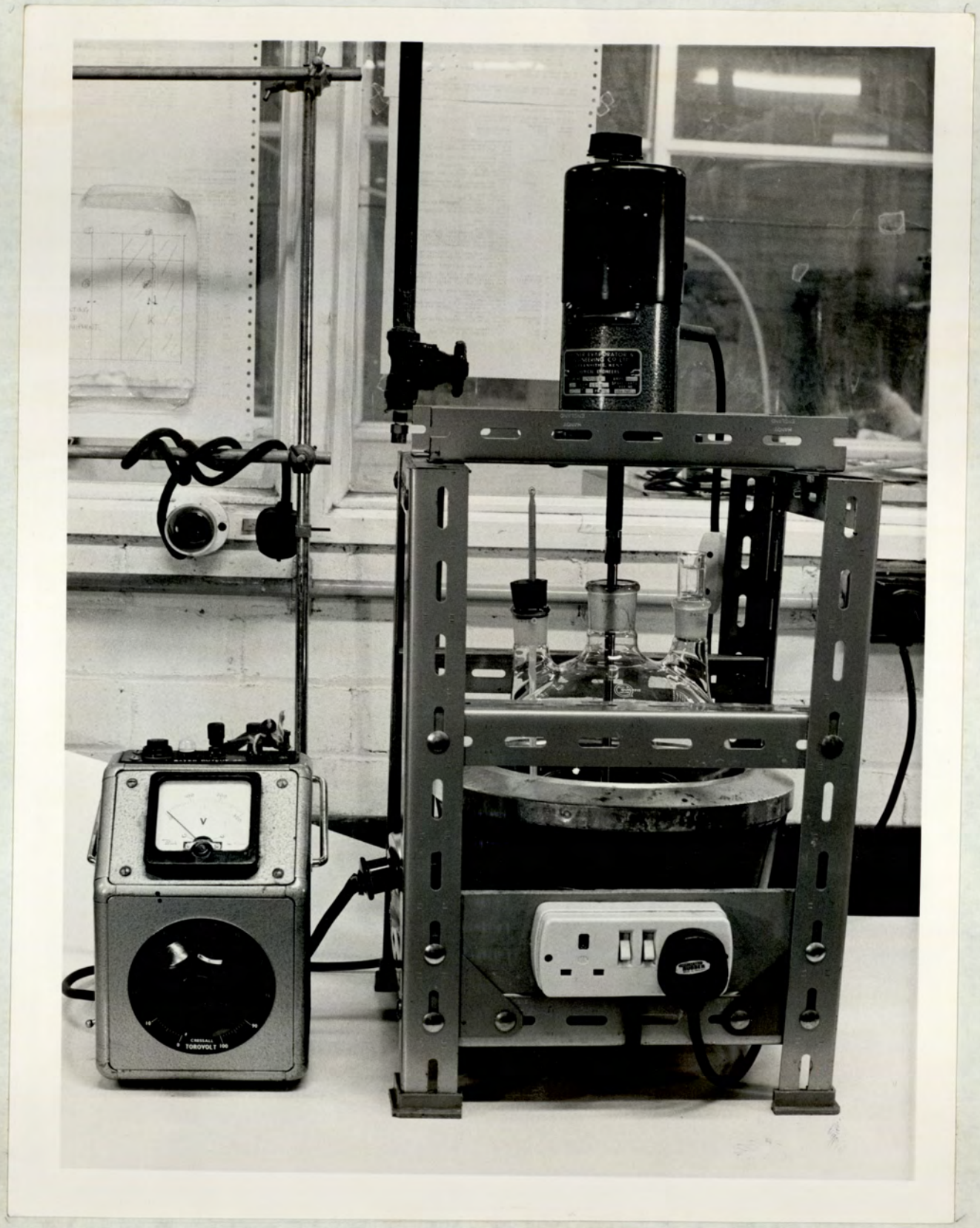

Fig. 5 Extraction Flask

CHAPTER 5

CRYSTAL GROWTH APPARATUS AND MATERIALS

5.1 Materials

a) Distilled water: Preliminary tests showed that there was no advantage in using de-ionized water and therefore freshly prepared distilled water was used throughout the work.

b) Charcoal: Two different grades of charcoal were used. The preliminary experiments were conducted with the type "Norit NK" which was very carefully washed with hydrochloric acid. However, repeated observation of oscillating growth rate (variation of growth rates with time under constant external conditions) necessitated the use of the purer grade "Norit SX1". No acid washing was required for this grade because of its high purity (Fe < 0.01% and Ca < 0.05%). All the reported crystal growth measurements in this work involved the use of the type "Norit SX1".

c) Pentaerythritol (Pe): Different batches of Pe were available and the one labelled by Rogers as "Batch D" was used in this work since it probably contained least (X). It was purified by hydrolysis, extraction, and recrystallisation as explained in section (4.3). A GC analysis of the purified material showed the presence of not more than 0.05% of di-Pe and the same of Formal. More than one half of the Pe was discarded in the purification process.

d) di-Pentaerythritol (di-Pe): di-Pe used in this investigation was obtained from the Hercules Powder Corp. as "Dipentek". Besides the possible presence of (X), it was found to contain about 4% of the

by-product Formal. The concentration of the Formal and that of (X) was reduced below the threshold limit by the same extraction technique as used for the extraction of (X) from hydrolysed Pe (section 4.3.2) and using the same charcoal/solids ratio.

e) Formal: Formal was not available as an isolated compound. Thus, batch G Pentaerythritol (containing < 0.01% di-Pe and about 5.20% Formal) was used for introducing formal as an impurity in the growth of crystals from pure Pe solutions. (X) was removed by the extraction of batch D with charcoal as previously described. This extraction technique also reduced the concentration of the formal from 5.2% to 2.69% (w/w) in the product.

f) Miscellaneous Impurities:

Impurity	Grade and Form	
NaCL	AnalaR	Crystalline
NaOH	AnalaR	Aqueous solutions
	AnalaR	Pellets
Non-idet P-40		
(Polysacharide		Flakes
(Sulphate		
White Spirit	S.L.R.	Aqueous solution
$Ca(OH)_2$	G.P.R.	Crystalline
Formaldehyde	G.P.R.	Aqueous solution
Methanol	AnalaR	Aqueous solution
H_2O_2		Aqueous solution
Silcolapse 437		Emulsion
" 5000		Emulsion

Impurity	Grade and Form
Oil	Low viscosity lubricating oil
"	High viscosity lubricating oil
" W.T.I.	Thermostat oil
Topanol O	Crystalline
D-Erythrose	Liquid
1,1,1 Trimethylolethane	Crystalline
Meso-Erythritol	Crystalline

5.2 Crystal Growth Apparatus

Four different cells were tried in order to overcome the risk of contamination from materials of construction, problems of secondary nucleation, and to confirm the existence of oscillating growth rates. The bulk of the experimental work was carried out in cells referred to as G_1 and S_2. The details of these two cells are as follows:

1. Glass Cell G_1 (Figure 6)

The cell was constructed of pyrex glass tube (C) and was surrounded with a glass water jacket (W). Pyrex glass optical flats were cemented to each end of the cell using Araldite resin AY 105 and HY 951 hardner. A 60 watt bulb was positioned as a source of light at O_1 and a coordinate microscope at O_2. The water was circulated through the jacket from a Townson and Mercer T.U.3 thermostat circulating unit controlled by a contact thermometer regulating the temperature to $\pm$ 0.03^{o}C. The carefully calibrated thermometer (T) and the crystal support (G) were held in position in the cell through

a rubber bung (B). Extreme care was taken to mount the cell assembly on as rigid a frame as possible to prevent any mechanical vibrations affecting the relative position of the crystal seed and the microscope. The cell capacity was 75 cm^3.

2. Metal Cell S_2 (Figure 7)

This cell was made of stainless steel (Type 316) and was in fact the body of a standard Bellingham and Stanley in-line sugar refractometer. The glass/metal seals were made with neoprene O-rings. The discharge end (E) was blocked with a stainless steel plug and neoprene O-ring seal during an experiment. The crystal supporting rod (G) was inserted through a rubber bung and rested on the steel plug. This helped in eliminating the continuous movement of the rod due to extraneous vibrations. The temperature control and measurement were as for the cell G_1. Before installation the cell was thoroughly polished with London Emery Flour. As for the cell G_1, great care was also taken for the cell S_2 to provide it with a rigid base. The other features of the cell are essentially the same as those for the cell G_1. The cell capacity was 275 cm^3.

3. Other Cells

Glass cell G_2 was similar to G_1 except that the light path was 25 mm longer and the cell protruded from the jacket so that an all fused construction was possible and the risk of contamination of the solution from the cement avoided. The cell was also of slightly larger diameter and had a capacity of 200 cm^3.

The original stainless steel cell S_1 made from 50 mm stainless

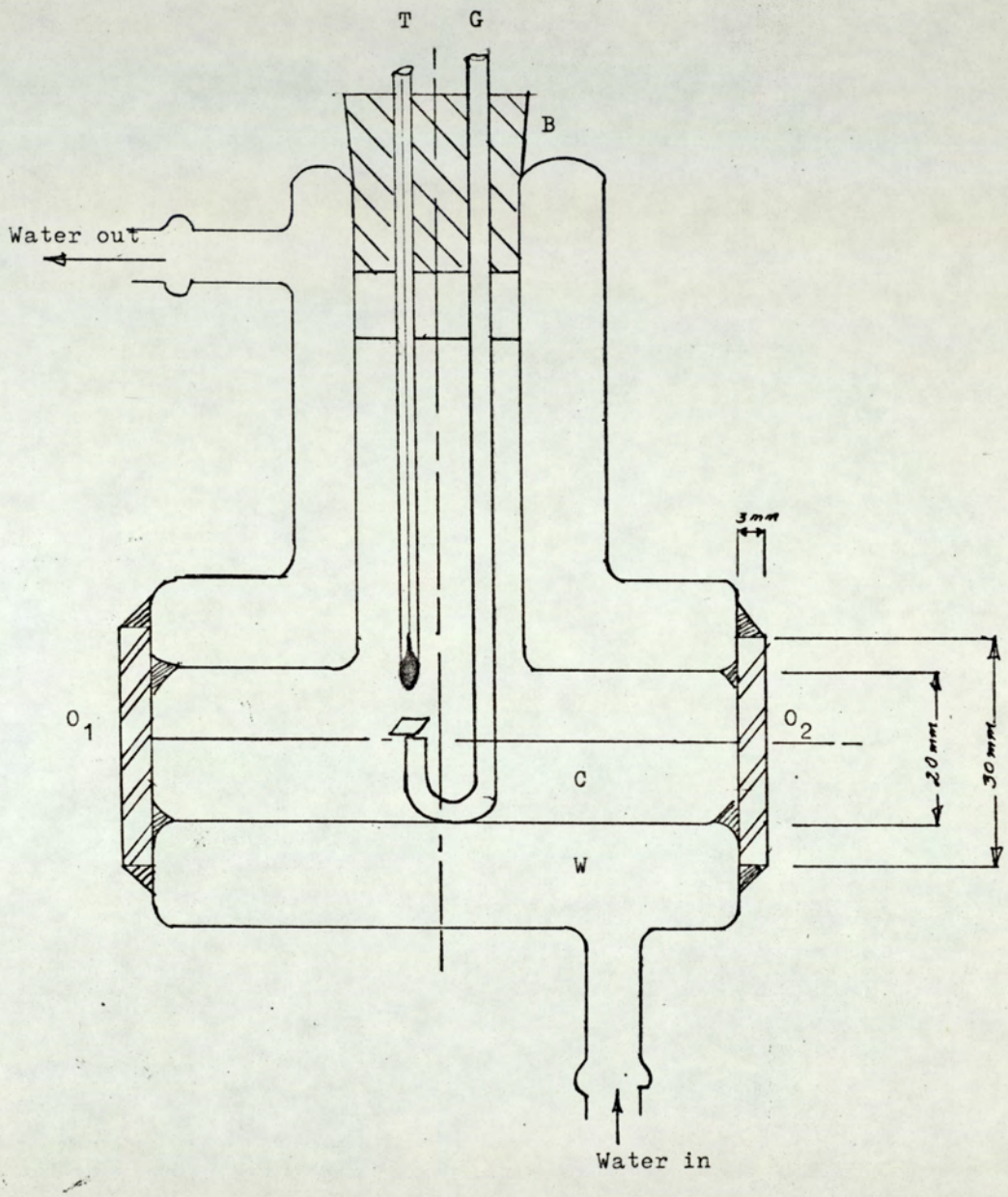

Fig. 6 Crystal Growth Cell G_1

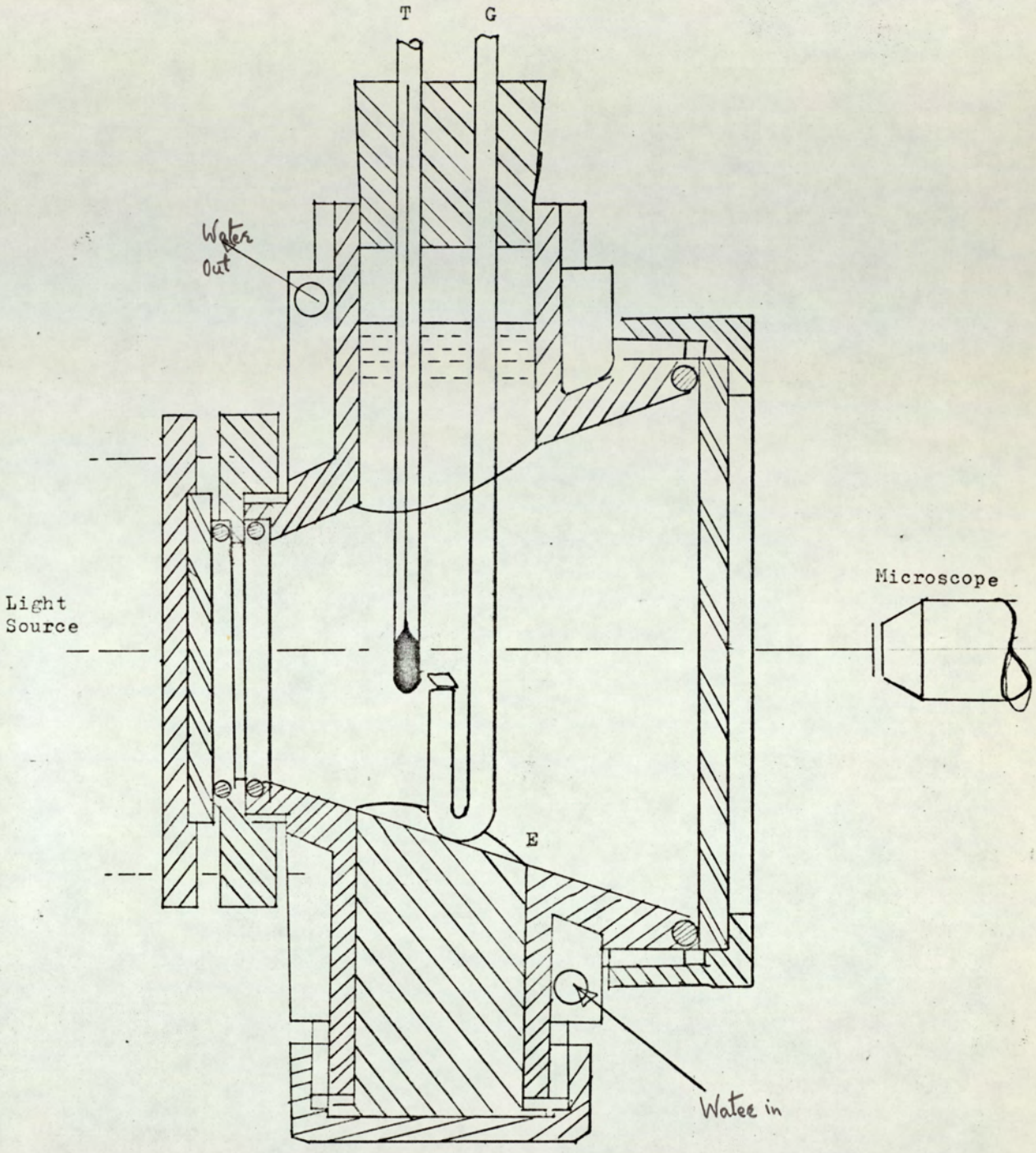

Fig. 7 Crystal Growth Cell S_2

tube and tin jacketed, created many nucleation problems and was therefore dispensed with at an early stage.

5.3 Preparation of Solutions

Several techniques were tried to achieve the preparation of solutions on volume basis (gPe/cm^3 solution). The non-availability of the densities of Pe solutions at that time and the essential requirement of the hot filtration of solutions through 0.1 micron filters necessitated the preparation of solutions on a weight basis (gPe/100g solution). However, checks were made to obtain the necessary correction factors for weighing hot solutions. The techniques used throughout the experimental work are described as follows:

5.3.1 Pure Solutions

The required quantity of hydrolysed and extracted Pe (determined by the desired supersaturation) was weighed in a 500 cm^3 beaker. 75% of the required amount of distilled water was poured into the beaker, the contents were covered with a watch glass and heated to dissolve the Pe and to remove the absorbed CO_2. The solution was then filtered at about 80°C through a heated millipore filtration assembly using a 0.1 micron membrane filter. The beaker was washed with 10 cm^3 of hot distilled water (at about 80°C) and the washings were also transferred to the filtration assembly. The filtrate was collected in the receiving flask and weighed. As it was at a much higher concentration than the desired one a necessary amount of hot distilled water was added to adjust the concentration. The

flask was then covered with a rubber bung and vigorously stirred for 2 to 3 minutes. The resulting well-mixed filtered solution was poured into the growth cell.

5.3.2 Solutions with added Impurities

The technique for preparing solutions with controlled amount of added impurities depended upon the nature of the impurity and can be summarised as follows:

a) Solid Impurity: In this case the required amount of impurity was added to the weighed pure Pe in the 500 cm^3 beaker. The rest of the procedure adopted was the same as for preparing pure Pe solutions.

b) Miscible Liquid Impurity: With substances like formaldehyde and hydrochloric acid a solution of pure Pe was first prepared and filtered through a 0.1 micron membrane filter. The required amount of the impurity was then added to the filtered solution and the necessary weight adjustment made to obtain a solution of required concentration.

c) Immiscible Liquid Impurity: With materials like Silcolapse and various oils an essential requirement of a successful experiment was the dispersion of these impurities in the pure Pe solution. A dilute aqueous solution (concentration in ppm) of the impurity was first prepared in a 10,000 cm^3 aspirator and was stirred at high speed (14000 rpm) for several hours. A cetain amount of this fine suspension was pippetted into the filtered hot solution of pure Pe. The necessary weight adjustments were made and the hot suspension was poured into the cell.

Checks were made on the effectiveness of the dispersion of these impurities in solutions of Pe left unstirred for a period of up to four hours. A Spekker Absorptiometer was used to compare the opacity of Pe solutions at a known concentration and containing a certain amount of an impurity with that of pure Pe solution at the same concentration and temperature. The opacity did not appear to change in unstirred solutions up to a period of four hours thereby indicating that the suspension was stable. It was also assumed that the adsorption of the impurity on the walls of the cells was negligible.

5.4 Cleaning Procedure

All glassware was cleaned before use, first in warm KOH-ethanol solutions to remove any trace of grease, next in warm chromic acid cleaning solution and finally thoroughly rinsed with distilled water. The only metal used was stainless steel in cell S_2. This was washed first with warm KOH-ethanol solution and then with distilled water.

5.5 Preparation of Seed Crystals

The various techniques tried to grow seed crystals with the least possible defects have been discussed in the section (10.1.2). The best quality crystals were obtained from the slow evaporation of stagnant aqueous solutions and were found to depend greatly upon the supersaturation attained at the time of nucleation. The required supersaturation was reached in the following way:

A solution of weighed quantity of hydrolysed and extracted Pe was first prepared with distilled water in a 500 cm^3 beaker under

boiling conditions. The necessary amount of hot distilled water was then added to the solution at the same temperature as that of the solution to obtain the required weight of solution. The beaker was then covered with a watch glass and cooled over a period of 4 to 5 hours on a hot plate to the room temperature. The beaker was then transferred to a wooden working table and the solution was allowed to evaporate for a few days at room temperature ranging from $10^{o}C$ to $15^{o}C$. The amount of evaporation of the solution was less than 5 cm^3/day. Nucleation began at least 24 hours after the room temperature was reached. The concentration difference at the stage of nucleation was estimated to be between 2.00 and 2.50×10^{-2} (KgPe/Kg solution). No seed crystals were added to the solution. Nucleation always commenced at the surface of the solution and these nuclei grew at a low rate (about 10^{-5} cm/min) yielding transparent crystals of nearly uniform size of ca. 2mm. These crystals were found to contain the crystallographic faces (110) and (001) apart from the face (101) usually reported in the literature. They were also found to contain physical imperfections exposed on air/crystal face (110). Some of these crystals fell from the surface due to gravity or due to a mechanical shock and nucleated more crystals at the bottom of the beaker. Once this happened, their growth was greater and exaggerated in different directions and they were found to be much less transparent than those which grew at the surface of the solution. The carefully selected seeds were taken from the surface of the solution and immersed in distilled water for a few seconds to remove any small crystallite which might have grown on their surface. They were then carefully stored.

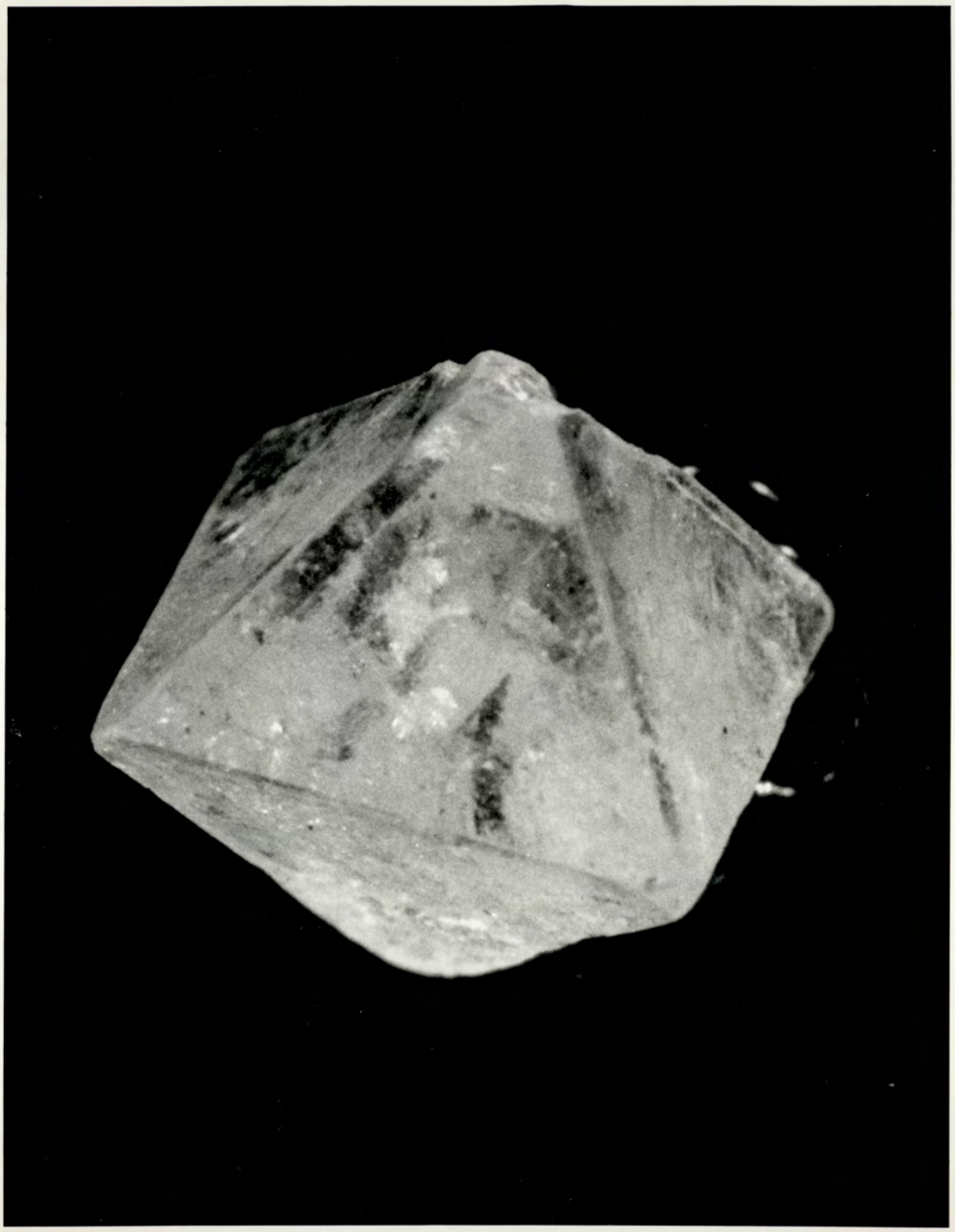

Fig. 8a CRYSTAL GROWN FROM IMPURE SOLUTIONS

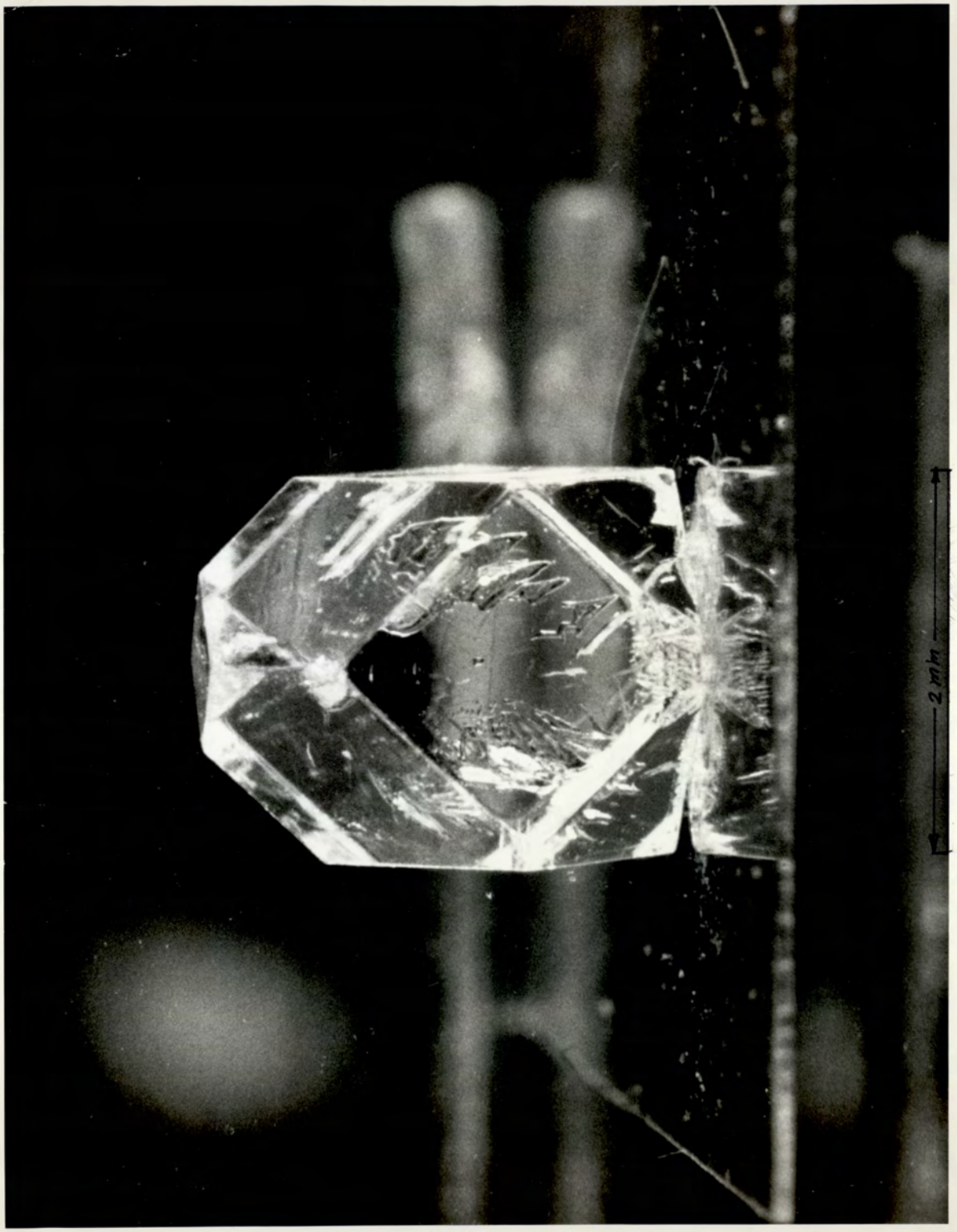

Fig. 8b Crystal Grown from Pure Solutions

5.6 Mounting of Seed Crystals

Various techniques have been tried for mounting the crystal seeds and are discussed in section (10.1.3). The following technique was found to be most successful and finally adopted throughout the experimental work.

A carefully selected seed crystal was washed in distilled water at room temperature for 15 - 20 s. The crystal was then mounted on one end of the glass rod with Durofix cement such that one of the (101) faces was as horizontal as possible. The crystal was kept in this position for 10 - 15 minutes while the cement set. It was then washed for 15 seconds in a beaker containing distilled water at a temperature of 5 - 10^{o}C higher than the working temperature of the cell. The seed was then quickly inserted into the solution in the cell and the glass rod slightly rotated in the solution to remove the film of distilled water which might have formed during washing.

5.7 Microscopy

Each of the crystal growth cells used in this work was fitted with optically flat glass discs to avoid errors in the growth measurement due to distortion.

For the cell G_1 a Griffin Co-ordinate microscope was used. The microscope was fitted with a standard x 10 RMS focussing Ramsden eyepiece and a x 3 achromatic objective giving a magnification of x 30. The eyepiece was fitted with a graticule (E18, obtained from Graticules Ltd., London) having 5 mm horizontal and vertical scales divided into 100 parts of 50 microns each.

For the cell S_2 a Griffin "Intermediate" Cathetometer was used having a microscope fitted with a standard x 7 RMS focussing Ramsden eyepiece and a x 3 achromatic objective giving a magnification of x 21. The eye-piece was fitted with a graticule (E17 obtained from Graticules Ltd.) having 10 mm combined horizontal and vertical scales divided into 100 parts of 100 microns each.

The calibration of the eye piece graticules E 17 and E 18 was carried out against a stage micrometer. The actual conditions of an experiment were simulated by inserting the stage micrometer at three different positions, within a range of 15 mm, in the two cells, filled with distilled water. The following calibration factors were obtained:

1 scale division on graticule E17 = 0.00384 cm

" " " " " E18 = 0.00238 cm

5.8 Determination of Representative Growth Rates

It was noted that at any particular condition of temperature and supersaturation, the linear growth rates fluctuated with time. The maximum growth rate during an experiment was found to be as high as 7 times the minimum value. The growth rates also differed from one seed to another under apparently similar conditions. Although for large growth rates (at high supersaturations and temperature) this difference became less noticeable, it was still too large for the growth rate values of an experiment to be averaged directly. However, at all working conditions, the amplitude of oscillation of the growth rate vs. time curve was observed to decrease gradually

to a certain minimum value of the oscillation. A constant growth rate could still not be obtained despite its almost constant supersaturation (Figures 10 - 12). This problem not only imposed the difficulties in deciding the representative growth rate of an experiment but it also prolonged its duration by a factor of ten in order to obtain the least possible oscillation of growth rate versus time curves.

However, four different values were selected in each experiment to represent the growth rate of the seed crystal used in that experiment. These different growth rates for each experiment are:

1. The highest growth rate, g(max).
2. The lowest growth rate, g(min).
3. The average of the growth rates under conditions of smallest possible fluctuations in growth rate versus time curve, g(avg 1).
4. The average of the whole experiment, g(avg 2).

These values of growth rate during an experiment are well described in figures 10 - 12.

5.9 Experimental Procedure

The following standard procedure was used throughout the experimental work.

1. The crystal growth cell was completely dismantled (feasible only for S_2) and thoroughly washed first under running tap water and then rinsed with distilled water for 5 - 10 minutes to dissolve any nuclei that might have been left over from the previous experiment.

2. The cell was reassembled, filled with distilled water, and was heated to a temperature at least $10^{o}C$ above the desired working temperature by pumping hot water through the cell jacket from the Townson and Mercer T.U.3 thermostat circulating unit. The difference between the desired working temperature of the solution and the set point on the thermostat contact thermometer depended upon various factors and were found by trial and error.

3. The required amount of Pe solution at known concentration was prepared by the technique described in section (5.3.1). The filtered hot solution was vigorously stirred in the buchner flask to achieve complete mixing of the contents and the solution was poured into the cell. The temperature of the solution in the cell was then gradually lowered to the working temperature by altering the set point on the contact thermometer and passing cold tap water through the cooling coil of the thermostat circulator.

4. A carefully selected seed crystal (prepared by the technique discussed in section (5.5)) was mounted on a glass rod by the technique described in section (5.6) and inserted into the cell. Adjustment of the crystal support rod was then made so that the mechanical vibrations in the rod could be minimized.

5. The previously levelled microscope was quickly focussed so that the inverted image of the crystal seed was superimposed on the eye-piece graticule. The microscope was then adjusted so that a certain figure on the graticule (usually 3.0) coincided with the (101) face of Pe crystal seed to be measured.

6. The stop clock was started immediately.

7. The time required for the growth of (101) face to traverse each graticule division was recorded. Readings were continued

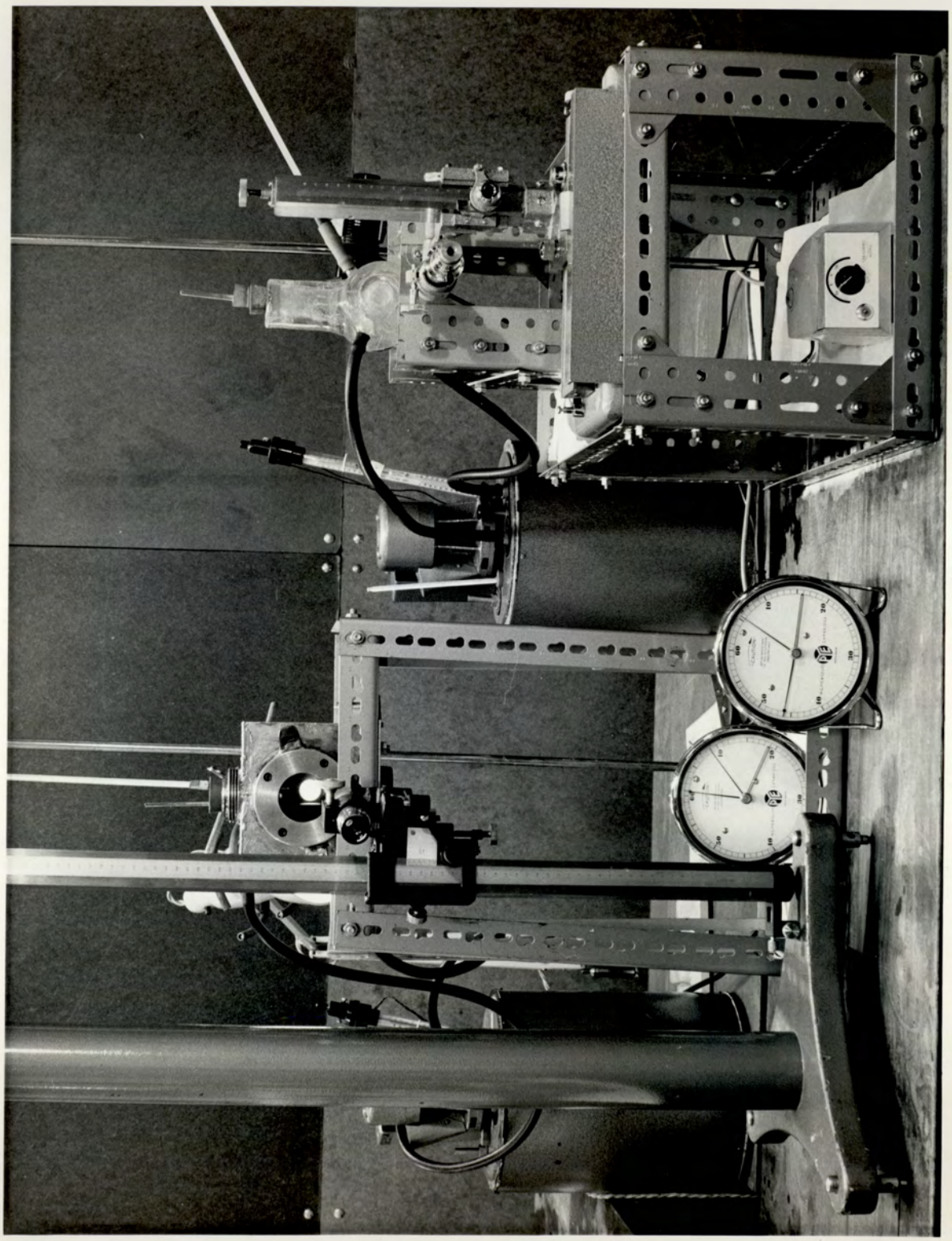

Fig 9 Crystal Growth Apparatus

until the difference between successive time intervals appeared to be a minimum (i.e. growth rate versus t curves had the minimum possible oscillations). In roughly half of the experiments this condition could not be achieved due to significant secondary nucleation and the tests were discarded and repeated.

8. The seed crystal was then withdrawn from the cell at the end of an experiment and the cell assembly was thoroughly washed with tap water and distilled water. If the seed crystal was required to be re-used or stored for sampling, it was first immersed in warm distilled water and later in acetone for 2 - 3 s, dried on a filter paper and stored in glass sampling bottles.

5.10 Analytical Technique

The analysis of Pe was carried out by the gas-chromatographic technique currently investigated by Simons[96] which was a modification of that originally proposed by Suchanec[95]. In the present work it was only used as a service.

The method consists of the formation of volatile silane ethers of solid hydroxyl containing compounds (Pe, its homologous and acetals) by reacting dried Pe with a mixture of hexamethyldisilazane and trichlorosilane in pyridine solution. The ethers of the form

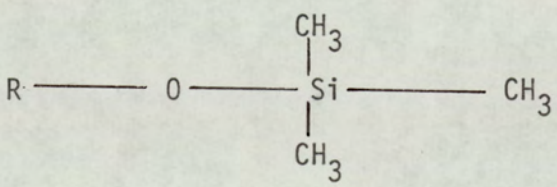

are formed very readily, with some heating, whilst the precipitated NH_4Cl does not interfere with the subsequent analysis.

The trimethylsilyle derivatives are very suitable for gas-chromatographic analysis in the temperature range of 150 - 350°C and give a very good resolution of peaks. A Pye series 104, Model 24 gas-chromatograph was used. The instrument was equipped with temperature programming, a flame ionization detector and a Kent, Mark 3, recorder. A 150 mm analytical column was constructed from 4 mm o.d. stainless steel (type 316). The column was packed with 10 wt % SE-30 on 100 - 120 mesh siliconized celite. A detection limit of 0.05% (w/w) of the impurities di-Pe and Formal was possible.

5.11 Epitaxial Growth Technique

It had originally been intended to measure growth rates in a flow type cell in which a crystal had been nucleated and grown on a substrate in order to avoid the difficulties anticipated in mounting individual crystals. A search through the periodic table suggested that only tin had crystal lattice dimensions near that of Pe, the lattice mismatch being ca.4%. It has been claimed by Van der Merwe[100] that such epitaxial growth may occur provided that the lattice mismatch does not exceed 10%.

Test tube scale experiments on a number of metal wires showed that tin was the only satisfactory metal substrate. Other materials such as mica and PTFE were not successful but the results were not necessarily consistent. For instance, it was found that although the thermometer bulb did not normally create nuclei, one in particular could not be used due to the prolific nucleation it caused. This method of studying growth rate was later pursued by Bankier[97].

based on techniques developed in the present work. Since the preliminary tests indicated that growth rates with hydrolysed and extracted Pe were not high enough to bring the system into the diffusion controlled regime, the flow cell was abandoned.

CHAPTER 6

RESULTS

6.1 Introduction

The results obtained from the crystal growth studies have been divided into two main sections:

1. The preliminary results which were obtained mainly from experiments performed under identical working conditions to develop the apparatus and experimental procedure, and
2. The main results which were obtained from the growth of Pe crystals in pure Pe solutions (i.e. solutions free from di-Pe, Formal and (X)) and in solutions containing controlled amounts of known impurities.

The preliminary experiments enabled an assessment to be made of the degree of success attained in the removal of the impurity (X) from the hydrolysed Pe, and helped to ensure that none of the foreign materials used in the main experiments had any effect on the growth of the crystals. The results obtained from these experiments are presented in Tables 2 and 3. The seed crystals were prepared from the slow vaporization of the stagnant aqueous solutions of Pe. Initially the hydrolysed Pe solutions were used for the seed preparation. However, after the successful extraction of the impurity (X) with activated charcoal, the crystal seeds were prepared from the hydrolysed and extracted solutions.

Using the apparatus and procedure developed in the preliminary

experiments growth rates were measured as a function of temperature, concentration difference, impurity concentration, and nature. The results obtained have been presented in several sections according to the presence or the absence of an impurity, or according to the significance of its effect on growth. The results have been presented in tabular and graphical form. The qualitative growth observations have also been discussed in individual sections.

6.2 Experimental Legend

D	Commercial batch D
DH	Hydrolysed batch D
DHE	Hydrolysed and extracted batch D
DHE (13X) C_1	Batch D hydrolysed, and extracted with molecular sieve type (13X); the extraction carried out once in the column
DHE (5A) C_3	Batch D hydrolysed, and extracted with molecular sieve type (5A); the extraction carried out three times in the continuous column
DHE (13X) B_6	Batch D, hydrolysed, and extracted with molecular sieve type (13X); the extraction carried out six times in the batch vessel
DHE (13X) B_3	Batch D, hydrolysed, and extracted with molecular sieve type (13X); the extraction carried out three times in the batch vessel
DHE (NK) B_1	Batch D, hydrolysed, and extracted with activated charcoal type (Norit NK); the extraction carried out once in the batch vessel

DHE (SX1) B_1 Batch D, hydrolysed, and extracted with activated charcoal type (Norit SX1); the extraction carried out once in the batch vessel.

DHE (SX1) B_6 Batch D, hydrolysed, and extracted with activated charcoal type (Norit SX1); the extraction carried out six times in the batch vessel.

DHE (SX1) B_3 Batch D, hydrolysed, and extracted with activated charcoal type (Norit SX1); the extraction carried out three times in the batch vessel.

6.3 The Preliminary Experiments (Results & Discussion) Table 2 and 3

6.3.1 Commercial batch D (Experiments 1, 2)

The growth of crystals in solution prepared from the commercial batch D was too slow to yield any reliable information. The seed crystal in experiment 1 grew at an estimated rate in the order of 10^{-6} cm/min for the first five hours. It then dissolved for about two hours. The growth then recommenced at a decreasing rate such that it was found to be decreasing even at the termination of the experiment. Because of this only the maximum growth rate value (7.99×10^{-6} cm/min) has been reported in the table 2 and was obtained when the growth recommenced after dissolution.

The dissolution of the seed in the experiment 2 occurred immediately and lasted for 3½ hours. The seed then began to grow and the maximum growth rate (3.25×10^{-6} cm/min) was obtained. The rate then decreased with time.

No change in the habit of the crystal was noted in either of the two experiments and no secondary nucleation was observed. The large difference between the two maximum growth rates and the variation of growth rate with time during each experiment was attributed to the presence of impurities. The seed crystals used in these experiments were also highly imperfect compared with those used in the later experiments.

6.3.2 Hydrolysed batch D (Experiments 3-5)

Experiments 3-5 conducted on this material gave growth characteristics identical to those obtained in experiments 1 and 2. The value of the maximum growth rates, however, was at least one order of magnitude higher. The continuously decreasing growth rates were attributed to the presence of the suspected impurity (X) in the Pe solutions. The increase in the maximum growth rates appeared to be due to the absence of the impurities di-Pe and Formal.

6.3.3. Hydrolysed and Extracted Material

6.3.3.1 Molecular Sieve Extracted (Experiments 6-15)

Experiments 6 and 7 were conducted on the Pe solution extracted once with molecular sieve (type 13X) in the continuous column after hydrolysis. Surprisingly the growth rates obtained were of the same order of magnitude as those of experiments 3-5 and were found to decrease continuously with time. Experiments 8-10 were carried out on the material extracted twice and three times with molecular sieve in the continuous column. The growth rates still continued to decrease in these experiments and the maximum growth rates obtained in the earlier periods of growth had the same order of

magnitude as those obtained in experiments 3-5. This created the suspicion that either the impurity (X) was still present in the Pe solutions or that perhaps another growth inhibiting impurity was picked up during the handling of the solutions. Experiment 11 was then conducted on the material extracted batchwise with molecular sieve (Rogers' technique). No improvement in growth rates was obtained. Experiment 12 was performed on the six times batchwise extracted material without any significant change in growth pattern. Since these results contradicted those obtained by Rogers, experiments 13-15 were carried out at higher supersaturation on the material extracted with different grades of molecular sieve. The growth rates still continuously decreased with time in each of these experiments and the maximum values obtained were of the same order of magnitude as those of experiments 3-5. All the other features were also similar. Thus no secondary nuclei were observed up to a measured duration of 48 h in either of these experiments. Therefore, experiments 6-15 suggested that molecular sieve do not extract a sufficient amount of the impurity (X) to increase the growth rate of Pe solutions.

6.3.3.2 Charcoal Extracted (Experiments 16-25)

Experiments 16 and 17 were conducted on Pe solutions which were hydrolysed and were extracted with activated charcoal (type Norit NK). A remarkable increase in growth rate of up to two orders of magnitude was obtained. The growth rate now appeared to increase and decrease at random with time instead of continuously decreasing as in experiments 1-15. The duration of the experiments was now limited by the onset of prolific secondary nucleation. In order to obtain a representative growth rate it was necessary to

perform an experiment for a reasonable length of time without secondary nucleation. Techniques for crystal washing were improved (section 10.1.1) and several trial experiments were performed to achieve the desired results. Since the results obtained were not accurate enough to be used for crystalliser design purposes (because of the presence of some more extractable impurity (X)) only some of these experiments (18-24) have been tabulated (Table 2). Experiments 22-24 indicated that a Δc of 2.00×10^{-2} (KgPe/Kg solution) at a temperature of $30^{o}C$ was the most suitable working condition to perform comparative tests, as representative growth rates could be obtained before the secondary nucleation was noticed.

These experiments also indicated the appearance of the crystallographic faces (110) and (001) after the crystal had been growing for some time. The size of these faces appear to vary with the growth rate of the (101) face. Experiment 25 performed on Pe solution extracted with a purer grade of charcoal (Norit SX1) did not show any difference in growth features or even in the growth rate. However, Norit SX1 was used throughout the rest of the work to reduce the number of suspected factors which could be the reason for the varying growth rates. A technique was also developed to obtain a representative growth rate under any working condition (section 5.8) and, therefore, four different growth rates have been reported from experiment 22 onwards in accordance with this technique. Experiments 16-25 suggest that the treatment of hydrolysed Pe solutions with activated charcoal under the conditions used here possibly removes the impurity (X) from the solution. In the absence of this impurity the growth rate of the (101) face exceeds those of the (110) and (001) faces and therefore causes the appearance of these faces.

6.3.4 Required number of Extractions

Experiments 26-30 indicate that no significant improvement in growth rate is obtained after two extractions of the hydrolysed Pe solutions with activated charcoal. Therefore it appears that a minimum of two extractions are required under the specified conditions to reduce the concentration of (X) below a threshold limit. The routine developed was to carry out three extractions in order to provide a safety factor.

6.3.5 Effect of Purer Seed Crystal

The previous experiments 1-30 were all conducted on seeds possibly containing the impurity (X). Experiment 31 was performed on a seed crystal grown from a solution which had been hydrolysed and extracted with charcoal. There was no apparent difference between the growth rates obtained from the two kinds of seed. However, all the future work was performed on purer seed crystals.

6.3.6 Charcoal Effect

Although the treatment of hydrolysed Pe solutions with activated charcoal has increased the growth rate of Pe crystals by up to two orders of magnitude it was difficult to ascertain whether it was due to the removal of (X) or due to the addition of some growth accelerating substance by charcoal. The following experiments were carried out at $T = 30^{o}C$ and $\Delta c = 2.00 \times 10^{-2}$ (KgPe/Kg solution) to resolve this. Extreme care was taken to maintain conditions of utmost purity i.e. no glue was involved in mounting the seed crystals. 1000 cm^3 of solution was prepared with hydrolysed Pe and was divided into several parts.

1. Experiment 32 was conducted on one part of hydrolysed solution. The growth rate continuously decreased after an intial maximum of 1.58×10^{-5} cm/min. All other characteristics were similar to those observed in experiments 3-5.

2. Sufficient charcoal was added to a second part of hydrolysed Pe solution in the cell G_1 to obtain a charcoal concentration of 1 (g/ 100 g solution). The solution was kept under the above working conditions for a period of two hours without any stirring. No secondary nucleation was observed. A pure seed crystal was inserted and (experiment 33) gave growth rates and growth features identical to those in experiment 32.

3. A third part of the hydrolysed solution was now extracted with charcoal (Norit SX1) and experiment 34 conducted on this hydrolysed and extracted solution gave growth features similar to experiment 30.

4. The charcoal used in experiment 34 was now boiled in 500 cm^3 of distilled water for two hours in the hope of back extracting impurity (X), and filtered hot. The filtrate was used in preparing a solution with hydrolysed and extracted Pe at similar working conditions. Experiment 35 performed on this solution gave a maximum growth rate of the same order of magnitude as that obtained in experiment 32 and the growth rate continuously decreased with time and no g(avg.1) or g(min) could be obtained.

Experiments 32-35 indicate that the impurity, which may be more than one compound, does exist and is extracted by charcoal, also that the enhancement of growth rate is due to its removal and not due to a growth accelerating additive from the charcoal.

6.3.7 Use of Deionized Water

It was suspected that the variation of growth rate with time observed might possibly be due to the presence of surfactants in distilled water. Solutions of pure Pe (hydrolysed and extracted) were prepared with deionized water. However, experiments 36 and 37 conducted on these solutions gave growth characteristics identical to those obtained in experiment 30.

6.3.8 Effect of Plasticizers

The crystal seeds used in all the previous experiments were glued to the support rod with Tensol cement. It was thought that perhaps the leaching of plasticizers from the cement was the cause of the fluctuating growth rates. Two different cements, "Durofix" and Polystyrene (the latter containing no plasticizer) were used in experiments 38 and 39 for mounting the crystal seeds. The growth rates still varied with time up to a measured period of two hours. In experiments 40-43 the three glues were added as dried chips to the solution to see if the plasticizers were leached from them. The experiments were carried out for several hours without any difference in growth pattern. In order to double check that the glues had no effect on growth rates, experiments 44 and 45 were performed in the two cells without using any glue for crystal mounting. The growth rate was found to be similar to that of experiments 28-30. These results suggested that the various glues had no detectable effect on the growth rate nor on the way the growth rate varied with time and it was therefore decided to use "Durofix" due to its convenience and speed of drying.

6.3.9 Effect of Neoprene and Araldite

Since the cells S_2 and G_1 had neoprene O-rings and Araldite cement as foreign materials, it was required to observe their effects on the growth rate of Pe crystals. Experiments 46-49 indicated no effect on growth rate or growth pattern.

6.3.10 Conditions of Utmost Purity

All the experiments conducted from experiment 33 onwards tend to suggest that the oscillating growth rates with time were not due to any added contaminant. However, for final confirmation, cell G_2 was made entirely from pyrex glass. The seed was also mounted to the support rod without any glue. Pe solutions were prepared from deionized water. Experiments 50 and 51 still gave the usual pattern of growth rates observed in experiments 28-30.

6.3.11 Different Size Crystals

Experiments 52 and 53 were conducted on seeds nearly twice as large with respect to the distance between opposite identical crystallographic faces as used in the experiments up to 51. However, the results showed no significant difference in growth rate or pattern, and hence indicated that the size of the crystals had no effect on crystal growth rate.

6.3.12 Conclusions

1. The growth rate of Pe crystals varies with time under constant external conditions of temperature and supersaturation. The variation of the growth rate is a real effect and is not due to any contaminant picked up during the handling of the solutions.

2. The growth rate of solutions containing di-Pe and Formal continuously decreases with time. Occasionally the temporary dissolution of seed crystals is also observed.

3. The removal of di-Pe and Formal increases the growth rate by at least one order of magnitude. The growth rate still decreases with time.

4. Activated charcoal extracts an impurity (X) from Pe solutions. A maximum of three extractions is required to reduce the concentration of (X) below a threshold limit in the hydrolysed Pe solutions.

5. The growth rate of extracted and hydrolysed solution is at least two orders of magnitude higher than that of the hydrolysed material and three orders higher than that of the commercial material containing di-Pe, Formal and (X).

6. The growth rate of hydrolysed and extracted Pe varies continuously with time and the maximum rate can be twice as high as the minimum.

7. The purification process makes the solutions very sensitive to secondary nucleation and thus limits the duration of an experiment and the range of useful supersaturation.

8. The increased growth rate of the (101) face causes the appearance of the crystallographic faces (110) and (001).

9. Molecular sieve does not extract a sufficient amount of impurity (X) to reduce it below the threshold limit for growth inhibition under the experimental conditions investigated.

10. Crystal growth rate does not vary with the size of the crystal over the experimental conditions investigated.

6.4 Main Results

Single crystals of purified Pe were grown in the cells S_2 and G_1 under different conditions of supersaturation, temperature and impurity concentration. The results have been presented in several sections according to the presence or absence of impurity and its nature.

6.4.1 Growth in the Absence of Impurities

Growth rates were measured for the (101) faces at normal temperatures of 10, 20, 30, 40 and 50°C, and at Δc between 0.25×10^{-2} and 2.60×10^{-2} Kg Solute/Kg solution. The upper limit of Δc was set by the immediate occurrence of secondary nucleation upon seed insertion. Within this range of Δc, an experiment was continued until secondary nucleation occurred. If this nucleation occurred before g(avg.1) was obtained the experiment was discarded. However, if the nucleation occurred after the attainment of g(avg.1) the experiment was considered successful. All successful results have been reported in the Tables (4-8). Three experiments were performed at each temperature and Δc to obtain more reliable average values.

The growth rate of a particular crystal at constant T and Δc changed markedly with time. In general the fluctuations in growth rate decreased with time, although under conditions of low growth rate there were occasionally short periods of much higher (or lower) growth rates. Under high growth rate conditions the initial growth rate may be higher or lower than the final mean value (i.e. g(avg.1)). The growth pattern also varied from one seed to another of the same size

and under similar conditions of T and Δc. Some of the typical growth patterns obtained are shown in figures (10-12).

The duration of an experiment varied from ca.1h to 24 h for higher or lower growth rate conditions respectively, but in no experiment with pure material did the rate become independent of time.

The fluctuation in growth rate resulted in a maximum and a minimum value in each experiment. Although these maximum and minimum values appear to be a function of Δc and T, the difference between them also varied with Δc and T and either a decrease or an increase in the difference between g(max) and g(min) could be observed at increasing values of Δc and T. Despite such unpredictable behaviour, the average growth rate of an experiment g(avg.2) until the time of secondary nucleation did not differ much from the near steady-state growth rate g(avg.1) especially at high growth rates. Growth was observed under all conditions except at $20^{o}C$ and Δc of 0.25×10^{-2}. Under this condition continuous dissolution of the seed was observed in experiments 117 and 118 and little or practically no growth was observed in experiment 116 (Table 7).

At $10^{o}C$ and $20^{o}C$ the face (101) appeared to grow smoothly and virtually free from any surface irregularities. At temperatures above $20^{o}C$, however, a continuous appearance and disappearance of steps and projections was usually observed, if the seed crystal was smooth initially. These projections normally emerged from near the faces

(110) and (001) and gradually spread over the entire face. The elevation of the face (101), as observed through the microscope, then appeared in several sections and layers. The thickness of the layers at the centre of the face was always several times that of the layers near the edges. The growth rate measured at the centre in such cases almost always had a very high initial value and decreased or fluctuated with time. If it decreased with time initially, then the various steps at different parts of the crystal face merged into one another and gradually a smooth layer was built up on the face. If, however, the growth rate at the centre fluctuated, the number of different layers continuously increased or decreased depending upon whether the growth rate was increasing or decreasing respectively.

If, however, the surface of the seed crystal was smooth but no projections were observed, the growth rate at the centre, in most of the cases did not have a very high initial value. Under these conditions the face was observed to grow in two sections. A faster growing layer was observed to start from near the face (110) and rapidly spread over the face. Occasionally such a layer stopped at the centre and its growth rate would appear to decrease until it was met by a similar layer approaching from the opposite side. At the meeting point a cavity was occasionally observed to develop for a considerable period during the subsequent growth. If, however, it was filled, solvent inclusion was observed.

When the crystal face was not smooth initially, the growth rate at the various defects appeared to be higher than at the centre of

the edge (no such relative growth rates were actually measured). Rapid healing of these defects was then observed until a smooth layer was built up on the entire surface. With a continuation in growth the surface again began to develop in projections.

The growth rate data obtained from these experiments have been plotted as log g versus log Δc in the figures (13-17) to test the application of dislocation theories. The theories predict a parabolic relationship between g and $\Delta c/c^*$ at low $\Delta c/c^*$ and a linear relationship at higher $\Delta c/c^*$. Because of the large fluctuation, four different values of growth rates have been plotted for each Δc and T in figures (13-17). These include

1. The highest of the three g(max) values.
2. The lowest of the three g(min) values.
3. The g(avg.1) for each of the three experiments.
4. The mean of the three g(avg.1), which is taken as the growth rate (g) for given values of Δc and T.

At 10^oC and 20^oC, g appears to fall reasonably well on the best straight line of slope 2 drawn through the data. At 30^oC and 40^oC, however, deviations appeared from this straight line for $\Delta c < 1.50 \times 10^{-2}$ and the growth rate dependence upon Δc decreased. The data at these temperatures can be represented by a curve of slope 2 at $\Delta c > 1.50 \times 10^{-2}$. At 50^oC, on the other hand, the growth rate fell on a straight line of slope 1.24. For visual comparison the curves from figures (13-17) have been redrawn without the experimental points in figure 18.

For the dislocation theories, the growth rate data can also be represented by an empirical equation of the form:

$$g = k(\Delta c)^n \tag{61}$$

where Δc = concentration difference (KgPe/Kg solution)

and k has an Arrhenius type dependence on temperature, i.e.

$$k = A_o \exp(-E/RT) \tag{62}$$

and

$$\ln k = \ln g \quad \text{for} \quad \Delta c = 1.00 \tag{63}$$

An activation energy plot for ln k vs. 1/T (k) has been shown in figure (19). The activation energy for growth = 8.47 kcal/ mol.

This activation energy applies for the data at 10, 20 and 50°C at all Δc studied;

for 30 and 40°C it is applicable only for $\Delta c > 1.50$.

The data were also plotted as log. g vs. 1/log S (figure 20) to examine the growth rate data in the light of the TDN theories. The theories predict a straight line relationship at a given value of T. It is quite apparent that no straight line can be drawn through the data. Rather, two straight line portions are observed at 30°C, 40°C, and 50°C, one of which appears to apply at high Δc and the other at low Δc. At 10°C and 20°C the data is scanty and only a curve can be drawn through the points.

Although the objectives of this investigation did not specifically include a study of the phenomenon of secondary nucleation

some observations concerning this phenomenon were made during the course of this investigation. The results provide some information concerning the mechanism by which secondary nucleation could occur in stagnant solutions.

The initial washing of the seed crystals (precuring) was found to be of vital importance in determining the time for secondary nucleation $t_{s.n}$, which also depended on T and Δc. Success was achieved in rather less than half of the total number of experiments conducted. The value of $t_{s.n.}$ varied with the growth rate. A plot of $t_{s.n.}$ vs. g(avg.2) has been shown in figure 21. It is clear that $t_{s.n.}$ continuously decreases with increasing g(avg.2). Below a g(avg.2) of 1×10^{-4} cm/min no secondary nucleation was observed even up to 48 hours. The shaded region of figure 21 shows that for g(avg.2) above 1×10^{-4} cm/min secondary nucleation was observed in practically all of the reported experiments within this region. If, however, the precuring of the seed was not successful due to improper washing or due to the mechanical weakness of the crystal, secondary nucleation occurred much earlier than $t_{s.n.}$ in which case the experiment was discarded. For g(avg.2) between 1×10^{-4} and about 7×10^{-4} cm/min only a few nuclei were observed at $t_{s.n.}$ and these grew very slowly with time without a large increase in their number.

In experiment 96 ($T = 30^{o}C$, $\Delta c = 1.08 \times 10^{-2}$ KgPe/Kg solution) only one secondary nucleus was observed growing at the bottom of the cell at $t_{s.n.}$ of 123 minutes. The continuation of the experiment to 48 hours increased the number of secondary nuclei only up to 5.

However, for g(avg.2) above about 7×10^{-4} cm/min several nuclei appeared at $t_{s.n.}$ and they rapidly increased in size and multiplied in number.

In the absence of a seed crystal, no secondary nucleation was observed up to a period of 48 hours at the temperature and concentration difference which corresponded to a g(avg.2) of less than about 7×10^{-4} cm/min. At higher values of g(avg.2), however, the appearance of a few tiny nuclei was observed at $t_{s.n.}$ and these nuclei rapidly multiplied themselves in number and size.

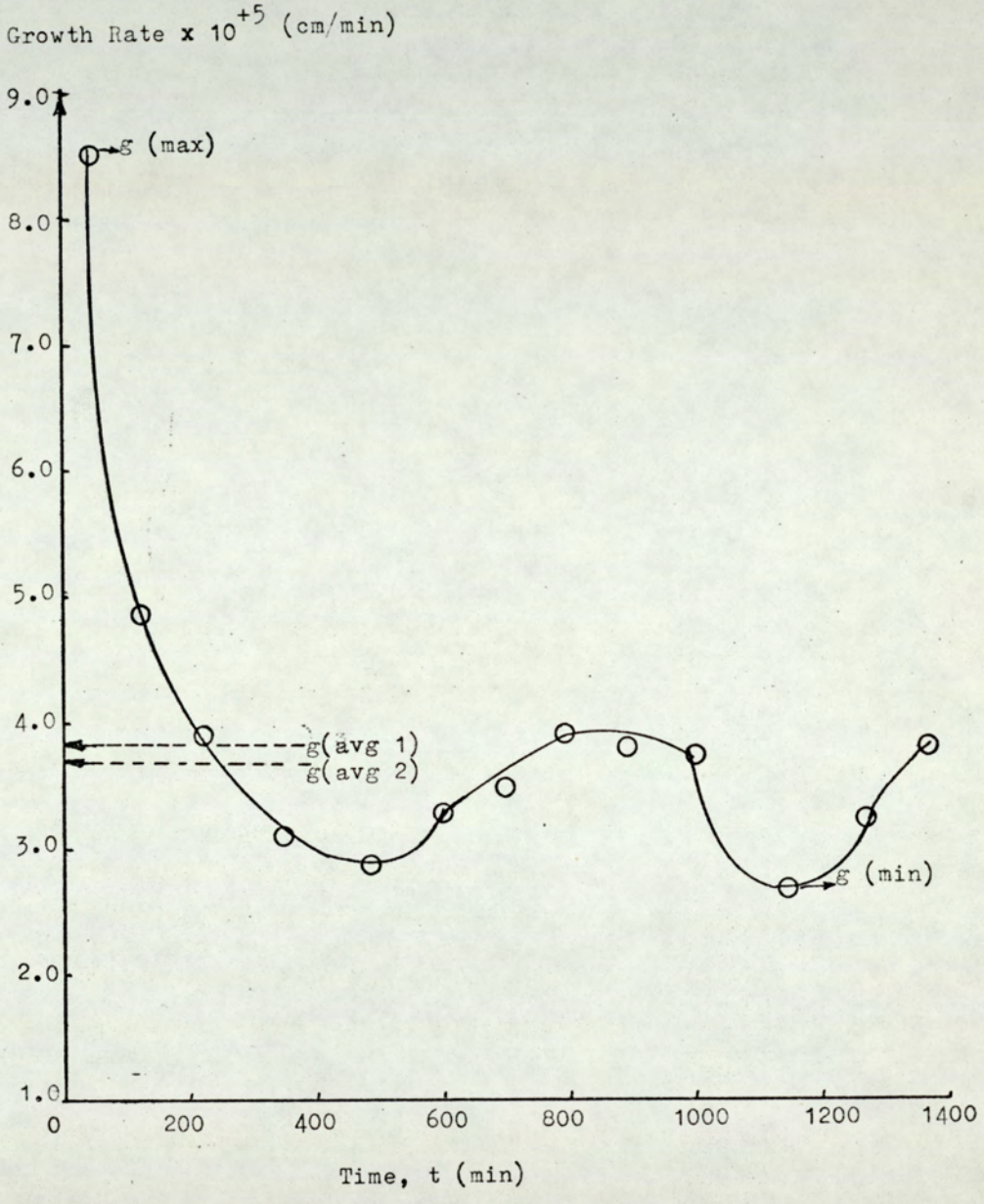

Fig. 10 Growth rate as a function of time

$T = 10^{0}C$, X = 0.146 Exp 130

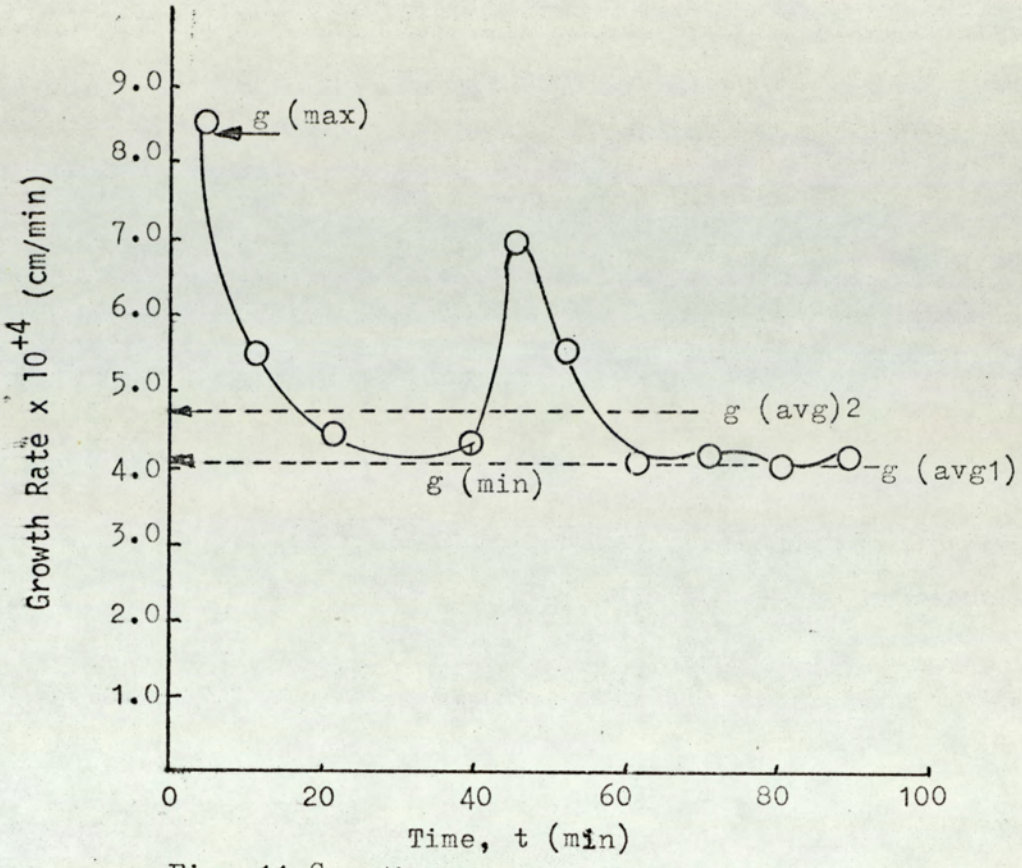

Fig. 11 Growth rate as a function of time

T = 30^{0}C, X= 0.274 Exp 92

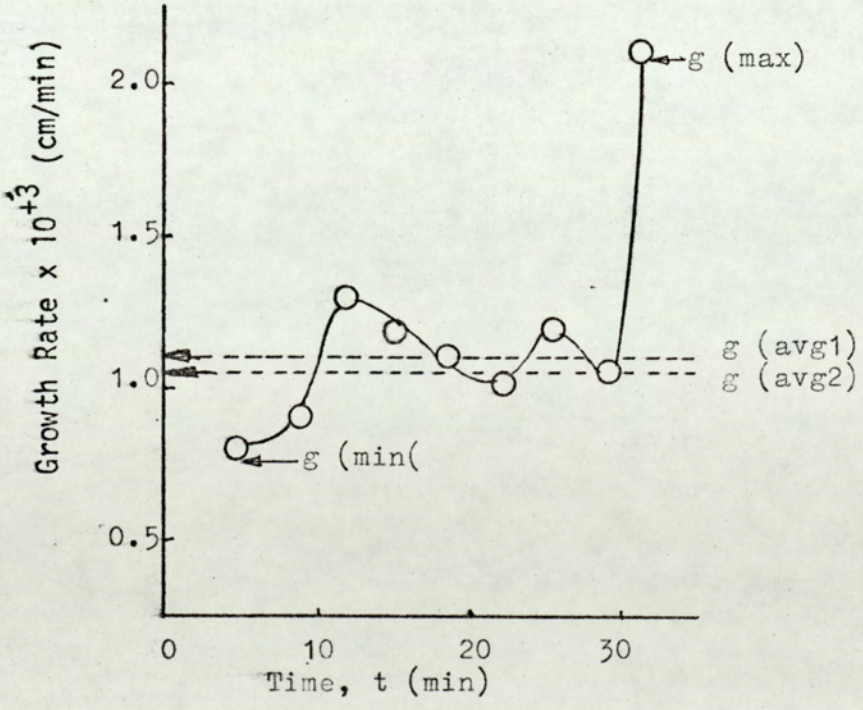

Fig. 12 Growth rate as a function of time

T = 50^{0}C ∓ X = 0.173 Exp 55

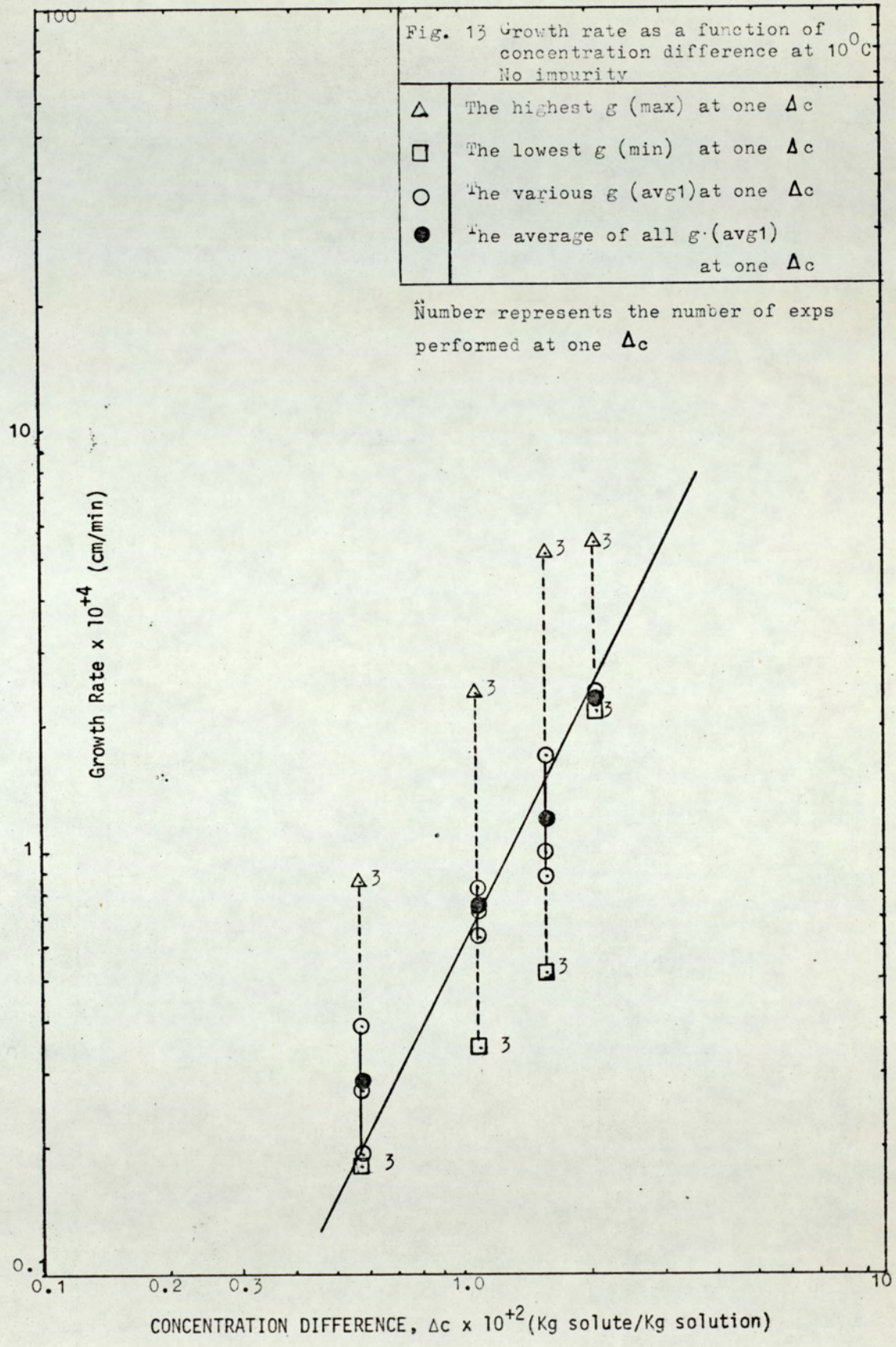
100
10
1
0.1
0.1
0.2
0.3
1.0
10
Growth Rate x 10+4 (cm/min)
CONCENTRATION DIFFERENCE, Δc x 10+2 (Kg solute/Kg solution)
Fig. 13 Growth rate as a function of concentration difference at 10°C No impurity
The highest g (max) at one Δc
The lowest g (min) at one Δc
The various g (avg1) at one Δc
The average of all g (avg1) at one Δc
Number represents the number of exps performed at one Δc

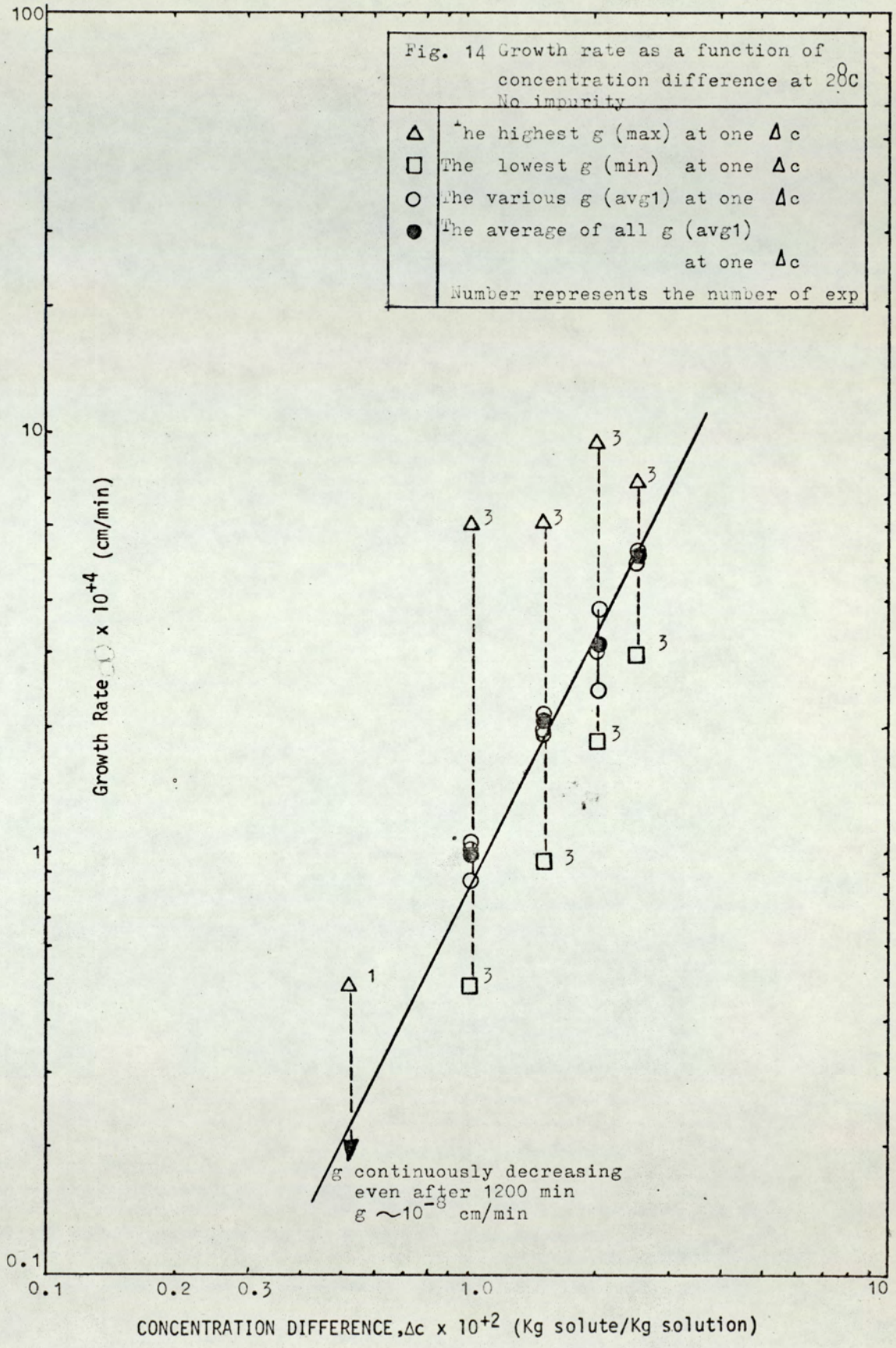
Fig. 14 Growth rate as a function of concentration difference at 28°C
No impurity
△ The highest g (max) at one Δc
□ The lowest g (min) at one Δc
○ The various g (avg1) at one Δc
● The average of all g (avg1) at one Δc
Number represents the number of exp
Growth Rate, g x 10^+4 (cm/min)
100
10
1
0.1
0.1
0.2
0.3
1.0
10
CONCENTRATION DIFFERENCE, Δc x 10^+2 (Kg solute/Kg solution)
g continuously decreasing even after 1200 min
g ~10^-8 cm/min

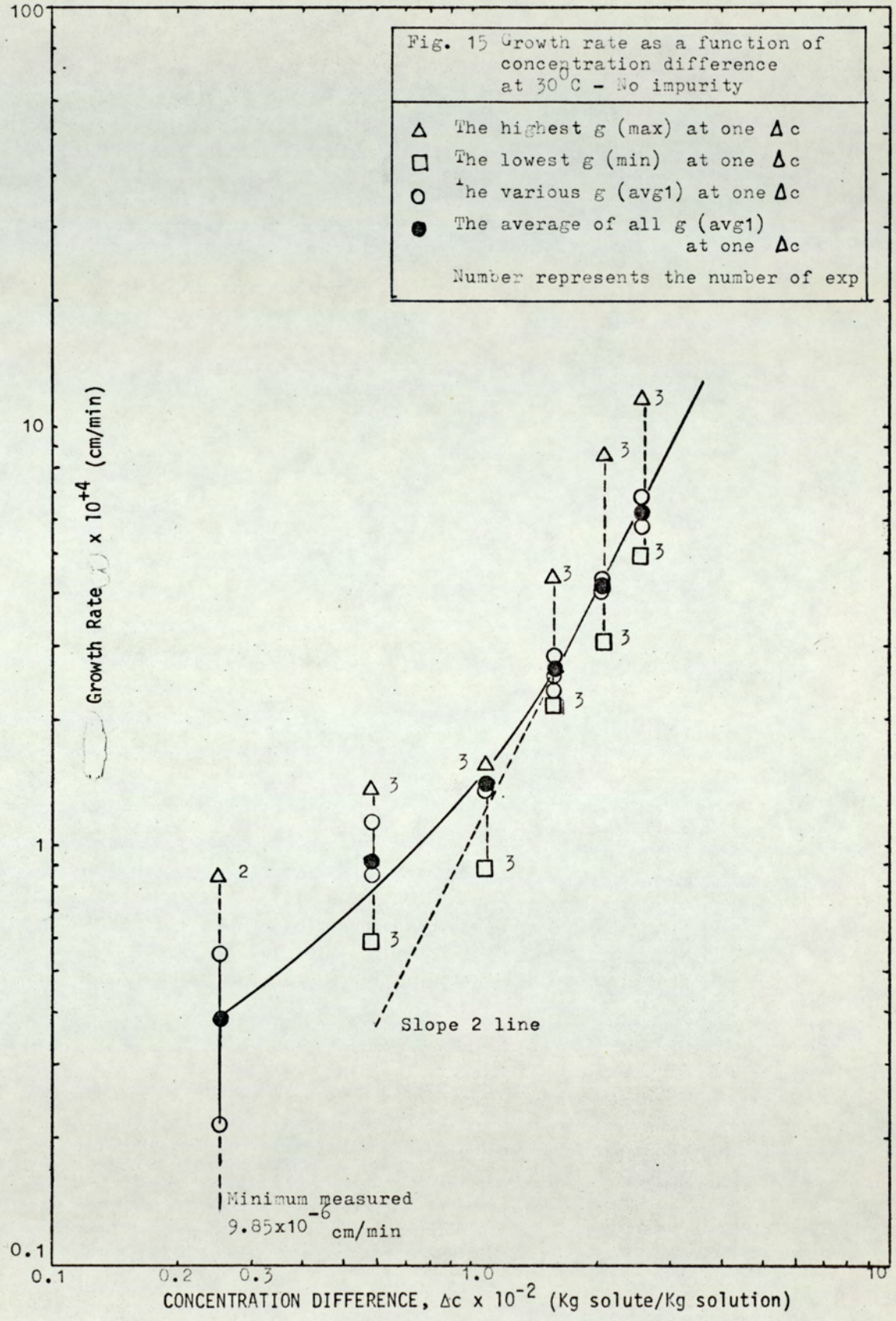
Fig. 15 Growth rate as a function of concentration difference at 30°C - No impurity
The highest g (max) at one Δc
The lowest g (min) at one Δc
The various g (avg1) at one Δc
The average of all g (avg1) at one Δc
Number represents the number of exp
Growth Rate x 10^+4 (cm/min)
100
10
1
0.1
0.1
0.2
0.3
1.0
10
CONCENTRATION DIFFERENCE, Δc x 10^-2 (Kg solute/Kg solution)
Slope 2 line
Minimum measured
9.85x10^-6 cm/min

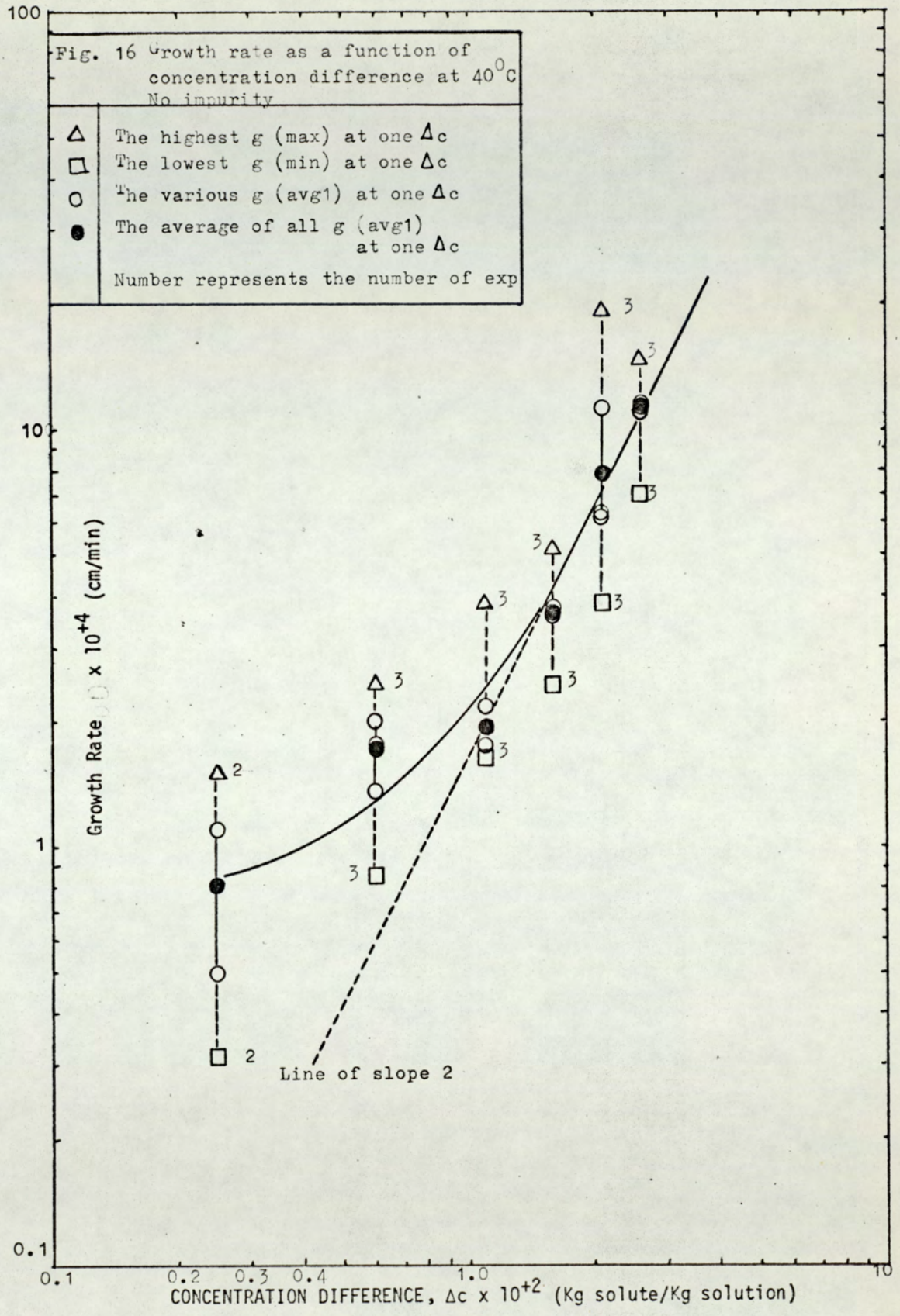
Fig. 16 Growth rate as a function of concentration difference at 40°C
No impurity
The highest g (max) at one Δc
The lowest g (min) at one Δc
The various g (avg1) at one Δc
The average of all g (avg1) at one Δc
Number represents the number of exp
Growth Rate x 10+4 (cm/min)
CONCENTRATION DIFFERENCE, Δc x 10+2 (Kg solute/Kg solution)
Line of slope 2
100
10
1
0.1
0.1
0.2
0.3
0.4
1.0
10

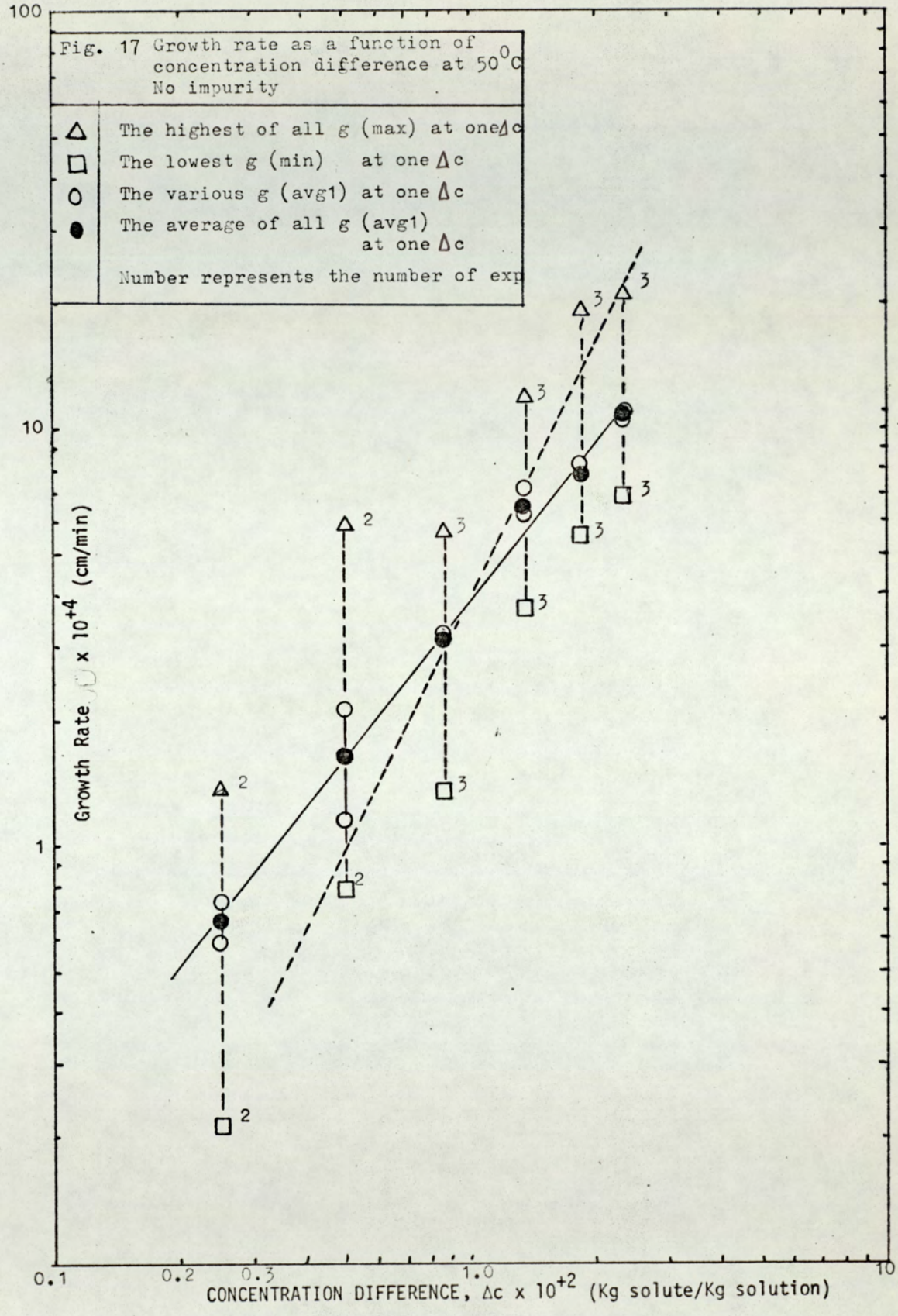
Fig. 17 Growth rate as a function of concentration difference at 50°C
No impurity
The highest of all g (max) at one Δc
The lowest g (min) at one Δc
The various g (avg1) at one Δc
The average of all g (avg1) at one Δc
Number represents the number of exp
100
10
1
0.1
0.2
0.3
1.0
10
Growth Rate x 10+4 (cm/min)
CONCENTRATION DIFFERENCE, Δc x 10+2 (Kg solute/Kg solution)

Fig. 18 g versus Δc at several temperatures- No impurity

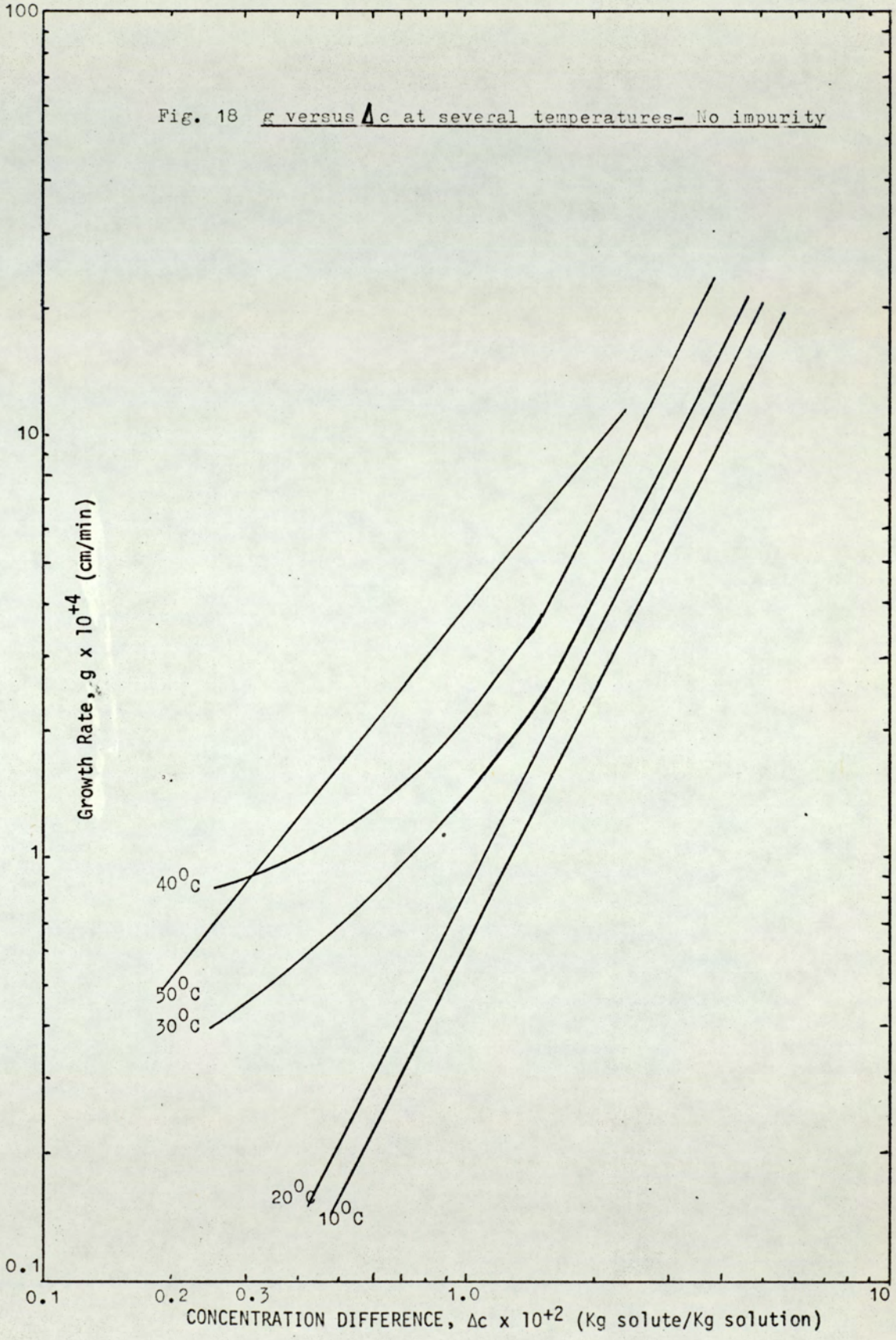

Fig. 19 Activation Energy Plot for Pure Pe

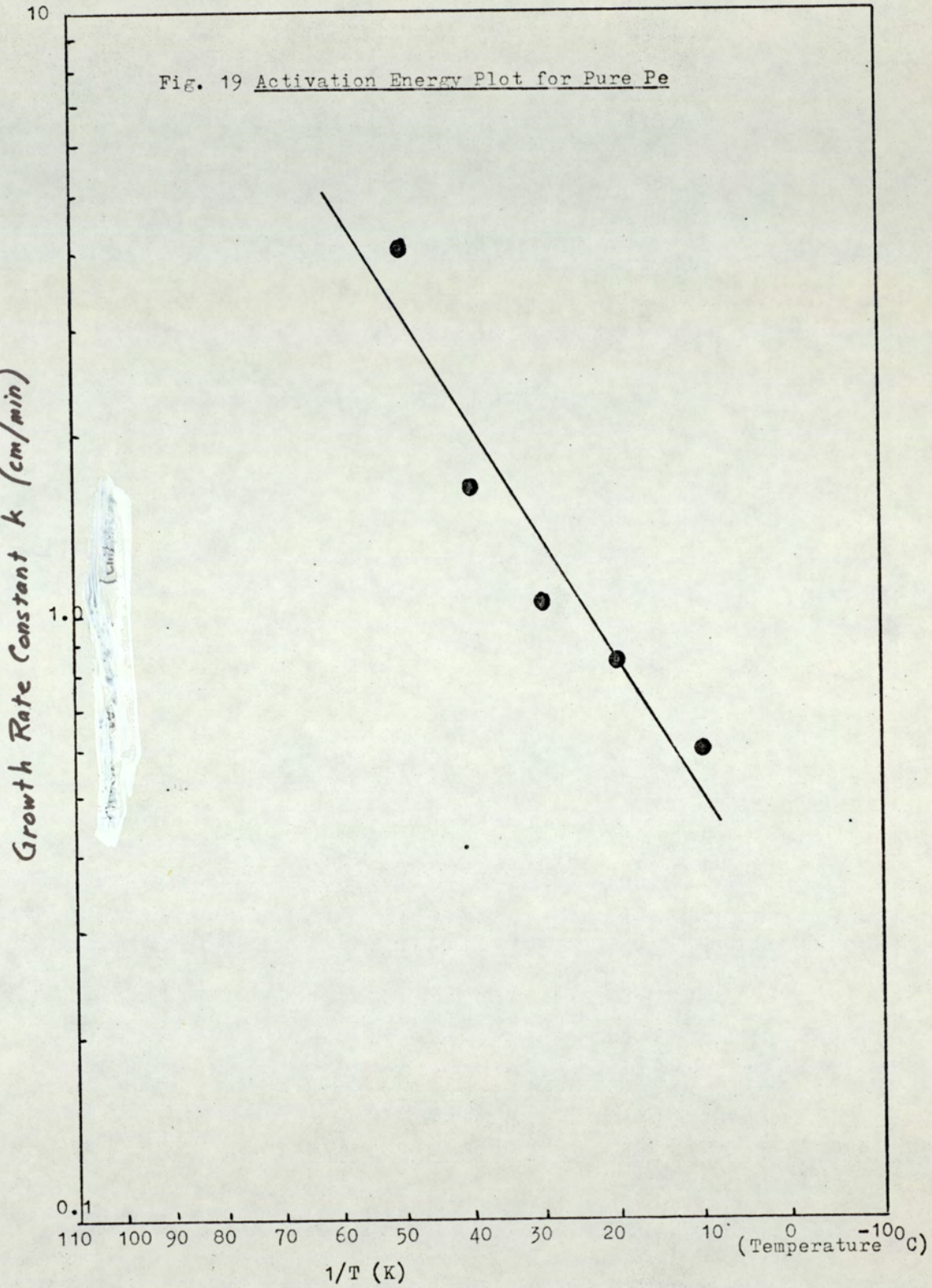

Fig. 20 Plot of log g vs. 1/log S for pure Pe
($S = c/c^*$)

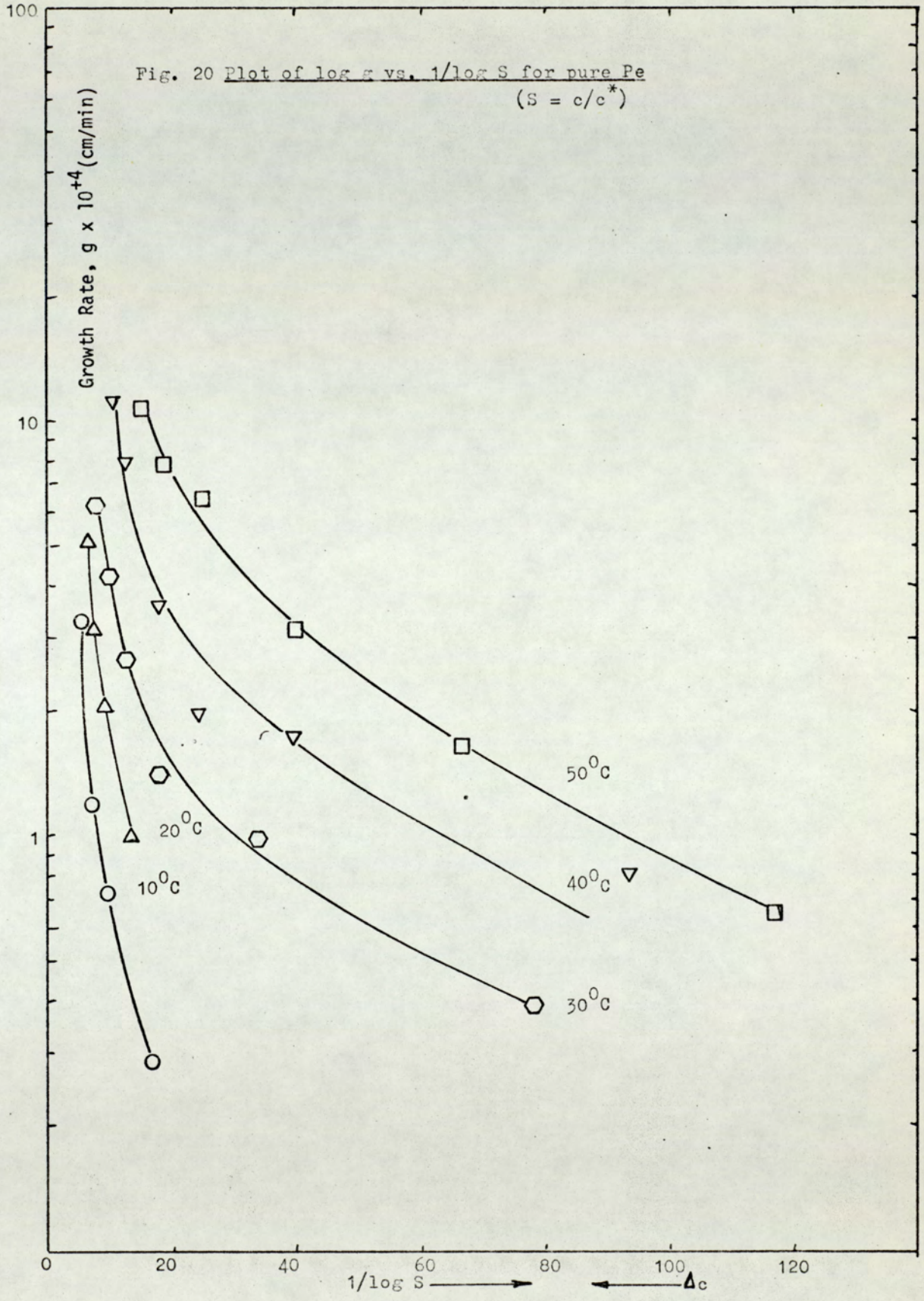

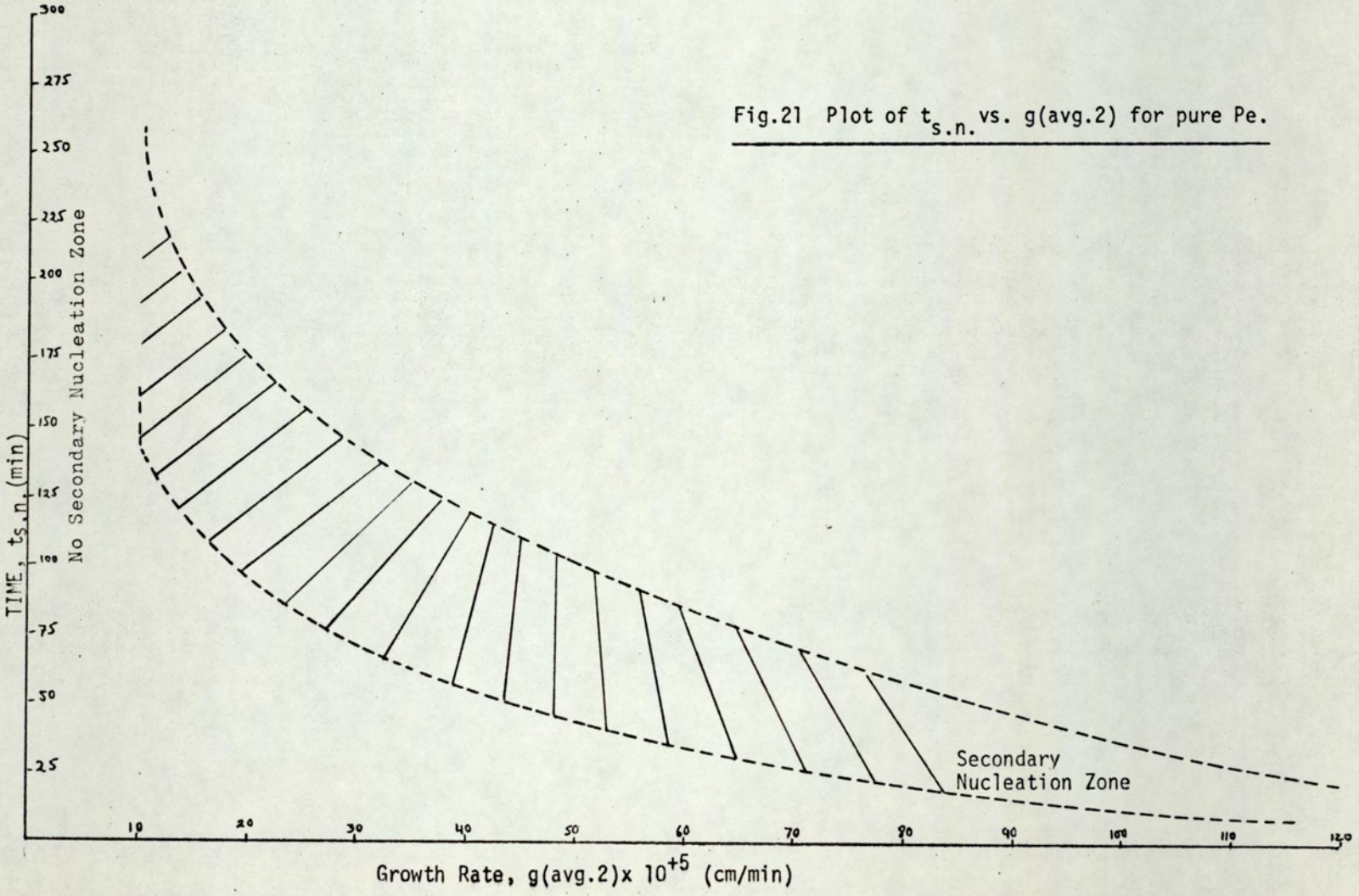

Fig.21 Plot of $t_{s.n.}$ vs. g(avg.2) for pure Pe.

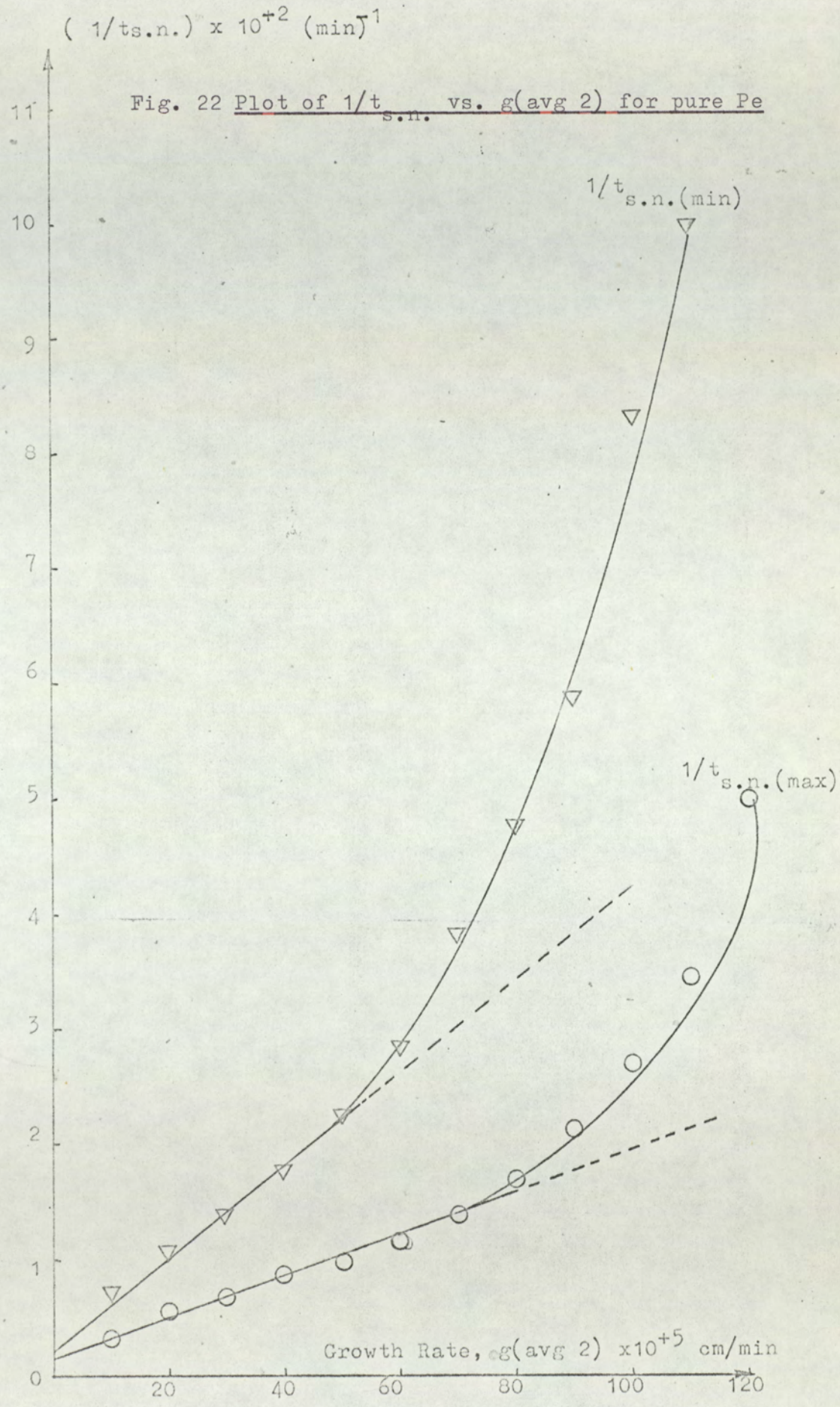

Fig. 22 Plot of $1/t_{s.n.}$ vs. g(avg 2) for pure Pe

6.4.2 Growth in the Presence of Impurities

6.4.2.1 Growth in the Presence of Di-Pe

Growth rates were measured for the (101) faces at 30 and 40°C in the presence of a controlled amount of di-Pe varying from $c_i = 0.05 \times 10^{-2}$ to 0.75×10^{-2} (kg di-Pe/kg solution). Oscillating growth rates consistently appeared in every experiment and the problem of secondary nucleation meant that only just under half the experiments attempted were successful. The quantitative results are presented in Tables (9-14) and figures (23 & 24). The growth rates at zero di-Pe concentration have been obtained from figures (15 & 16).

The large oscillation of the growth rates necessitated the plot of only g vs. c_i. The values of g(min), g(max), and g(avg.1) for every working condition are given in Tables (9-14). The standard deviations of g(avg.1), have been tabulated in appropriate figures (figs. 23,24). The calculation method for these standard deviations is not strictly justified mathematically as the deviations for each of g(avg.1), have been obtained about their own g (for each c_i) rather than about one g for all c_i. However, the method used here is helpful in indicating the spread of the data in figures (23 & 24), and for the present requirements it seems useful.

The presence of di-Pe in the solution seems to yield both an increase and a decrease in growth rate over that obtained for pure Pe solutions. At 30°C, an initial decrease in growth rate is followed by a rapid increase at a Δc of 2.23×10^{-2} (fig.23,curve 1).

A maximum is obtained at a critical di-Pe concentration of 0.15×10^{-2} after which the rate gradually decreases again. There is a slight suggestion of a second maximum at $c_i > 0.75 \times 10^{-2}$. At lower value of Δc, the increase in growth becomes more gradual and a maximum is obtained at $c_i = 0.40 \times 10^{-2}$ (fig. 23, curve 2). At still lower values of Δc, (curves 3 and 4) the growth rate appears to decrease gradually and the fluctuations are well within the experimental variations. At $40^{o}C$ the maximum in growth is obtained for a value of c_i lower than that for the corresponding Δc at $30^{o}C$ (figure 24, curve 1). The increase in growth is also more gradual than the corresponding increase at $30^{o}C$. The growth pattern at lower Δc is similar to that obtained at the corresponding Δc at $30^{o}C$ (figure 24, curve 2).

The oscillation of growth rates with time was not much different from that obtained under pure conditions when no di-Pe was present in the solutions and both a higher or a lower initial growth rate was possible. Below a growth rate of g(avg.1) 5.00×10^{-4} cm/min, the initial growth rate was always the highest. At high values of growth rates the appearance and disappearance of projections was similar to that observed at corresponding growth rates in the pure solutions.

A plot of $t_{s.n.}$ vs.g(avg.2) has been presented in fig.25. $t_{s.n.}$ appears to increase continuously with decreasing g(avg.2) and for g(avg.2) below 1×10^{-4}cm/min practically no secondary nucleation was observed for any length of measured time up to 48 hrs. This effect was further investigated for a $c_i = 0.75 \times 10^{-2}$ and $T=30^{o}C$ with increasing

values of Δc (fig. 23). A Δc of 4.23×10^{-2} was found to be the maximum permissible concentration difference at which an experiment could be carried out without any secondary nucleation. In the absence of di-Pe such a limiting value was found to be 2.58×10^{-2}. The shaded region in figure 23 shows the area within which or above which it is impossible to avoid secondary nucleation.

No change in crystal habit was noticed under any working conditions. In order to determine the mechanism of growth enhancement and growth retardation, experiments 141 ($c_i = 0.15 \times 10^{-2}$) and 155 ($c_i = 0.75 \times 10^{-2}$) were conducted with larger seed crystals for periods of up to 8 and 16 hours respectively. No growth rate measurements were made because of an enormous amount of secondary nucleation. A gas chromatographic analysis showed the absence (i.e. > 0.05%) of any di-Pe in the seed crystals thereby indicating that di-Pe was not incorporated into the growing crystals. The chromatographic analysis was performed on the grown seeds after they were freed from the daughter crystals by dissolution in distilled water.

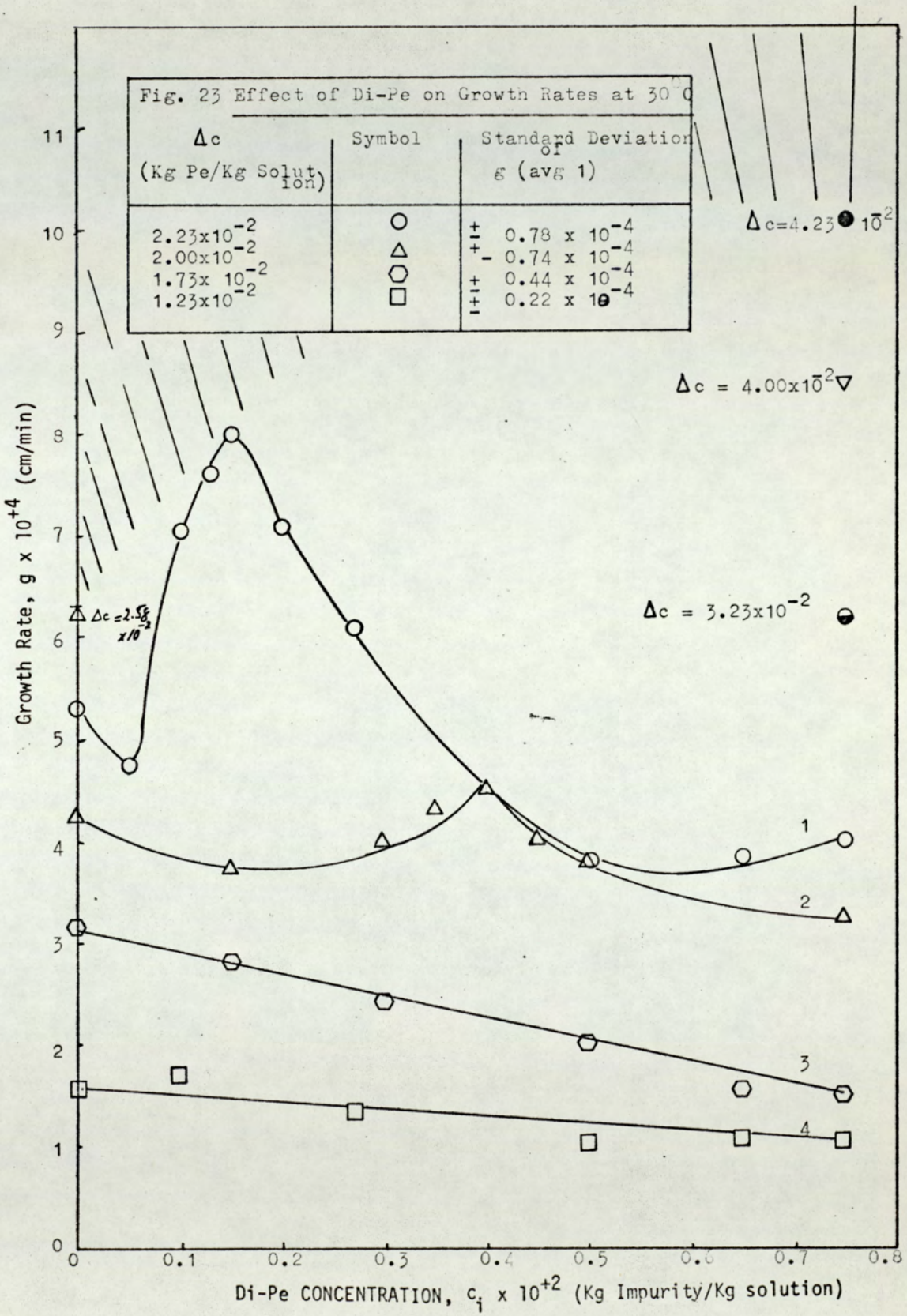
Fig. 23 Effect of Di-Pe on Growth Rates at 30° C
Δc (Kg Pe/Kg Solution)
Symbol
Standard Deviation of g (avg 1)
2.23x10^-2 ± 0.78 x 10^-4
2.00x10^-2 ± 0.74 x 10^-4
1.73x 10^-2 ± 0.44 x 10^-4
1.23x10^-2 ± 0.22 x 10^-4
Δc=4.23 10^-2
Δc = 4.00x10^-2
Δc = 3.23x10^-2
Δc =2.5 x10^-2
1
2
3
4
Growth Rate, g x 10^+4 (cm/min)
Di-Pe CONCENTRATION, c_i x 10^+2 (Kg Impurity/Kg solution)
0
0.1
0.2
0.3
0.4
0.5
0.6
0.7
0.8
1
2
3
4
5
6
7
8
9
10
11

Fig. 24 Effect of Di-Pe on Growth Rates at 40°C.

Δc (Kg Pe/Kg Solution)	Symbol	Standard Deviation of g (avg 1)
2.23×10^{-2}	○	0.73×10^{-4}
1.23×10^{-2}	□	0.33×10^{-4}

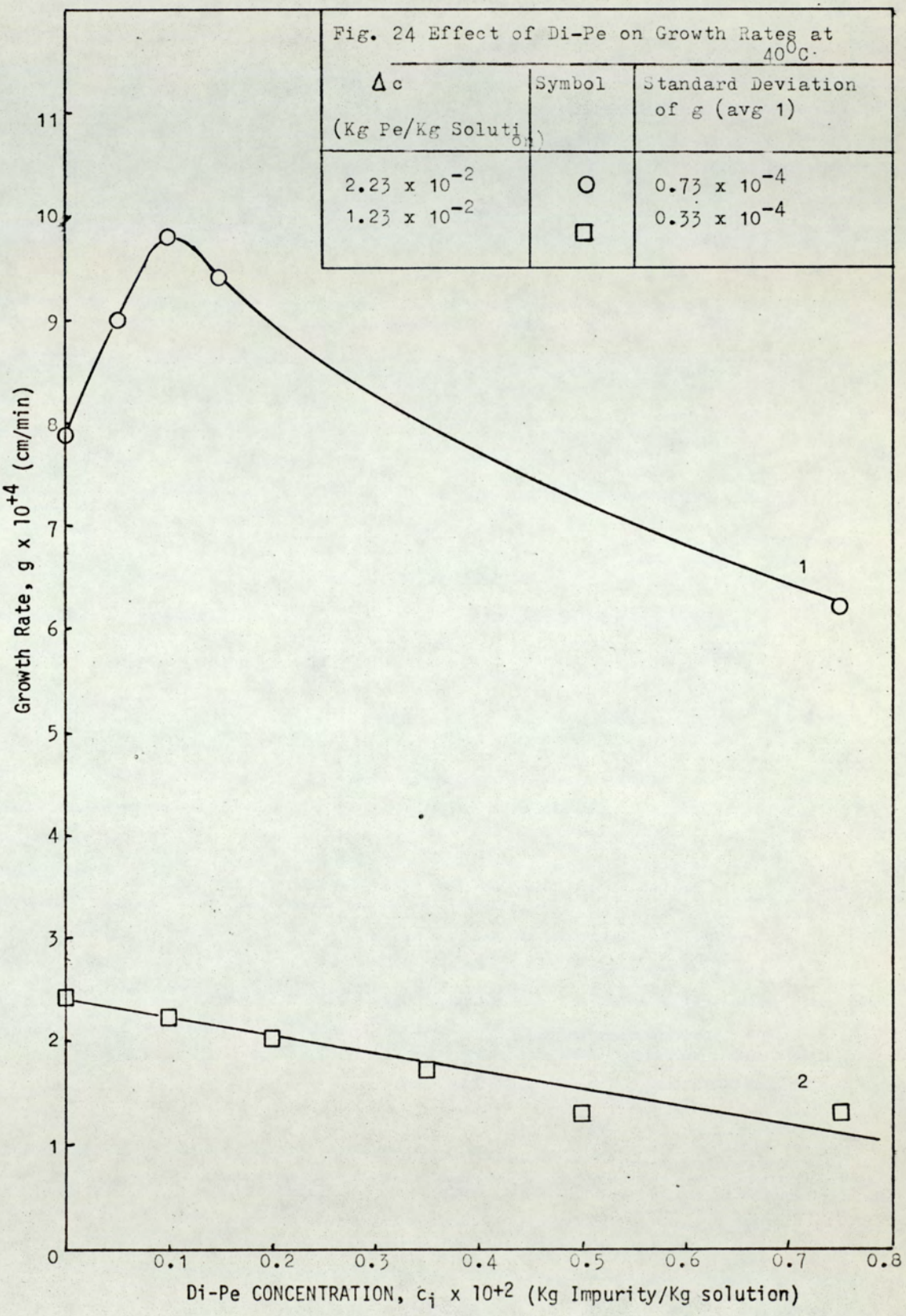

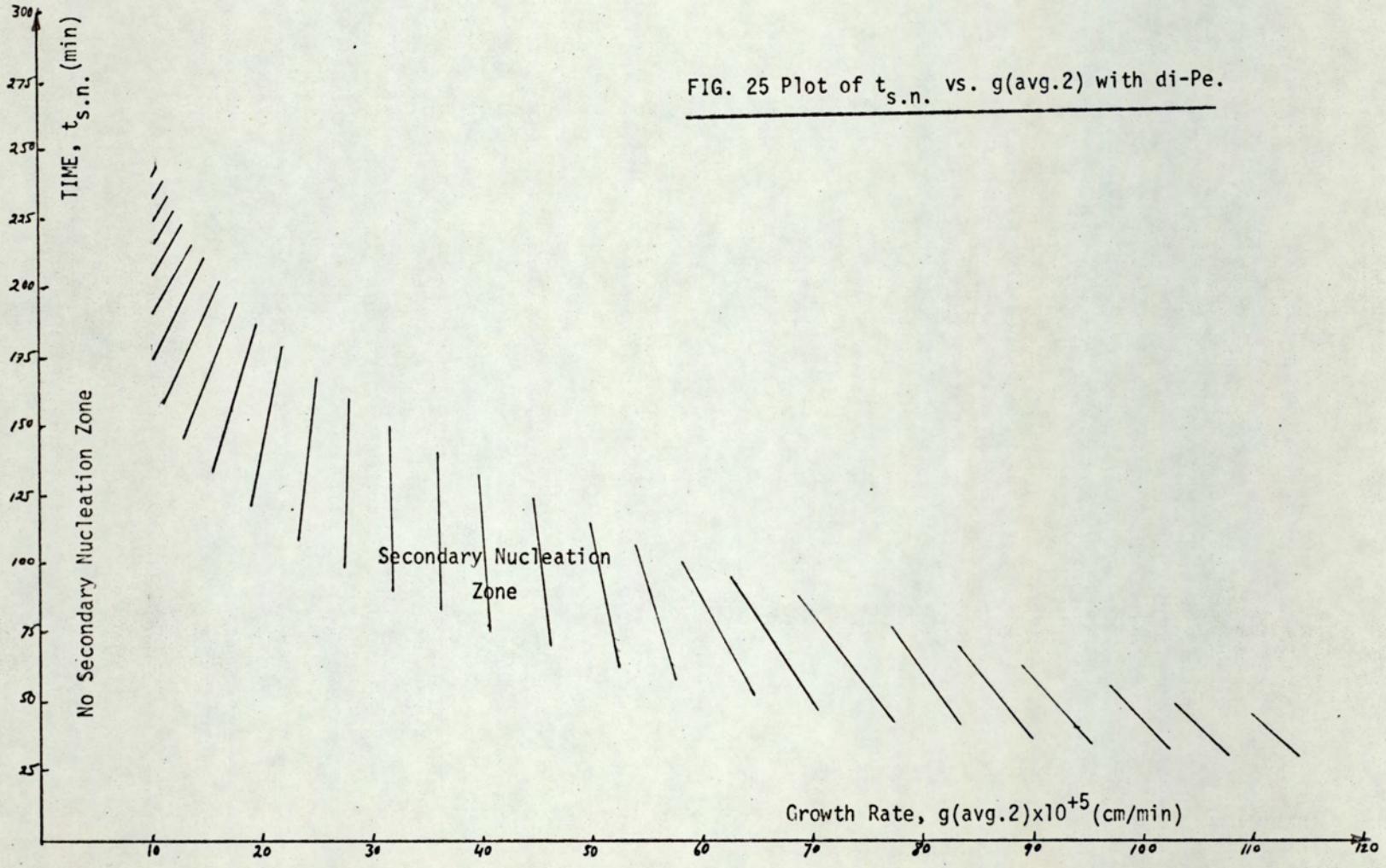

FIG. 25 Plot of $t_{s.n.}$ vs. g(avg.2) with di-Pe.

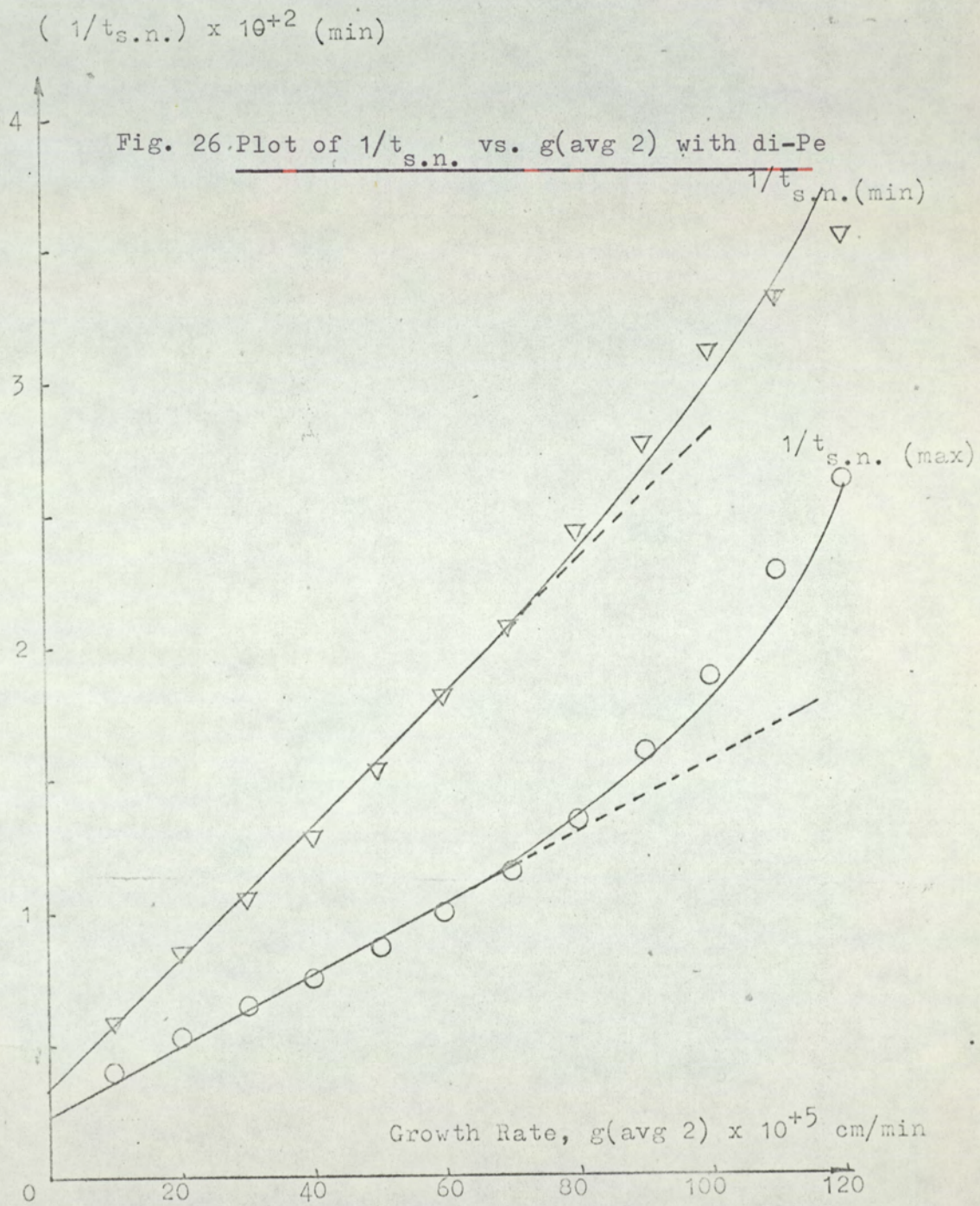

Fig. 26 Plot of $1/t_{s.n.}$ vs. g(avg 2) with di-Pe

6.4.2.2 Growth in the presence of Formal

Growth rates of the face (101) were measured at $30^{o}C$ and $40^{o}C$ in the presence of Formal concentrations (c_{if}) varying between 6.64×10^{-5} and 2.17×10^{-3} (Kg Formal/Kg solution) at different Δc up to 4.00×10^{-2} (KgPe/Kg solution). The results are shown in figures (27 and 28) and the data represented in Tables (15 - 18). Growth rates for zero c_{if} have been obtained from figures (15 & 16) by extrapolation. The shaded areas in figures (27 & 28) indicate the absence of any measurable growth using the single crystal technique.

The presence of Formal decreases the growth rate of Pe crystals under all the conditions investigated. At $30^{o}C$, the growth rate decreases very sharply with increasing c_{if} at a Δc of 1.23×10^{-2}. At any formal concentration above a critical value ca. 0.025×10^{-2} the growth rate continuously decreased up to a measured duration of 34-46 hours after which it finally ceased. At $\Delta c = 2.23 \times 10^{-2}$ the initial decrease in growth rate with increasing c_{if} is less sharp but nevertheless the growth ceases for $c_{if} > 0.135 \times 10^{2}$. At a higher temperature (figure 28), the initial decrease in growth rate becomes even more gradual and much higher values of c_{if} are obtained (it should be noted that the values used for Δc were higher at the higher temperature).

At a lower temperature of $30^{o}C$, an increase of 1.00×10^{-2} in Δc raises the value of c_{if} by more than a factor of five whereas at $40^{o}C$ the corresponding increase in c_{if} is less than 2.

The initial growth rate for any experiment was always the highest value obtained, i.e. g(max), the growth rate then decreased continuously and no increase in growth rate was obtained for any of the working conditions investigated.

Secondary nucleation was obtained only at growth rates higher than about 8×10^{-4} cm/min. Below this value an experiment could be conducted for any length of time with only the main seed crystal in the solution.

Although no relative growth rate measurements of the faces (101), (110) and (001) were made, the faces (110) and (001) grew out of existence within a few hours of growth and never reappeared in any of the experiments. The final shape of a grown crystal was always the one bounded with the triangular faces (101) well quoted in the literature. The originally transparent crystals became translucent due to the deposited growth material. A gas chromatographic analysis of the seeds grown in the experiments in the presence of Formal indicated the presence of Formal in them.

The surface free energies of the face (101) were calculated for conditions of temperature, supersaturation and Formal concentration at which growth ceased (section 10.3.1). An average value of the order of 30 ergs/cm^2 was obtained.

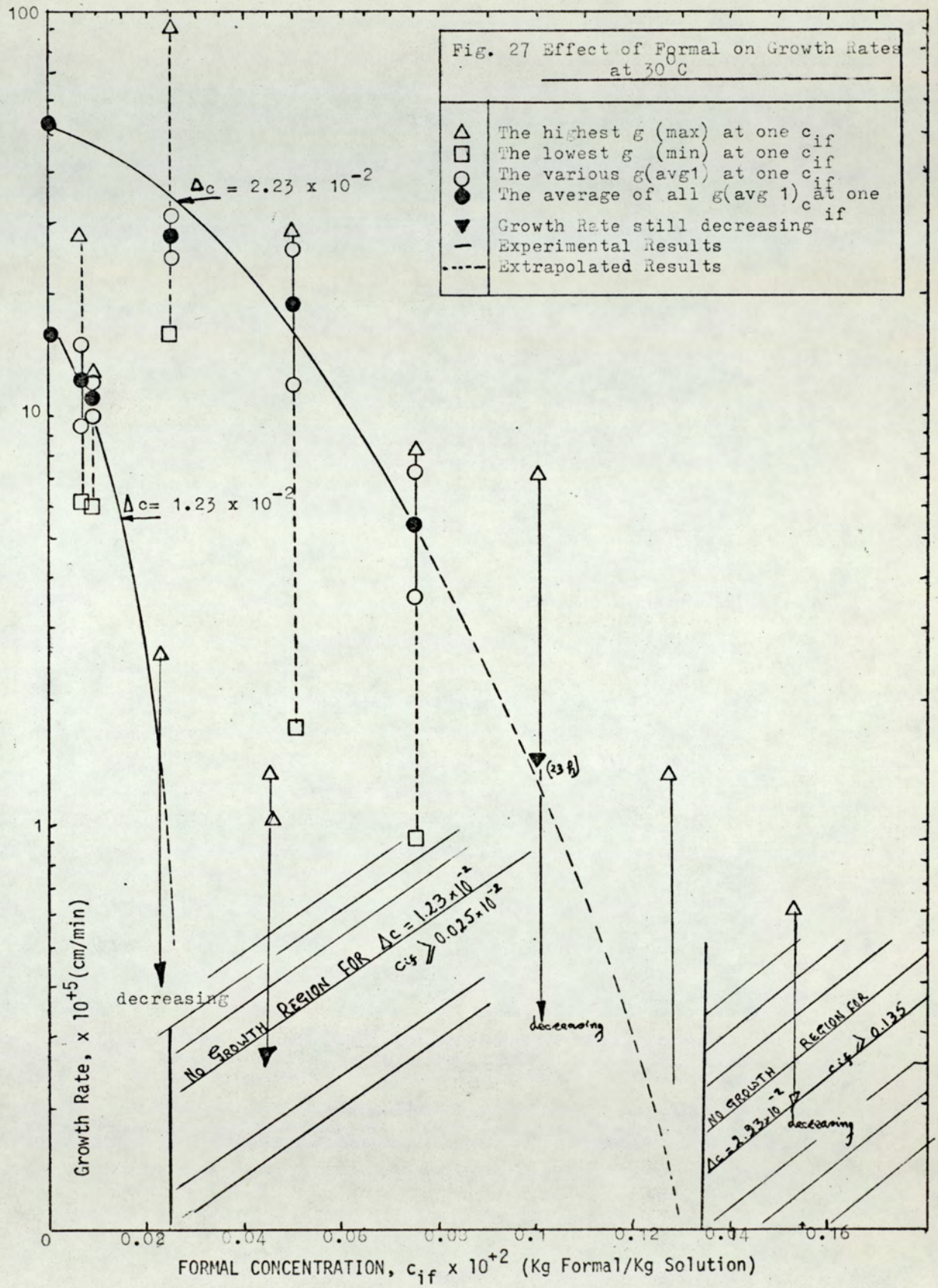
Fig. 27 Effect of Formal on Growth Rates at 30°C
The highest g (max) at one c_{if}
The lowest g (min) at one c_{if}
The various g(avg1) at one c_{if}
The average of all g(avg 1) at one c_{if}
Growth Rate still decreasing
Experimental Results
Extrapolated Results
$\Delta c = 2.23 \times 10^{-2}$
$\Delta c = 1.23 \times 10^{-2}$
decreasing
No Growth Region for $\Delta c = 1.23 \times 10^{-2}$ $c_{if} \gg 0.025 \times 10^{-2}$
(23 hr)
decreasing
No Growth Region for $\Delta c = 2.23 \times 10^{-2}$ $c_{if} \gg 0.125$
decreasing
Growth Rate, x 10^{+5} (cm/min)
100
10
1
0
0.02
0.04
0.06
0.08
0.1
0.12
0.14
0.16
FORMAL CONCENTRATION, c_{if} x 10^{+2} (Kg Formal/Kg Solution)

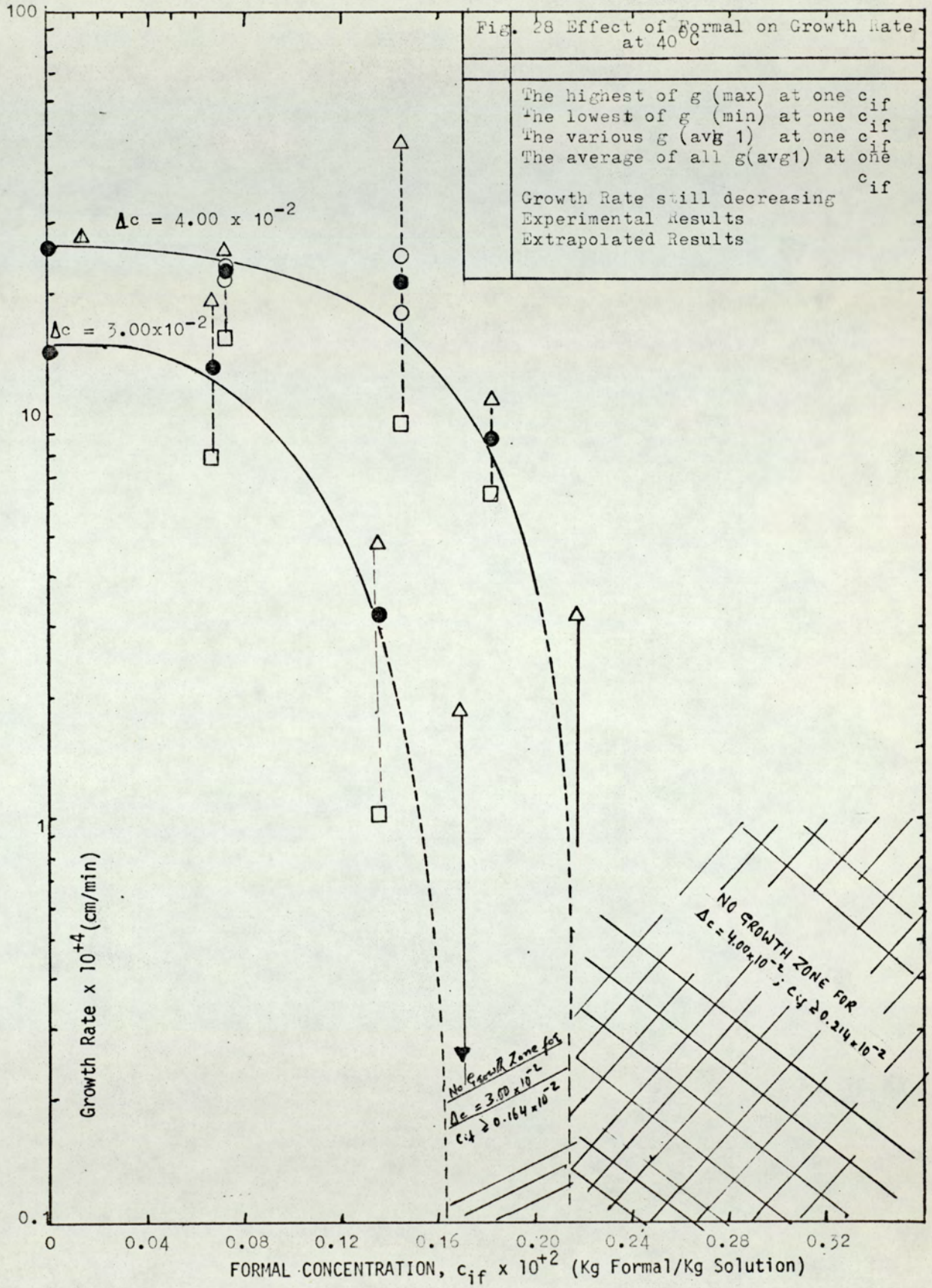
Fig. 28 Effect of Formal on Growth Rate at 40°C
The highest of g (max) at one c_{if}
The lowest of g (min) at one c_{if}
The various g (avg 1) at one c_{if}
The average of all g(avg1) at one c_{if}
Growth Rate still decreasing
Experimental Results
Extrapolated Results
$\Delta c = 4.00 \times 10^{-2}$
$\Delta c = 3.00 \times 10^{-2}$
No Growth Zone for $\Delta c = 3.00 \times 10^{-2}$; $c_{if} \geq 0.164 \times 10^{-2}$
NO GROWTH ZONE FOR $\Delta c = 4.00 \times 10^{-2}$; $c_{if} \geq 0.214 \times 10^{-2}$
Growth Rate x 10^{+4} (cm/min)
100
10
1
0.1
0
0.04
0.08
0.12
0.16
0.20
0.24
0.28
0.32
FORMAL CONCENTRATION, c_{if} x 10^{+2} (Kg Formal/Kg Solution)

6.4.2.3 Growth in the presence of Miscellaneous Impurities

In order to identify the impurity (X) which was believed to be present in the commercial Pe in trace quantities, the effect of several materials on the growth rate of Pe crystals was determined at T = 30°C and $\Delta c = 2.23 \times 10^{-2}$ (KgPe/Kg solution). It was anticipated that some of these materials might have been added either as reagents during synthesis reaction or else as (accidental) additives (such as lubricants) during processing. The results obtained are presented in Table 19.

Of all the impurities tried only NaOH, HCHO, and 1,1,1,trimethylolethane caused a significant reduction in growth rate and changed the crystal habit. At a $c_i = 1.00 \times 10^{-2}$ (Kg Impurity/Kg solution), NaOH reduced the growth rate by about 66% whereas HCHO reduced it by an order of magnitude. 1,1,1,trimethylolethane reduced the growth rate by 70% at the same concentration. A higher concentration of $c_i = 2.13 \times 10^{-2}$ was used only for NaOH out of these three impurities and complete inhibition of growth was observed. No secondary nucleation was observed for any length of time and the faces (110) and (001) rapidly grew out of existence with NaOH and HCHO impurities.

The addition of H_2O_2 or even the passage of CO_2 through the purified and unextracted Pe solutions did not produce any increase in growth rate. The addition of White Spirit reduced the growth rate by about 50% and no change in crystal habit was observed.

The addition of two grades of lubricating oil appeared to

catalyse the formation of secondary nuclei from the very beginning of an experiment. Thus with these two impurities in solution, an experiment had to be continued even in the presence of secondary nuclei.

CHAPTER 7

DISCUSSION

7.1 Accuracy of Measurement

7.1.1 The Determination of Growth Rates

It was unlikely that the seed crystal was mounted with its measured (101) face more than 10 degrees from the horizontal. Hence the maximum error due to this cause would be to make the growth rate smaller by 1½%. Since the growth rates are based on the time of growth between the eyepiece graticule divisions, the time error at low growth rates (ca. 10^{-5} cm/min) is (say) ± 10 min in 400 min, and at high growth rates (ca. 3×10^{-3} cm/min) it is (say) ± 5 seconds in 80 seconds. The growth rate error is therefore ± 2.5 to ± 6.3% respectively and the true overall rate may be in the range (+ 1%, -4%) to (+ 4.8,-7.8%) respectively. The actual error may tend to be at the extremes of these limits towards the end of an experiment due to the loss of focus with growth.

7.1.2 The Determination of Supersaturation (Δc)

The accuracy of the chemical analysis is claimed by Simons[96] to be better than ± 0.05%. Although bad practice, it was necessary to make up and weigh hot solutions - calibration showed that weighing solutions at up to 75°C caused an error of < 0.01 g and was therefore negligible since the masses involved ranged from ca.15 to 65 g Pe in 400 g of solution (an error of less than 0.07% at worst).

The largest single error is in the filtration when up to 0.1 g of Pe may be lost. It is also unlikely that the solubility data of Rogers'[84] is better than ± 0.1% (absolute).

Hence from the theory of combination of errors

$$\Delta c = \frac{M}{M+W} - c^* \quad \text{(mass fraction)} \tag{64}$$

and $$(\delta\Delta c)^2 \simeq \left(\frac{\partial \Delta c}{\partial M}\right)^2 (\delta M)^2 + \left(\frac{\partial \Delta c}{\partial W}\right)^2 (\delta W)^2 + \left(\frac{\partial \Delta c}{\partial c^*}\right)^2 (\delta c^*)^2 \tag{65}$$

$$\therefore \quad (\delta\Delta c)^2 \simeq \frac{W^2}{(M+W)^4} (\delta M)^2 + \frac{M^2}{(M+W)^4} (\delta W)^2 + (\delta c^*)^2 \tag{66}$$

(i) For the lowest supersaturations

$M = 15$ g, $W = 385$ g

$\delta M = \pm 0.1$

$\delta W = \pm 0.01$

$\delta c^* = \pm 0.001$

Hence $(\delta\Delta c) \simeq \pm 0.00025$

and $\Delta c = 0.0025$

i.e. $$\frac{\delta(\Delta c)}{\Delta c} \times 100 = \pm 10\%$$

(ii) For the highest supersaturation

$M = 65$ g $\qquad W = 335$ g $\qquad \Delta c = 0.025$

$$\frac{\delta(\Delta c)}{\Delta c} \times 100 = \pm 1\%$$

The maximum amount of seed growth $\simeq 0.015$ g; this would reduce the supersaturation in the worst case of the smaller cell G_1 (less volume of solution) by,

$$\delta\Delta c = \frac{0.015}{M^1 + W^1}$$

where $M^1 + W^1$ = mass of solution in the cell

$\sim$ 100 g

$\therefore \delta\Delta c = 0.00015$

At the lowest supersaturation error = $\frac{0.00015 \times 100}{0.0025}$ = 6% reduction

At the highest supersaturation error = $\frac{0.00015 \times 100}{0.025}$ = 0.6% reduction

Thus combining all the error in supersaturation, a total error of (+ 4%, -16%) at the lowest Δc and (+ 0.4%, -1.6%) at the highest Δc should be expected in the plots of log g versus log Δc.

7.1.3 The Determination of Temperature

The thermometers used were graduated in 0.10^{o}C and could be estimated to about 0.05^{o}C. The steam point and the transition point of hydrated Sodium Sulphate were checked for one test thermometer (under total immersion) and the values were found to be correct to within reading error. All thermometers used in the experimental work were checked against this test thermometer and the necessary correction factor applied. For the temperatures used in this work the correction for partial immersion was less than the reading error and therefore neglected.

7.1.4 The Determination of Impurity Concentration

(i) Di-Pe: The di-Pe was measured up to ± 0.0001 g. Thus, for the

minimum di-Pe concentration of 0.20 g/400 g solution, a maximum error of ± 0.05% was estimated.

(ii) Formal: The accuracy of Formal concentration is difficult to determine because of its non-availability as an isolated compound and because of its concentration variation in the extracted (un-hydrolysed) Pe. However, a maximum of ± 0.50% can be estimated.

7.2 Purification of Pe and Identification of (X)

The sequence of the purification procedure is important[99]. As stated earlier, a number of authors were unsuccessful in obtaining pure Pe by charcoal extraction[86,87]. This was probably due to their failing to remove di-Pe and Formal first and therefore these compounds saturated the charcoal before the critical impurity was adsorbed. Partly owing to its resistence to acid hydrolysis the impurity was originally thought to be a lubricant accidentally picked up during processing. However, the experiments reported here with selected impurity addition suggest that this is not so.

The work carried out by Farazmand[101], using the charcoal extraction technique developed in this work, has confirmed that impurity (X) does exist and that it is removed by activated charcoal (as suggested in the present work) as opposed to the addition of a counteracting impurity coming from the charcoal. It now appears that it may be a reaction by-product which does not contain an ether linkage (and therefore is not attacked by acid) and several possible compounds have been suggested and their effect on the growth rate of Pe crystals tested (Table 19). Only 1,1,1,trimethylolethane had any serious effect on the growth rate, but even this was not as

great as could have been expected if this were indeed the identity of impurity (X).

7.3 Growth Mechanism

Pure Solutions:

a) Diffusion Controlled Process: For a liquid phase bulk diffusion controlled process a plot of log g versus log X should be a straight line of slope unity. The results show that the minimum slope obtained had a value of 1.24 at the highest T of 50°C. At lower temperatures the slope was higher. Theoretical growth rates for a purely diffusion controlled process were calculated by substituting the estimated diffusivity of Pe in water from Spaldings correlation[102] into Ficks equation of 3D diffusion:

$$g = 2 D H \Delta c / L M \qquad (67)$$

These growth rates were found to be much higher than those measured under all working conditions. The energy of activation for crystal growth was found to be 8.47 Kcal/mol. Thus it appears that under the conditions investigated in this work the growth of Pe crystals is not purely diffusion controlled. This conclusion is further supported by the observed continuous variation of growth rate with time which cannot be explained by a purely bulk diffusion controlled process.

b) Two-Dimensional Nucleation: According to the equation (7) the TDN mechanism predicts a linear relationship between log g and 1/log (1+X). Correlation of the experimental growth rate results on this basis is unsatisfactory because of the non-linearity of the plot. Furthermore the observed growth rates at very low values of X of the order of 0.02 strongly suggest that at least TDN is not the rate controlling process.

c) Compound Growth Model: The compound models proposed by Bennema[38] and Botsaris et.al.[39] were suggested to fit the growth rate data of Potash alum and to explain the deviation from linearity between g versus X curves at high values of X. If both these authors' growth rate data are equally reliable a combination of them shows that the transition of the dependence of g on X, as X increases, is not from second to first power but the reverse. This result has not been explained by any theory and even the existence of a compound model is suspect[16]. A plot of log g versus 1/log (1+X) for the present data suggests the apparent existence of two straight lines for each temperature of 30, 40 and 50°C. Similar behaviour has been reported by Liu,et.al.[34] for the growth of $Mg.SO4\ 7H_2O$ and by Michael et.al.[103] during the growth of Adipic acid crystals. The latter group of authors combined the TDN and the dislocation theories and proposed a compound model. They proposed a distribution of sizes for surface nuclei at screw dislocations, the probability of activation of each size being dependent on supersaturation.

d) Dislocation Controlled Growth: The observed distinct surface imperfections and growth at low supersaturation ($X \leq 0.018$) strongly suggests that the growth of Pe crystals is dislocation controlled. The growth rates have a second order dependence on supersaturation at 10 and 20°C. At 30 and 40°C, however, a plateau is observed for Δc below 1.50×10^{-2} (Kg Solute/Kg Solution). At 50°C, the dependence on supersaturation is only 1.24. The theory of growth from dislocation predicts that growth rate should be proportional to the second power of supersaturation for low supersaturation and proportional to the first power of supersaturation for high supersaturation. Low supersaturation probably means X below 0.01.

A plateau similar to that observed at 30 and 40°C, at $\Delta c < 1.50$ has also been reported by Botsaris et.al.[39] for the growth of Potash alum crystals for $0.09 < X < 0.13$. It was suggested that this was due to an instability in growth process arising beyond a point at which the crystallisation was no longer bulk-diffusion (dislocation) controlled. The instability was suggested to arise either from the adsorption of a time-dependent impurity on the crystal surface or from the interference between MNTDN process and dislocation controlled surface diffusion process. Thus within this region of super-saturation, it was stated, a crystal could switch over from a higher to a lower growth rate and vice versa. Liu, et.al.[34] have also shown that the growth rate data for citric acid obtained by Cartier et.al. indicated that the dependence of growth rate on supersaturation decreased with decreasing supersaturation. Ovsienko et.al.[54] have also reported the existence of a plateau in the plot of growth rate versus supercooling for the growth of Salol crystals from melts. No explanation was offered for this phenomenon.

7.4 Effect of Impurities

7.4.1 Effect of Di-Pe

The presence of di-Pe gives rise to two main effects; a growth rate enhancement at low impurity concentrations and high supersaturations, and a growth rate depression at low supersaturations and high impurity concentrations.

7.4.1.1 Proposed Mechanisms of Growth Increase

The observed increase in growth rate (by as much as 60%) in the presence of di-Pe at 30 and 40°C (figures 23 & 24) is

real. Possible mechanisms proposed in the past are discussed in the following section.

a) Increased rate of TDN.

Impurities which reduce the nucleus edge free energy can increase the rate of TDN. Sears[74] proposed that this mechanism accounts for the observed increase in the rate of growth of thin plates of Lithium fluoride by the addition of 2×10^{-6} mole fraction of Ferric fluoride. The results of the present investigation, however, indicate that TDN as such is not involved in the growth of Pe crystals from aqueous solutions. In addition it seems unlikely that large di-Pe molecules could adsorb sufficiently rapidly (i.e. during nucleus formation) to reduce edge free energy and increase the growth rate of TDN.

b) Surface Flow of Solute.

It has occasionally been found that a rapidly growing face tends to impoverish the solution on adjacent faces and slows them down. Conversely, it has been suggested that faces adjacent to the retarded face tend to grow faster than otherwise[24,56]. It is suggested that this is due to the surface flow of solute from one face to another. Since the growth rate of only (101) face was measured this point cannot be ascertained with any certainty. However, if the observed increase in growth rate of (101) face was due to the retardation of growth on (001) and (110) faces, the face (101) should grow out of existence with time for a particular di-Pe concentration according to the overlapping principle. No such evidence was detected even for the maximum velocity increase obtained in the presence of di-Pe concentration of 0.15×10^{-2} at $\Delta c = 2.23 \times 10^{-2}$.

c) Reduction in Solubility.

Several instances have been reported where an impurity causes an enhancement in growth rate by decreasing the solubility of the crystallising material.[76] Appropriate corrections were made for the effect of di-Pe's presence on the solubility of Pe. Besides, di-Pe slightly increases the solubility of Pe and so the growth rate should decrease.

d) Increase in Dislocation Density by Impurity Incorporation.

It has often been proposed that impurity incorporation into a crystal lattice could disrupt the lattice and thereby create dislocations, possibly resulting in increased growth rates[54,67,69]. Frank's[15] treatment indicates that an increase in the number of dislocations should not markedly increase the growth rate since only most active dislocations or group of dislocations will determine the steady-state growth rate. However, it can be argued that the dislocations induced by impurity incorporation may be the most active. The effect would be expected to increase with the increase in impurity concentration until the retarding effect of the impurity overshadows the accelerating effect due to the creation of dislocations.

No di-Pe was actually detected by GC analysis in the seeds grown from solutions containing di-Pe. The results obtained from the X-ray analyses of seeds grown in the presence of di-Pe also do not show any straining of the Pe crystal lattice[96].

e) Negation of the effect of Another Impurity.

It has been reported that some cases of accelerated growth may be due to the negation of the retarding effect of another impurity[104].

It is thought in the present work that Formal and (X) in addition to di-Pe are alcohols. In the absence of a dehydrating agent it is not considered likely that a mutual reaction between any of these is possible and therefore any negating effect seems impossible.

f) Increased Rate of Step Generation

It has been suggested by Beck[29] that impurity adsorption at the dislocation centre could cause an increase in growth rate of a face containing the dislocation. Such an adsorption has been considered to reduce the edge energy of the step at the dislocation centre by effectively providing kinks in the highly curved step. This would in turn reduce the critical radius of curvature (ρ_c) and hence[15] increase the rate of step generation ($\omega/2\pi$). One could expect this enhancing effect to be significant only at low surface concentrations of impurity; as the concentration is raised the retarding effect of the impurities on step propagation should become increasingly important.

The adsorption of impurities on the dislocation centre could be considered to provide active sites on which Pe molecules might attach. That is, when the curvature at the dislocation centre is at its critical value (ρ_c) the addition of Pe molecules is extremely difficult because of the general curvature of the step and the resulting lack of neighbouring lattice molecules with which additional molecules may interact. However, even on a step of high curvature di-Pe may be adsorbed, thereby providing a stable kink at which a new row of Pe molecules may be initiated. In this way the step will move away from the dislocation more rapidly, with the result that the overall rate of step propagation will be increased.

This increase in step generation caused by the lowered edge energies of steps can account for the growth enhancement by di-Pe at one supersaturation. However, as the di-Pe concentration is increased, the increased retardation of step movement away from the dislocation by impurity adsorption may decrease the rate of new layer generation, and the overall growth rate of the crystal face is lowered. Thus the process appears to be a function of the concentration of di-Pe in the bulk of the solution which presumably alters its surface concentration. However, an interaction of the surface concentration of di-Pe with supersaturation is inevitable. The impurity would be expected to be either incorporated into the growing crystal or desorbed back into the solution and the surface concentration of the impurity would therefore depend upon super-saturation. Since the GC analysis indicates little or no incorporation of di-Pe into seed crystals, one would expect that the amount of di-Pe required to increase the activity of dislocation should decrease with decreasing supersaturations. The growth rate results are contrary to this (figures 23 & 24). This sugests that some di-Pe is incorporated into the growing crystal; the amount being beyond the detection limits of the Gas chromatographic technique used in this work. Thus with decreasing supersaturations more di-Pe would be expected to be incorporated and would therefore require higher impurity concentration in the bulk of the solution. An increase in temperature would similarly require less bulk impurity concentration at corresponding supersaturation.

7.4.1.2 Growth Reduction

Since the decrease in growth rate observed in the presence of di-Pe is very small under all the conditions investigated,

one could expect that the adsorption of di-Pe would be very small. Gas chromatographic analyses of the seeds grown in solutions containing di-Pe confirm this. It is however possible, as proposed above, that the little di-Pe adsorption and subsequent incorporation into the growing crystals is beyond the detection limit of the analytical technique used. However, its little effect on growth rate suggests that di-Pe is likely to have been weakly adsorbed on the growth steps.

7.4.2 Effect of Formal

The effect of Formal was always found to be the reduction of growth rates under all conditions investigated. At all supersaturations the growth was completely inhibited beyond a certain critical Formal concentration (X_c). The value of X_c increased with supersaturation and temperature (figures 27 & 28). The significant reduction in growth rate of the (101) face resulted in the change in the crystal habit and the faces (110) and (001) were found to grow out of existence.

The observed drastic growth rate reducing effect suggests that the rate of step propagation is severely hindered by the strong adsorption of Formal onto the crystal surface with the resultant incorporation into the crystal lattice. The results obtained from the gas chromatographic analyses of the seeds grown from solutions containing Formal show that Formal is in fact incorporated into the growing crystals. The interaction between impurity concentration and supersaturation can be explained either in terms of Frank's mechanism of time-dependent impurity adsorption[5] or by the mechanism

proposed by Cabrera and Vermilyea[42]. Both mechanisms require the impurity adsorption to take place on the plane region between the growth steps on a crystal surface.

In terms of Frank's mechanisms the motion of steps is hindered by their overtaking the adsorbed impurities. The impurities are rendered ineffective either by being incorporated into the crystals or by being desorbed after the passage of a step over a portion of the surface containing the impurity. If the equilibrium impurity adsorption were not attained then the impurity concentration at a point on a crystal surface would depend upon the time interval between the passage of two successive steps at that point. Thus at high supersaturation when the step flux at a point is sufficiently high the impurity concentration might be too small to cause any significant reduction in growth rate. If the step flux are reduced due to smaller supersaturation or higher surface impurity concentration, the steps would have higher impurity concentrations to be overtaken. This would slow the step propagation resulting in more impurity adsorption. Such a self aggregating process might continue until equilibrium adsorption of the impurity were attained. The process thus depends upon the initial surface impurity concentration which in turn depends upon the supersaturation and bulk impurity concentration. Such a process can explain the drastic reduction in growth with a slight increase in impurity concentration. However, it does not explain the complete inhibition of growth.

The mechanism proposed by Cabrera and Vermilyea explains

the reduction in growth rate in terms of an advancing step having to force its way between two adsorbed impurity molecules. The higher impurity concentrations will reduce the distance between adsorbed impurity molecules, ρ_x, decrease the radius of curvature of the advancing effect, ρ, and hence decrease the step velocity as proposed by the equation (11). Thus the growth rate of the crystal face will decrease. If the impurity concentration is such that ρ is comparable with ρ_c, the advance of a step will cease and complete growth inhibition will be observed. Such a critical impurity concentration, Xc, at which growth ceases has been occasionally reported in the literature[29,77]. If, however, the supersaturation in the bulk of the solution is increased, ρ_c will decrease and therefore greater impurity concentration will be required to reduce ρ to be comparable with ρ_c. An increase in temperature will have the same effect. It implies from this theory that for every supersaturation there exists a certain critical impurity concentration above which no growth should occur.

The change in crystal habit suggests that Formal is adsorbed onto the face (101) preferentially more than on the faces (001) and (110).

7.4.3 Effect of other Impurities

Of all the other impurities used only NaOH, HCHO and 1,1,1,trimethylolethane had a significant reducing effect on growth rate. NaOH was found to completely inhibit the growth rate above Xc. For the other impurities Xc was not determined. The

observed change in crystal habit (disappearance of (001) and (110) faces) and the severe reduction in growth rates suggest that these impurities are strongly adsorbed onto the (101) face. It is suggested that like Formal, these impurities are adsorbed between the growth steps and are subsequently incorporated into the growing crystals. The growth retardation can probably be explained in terms of the mechanism proposed by Cabrera and Vermilyea.

7.5 The Rythmicity of Crystal Growth

The growth rates of Pe crystals in pure solutions and in solutions containing added impurities have been found to vary continuously with time and from seed to seed under constant supersaturation and temperature. Although the amplitude of oscillation decreases with an increase in supersaturation, the difference in average growth rates of different experiments increases with an increase in supersaturation. Both high and low initial growth rates are possible except at very low supersaturations and temperatures where the initial growth rates are generally the highest. A growth reducing impurity generally yields highest initial growth rates and reduced its amplitude of oscillation.

The basic theory of crystallisation suggests that the linear growth rate of a crystal face should be independent of time under steady-state conditions. The steady-state has tentatively been assumed to depend only upon external conditions in the bulk of the pure solution. The concept of a pure solution appears to be hypothetical as occasionally a solvent has been found to act as an

impurity[69], and in any case trace impurities are always present. Besides, even the growth of crystals from melts has been found to change with time under constant external conditions existing in the bulk of a system[54]. This suggests that the attainment and the maintenance of steady-state conditions also depends upon factors other than the conditions in the bulk of the system. These uncontrollable factors can be associated with the external conditions existing at the surface of a crystal. A change in these can arise due to one or more of the following causes:-

1. Mechanism of growth: Sheftal[19] has suggested that growth by TDN can give rise to substantial changes in temperature and supersaturation existing at the surface of a crystal. Such changes can occur because of the chance formation of two-dimensional nuclei and their subsequent rapid lateral growth across the crystal surface. Since the growth of Pe crystals does not appear to be surface nucleation controlled, such a change cannot be attributed to the observed oscillating growth rates in the present work.

2. The formation of inclusions: The formation of inclusions has been suggested to be a rythmic process which can cause a periodicity in the conditions existing on the surface of a crystal[19]. Thus rapid increase in growth rates have been occasionally attributed with the formation of inclusions[69]. The inclusion formation was only seldom observed in Pe crystal growth.

3. Change in control mechanism: It has been suggested that the growth of a crystal takes place by more than one mechanism at all conditions[39]. The controlling mechanism has been suggested to vary with supersaturation. A change in controlling mechanism

from a dislocation controlled growth to surface nucleation controlled growth is likely to cause fluctuation in growth because of the nature of the TDN process. However, if the oscillation in growth rate is observed during both processes, the scale of oscillations has been suggested to decrease with a change in controlling mechanism from dislocation controlled growth to surface nucleation controlled[20,54]. In the present work the amplitude of oscillation was not found to follow a particular pattern with an increase or decrease in supersaturation which could change the controlling mechanism.

4. Impurity adsorption: Several reports appear in literature in which the adsorption of an impurity has been expected to cause instability in the growth process[16,25,39,67,68]. The main suggestions have been that an impurity can increase the growth rate in several ways: by decreasing the energy of formation of two-dimensional nuclei, by increasing the rate of step generation, or by increasing the number of screw dislocations. A decrease in growth rate has been attributed to the poisoning of active sites by the adsorbed impurities. However, none of these mechanisms seems to offer a suitable explanation of the continuous change in growth rates observed in the growth of Pe crystals at all supersaturations. A better explanation can be offered if one assumes the continuous formation and disintegration of macroscopic steps from and into microscopic steps due to an impurity adsorption. Frank[5] has suggested that such a process is continuous and depends upon the surface concentration of the time-dependent adsorbed impurity. The variation in growth rate with the formation and disintegration of macroscopic steps has actually been observed with a change in

supersaturation[43]. A more convincing argument of the presence of an impurity leading to instabilities in the growth process comes from the mathematical analysis of Ohara[16]. He deduced that for any $X >> X_c$ there can be two different growth rates for a single set of experimental conditions.

It is likely that even the purest Pe used in this work (hydrolysed and extracted) contained trace quantities of Formal and (X). The interaction of these impurities with the growth process might lead to such fluctuations or it might have been possible that this effect was caused by the presence of solvent water.

5) Activity of a Dislocation: The linear growth rate of a crystal face is proportional to the rate of generation of steps (i.e.the activity of dislocation)

$$g \alpha \omega/2\pi$$

A change in the activity of a dislocation will therefore alter the growth rate. Frank[15] has suggested that the activity of a group of dislocations depends upon the number of interacting spirals, their sign, and their distance apart. The absolute value has been suggested to vary from zero to as much as the number of dislocations contained within the group. In the case of random distribution of screw dislocations the resultant activity is always that of the most active group of dislocations. Thus, many authors have attributed the observed variation in growth rate in their work to the changing activity of the dislocations[53,54,60,64,65].

The continuous variation in growth rate of Pe under all conditions of temperature could be a result of the changing activity of dislocations due to mutual annihilation and co-operation of spirals. However, if this was the only reason responsible for the changing growth rates, the maximum values of growth rates should follow a linear law as suggested by Frank. Such a dependence of maximum growth rate on supersaturation has actually been observed in the growth of Salol crystals from the melt[54]. The growth rate results of Pe show that apparently such a dependence is not obtained and that the maximum and the minimum growth rates have the same dependence on supersaturation as that of representative growth rates g. However, there is a certain amount of unreliability in the initial value of g due to the time needed to take the first reading.

The above discussion suggests that the observed rythmicity in the growth rate of Pe crystals may be due to either or both of the effects of impurities and that of the interaction between spirals.

7.6 Secondary Nucleation

7.6.1 Pure Solutions

The hot filtration of pure Pe solutions through 0.1 micron filters increases the supersaturation above which the growth of a single crystal without excessive secondary nucleation was found impossible. This suggests that the presence of particles > 0.1 μm activates the process of nucleation. The presence of heterogeneous particles has usually been suggested to facilitate nucleation by causing a reduction in the overall free energy change required due

to two-dimensional nucleation. The most active hetero nuclei in liquid solutions have been suggested to lie in the range 0.1 to 1 μm.[79] Belyustin and Rogacheva[52] suggested that these particles were activated on the surface of a Salol crystal (or on a left-handed quartz crystal) and converted into crystallisation nuclei. However, they did not explain the formation of relatively greater proportions of right-handed Salol crystals in the presence of a left-handed quartz crystal. Besides, the necessity of a crystal surface to activate these heterogeneous particles was also not explained. Thus it appears that the presence of these hetero particles in pure Pe solutions may activate primary nucleation rather than secondary nucleation.

The insertion of the seed crystals in filtered solutions resulted in the immediate appearance of secondary nuclei at the bottom of the cell. In fact these nuclei were actually observed to fall from the surface of the solutions and also from that of the crystal seed. The fact that careful pre-washing of the seed eliminated the appearance of nuclei under all working conditions for a considerable time strongly favours the concept of initial breeding as proposed by Strickland-Constable[44].

The time for the appearance of nuclei after the elimination of initial breeding, the induction period ($t_{s.n.}$) decreased as growth rate increased (figure 21) except at growth rates below 1×10^{-4} cm/min when no nuclei were observed for very long periods. Although the exact mechanism of the formation of these nuclei is not clear, it appears to be due to the detachment of some kind of

microsurface irregularities or loosely bonded molecular units the number of which increases with the growth rate. The increase in local supersaturation in the vicinity of the crystal surface due to the decreased solubility in the ordered water layer could be another possibility. The two mechanisms can be operating together as has been suggested by Denk and Botsaris[48].

The dendritic model of secondary nucleation does not seem to be applicable here as no dendrite formation was observed. Similarly the ICG nucleation model[50] is not acceptable because of the solutions being essentially pure. Even if an impurity is present (e.g. (X)) its concentration is likely to be more in Pe solutions unextracted with charcoal, in which case the effect ought to be more pronounced. The reverse was found to be true i.e. the critical supersaturation was much higher in unextracted solutions than in extracted solutions.

7.6.2 Solutions with added Impurities

The addition of certain impurities like di-Pe, Formal, HCHO and NaOH to filtered pure Pe solutions appear to reduce or completely prevent the appearance of secondary nuclei at all supersaturations used. In other words these impurities increased the maximum supersaturation above which crystal growth without excessive secondary nucleation was found to be impossible. Thus the presence of 0.75 g of di-Pe increases this supersaturation from about 2.60×10^{-2} to 4.23×10^{-2} (fig.23) at one temperature. Within the operable conditions of temperature and supersaturation in the presence of

di-Pe, $t_{s.n.}$ continuously decreases with growth rate (figure 25). With the exception of di-Pe, all the other nucleation suppressing impurities were found to reduce the crystal growth rate.

Numerous instances have been reported where impurities have been found to inhibit nucleation, or at least raise the maximum supersaturation at which well-formed crystals could be grown without secondary nucleation occurring. The effect of the impurity has usually been considered to be either due to the complete poisoning and inactivation of the homogeneously formed embryos or heterogeneous nuclei (which might exist in the most carefully purified solutions) or else retardation of growth on these nuclei.

With di-Pe in question, the ICG nucleation model does not seem to apply as no incorporation of the impurity was observed.

CHAPTER 8

CONCLUSIONS

1. The growth rate of Pe crystals varied with time under constant external conditions of temperature and supersaturation. The maximum growth rate can be many times higher than the minimum. The growth rate also varied from one seed to another of the same size and under the same conditions of temperature and supersaturation.

2. The crystals grown from the commercial Pe have a growth rate $< 10^{-6}$ cm/min and contain only the triangular (101) faces. The removal of the by-product impurities by acid hydrolysis increases the growth rate by at least an order of magnitude.

3. Treatment with activated charcoal reduces an impurity (X) below a threshold limit in the hydrolysed Pe. A maximum of three extractions is required.

4. The removal of (X) increases the growth rate further by at least an order of magnitude. The crystals grown from the hydrolysed and extracted Pe contain crystallographic faces (101), (001) and (110).

5. The purification of Pe makes the solutions very sensitive to secondary nucleation and limits the duration of an experiment and the range of useful supersaturation.

6. The growth rate of pure Pe does not depend upon the size and the purity of the seed crystal.

7. Growth of the purified material was observed under all conditions down to a supersaturation of the order of 0.02.

8. The growth rates estimated for a purely diffusion controlled process were more than an order of magnitude higher than the experimental values.

9. The growth of purified Pe is dislocation controlled. The data satisfies a parabolic law of the dislocation theories over most of the conditions of temperature and supersaturation. The rate constant is given by

$$k = A_o \exp(-8470/RT)$$

and $A_o = 4.62 \times 10^6$

10. Secondary nucleation is greatly reduced by the filtration through 0.1 μm size filters and by careful washing of the seed crystal.

11. The mechanism of secondary nucleation appears to depend upon the growth rate value. At low growth rates it involves initial breeding by the seed crystals, and at high growth rates it probably occurs by the detachment of surface irregularities or loosely bonded molecular units.

12. The addition of di-Pe enhances the growth rate at low concentrations and high supersaturations. At high di-Pe concentrations and low supersaturations the effect is generally to reduce the growth rate.

13. The addition of Formal always reduces the growth rate drastically and above a critical Formal concentration the growth ceases. An average surface energy per unit area of the order of 30 ergs/cm^2 has been calculated for the face (101) when the growth is completely inhibited.

14. The faces (110) and (001) rapidly grow out of existence in the presence of Formal thereby suggesting that Formal is preferentially adsorbed on the face (101).

15. NaOH, HCHO, and 1,1,1, trimethylolethane greatly reduce the growth rates.

16. The impurity (X) appears to be 1,1,1,trimethylolethane or a similar compound.

17. The enhancement in growth by the addition of di-Pe is probably due to its adsorption in the vicinity of the dislocation centre thereby increasing the rate of step generation.

18. The reduction in growth rate by Formal addition is probably due to its strong adsorption on the planar regions between the growth steps on the (101) face.

19. The oscillation of growth rate appears to be due to the combined effect of impurity adsorption and the interaction between the growth spirals.

CHAPTER 9

FUTURE RECOMMENDATIONS

1. The growth of Pe crystals appears to be dislocation controlled under the conditions investigated. However, the mode of dislocation control is not certain. It is suggested, therefore, that the velocity effects on the growth of Pe crystals should be determined.

2. The use of single crystal growth technique involves the tedious mounting of crystals and the difficult prevention of secondary nucleation. Besides, the initial growth rates also depend upon the state of the crystal seed. Other crystal growth techniques like the nucleation and growth on a substrate should be investigated for comparison of data.

3. The growth rates of the crystallographic faces (001) and (110) should be measured to obtain a complete picture of Pe crystal growth.

4. The use of a linear microscope limits the observation only to the elevation of the face whose growth rate is to be measured. A close observation of the surface structure of the various faces should be determined along with their growth rates to elucidate the mechanism of growth oscillations. It is therefore suggested that use be made of a cinematograph or an interference microscope for future work on single crystal growth.

5. The identity of the impurity (X) has been suggested to be a compound 1,1,1,trimethylolethane in the present work because of its reducing effect on the growth rate of Pe crystals. It is likely, however, that other compounds similar in structure to 1,1,1,

trimethylolethane might have a greater growth reducing effect. The effect of compounds such as trimethylolpropane on the growth rates should therefore be determined. The formation of such a compound should also be established in the Pe preparation.

6. Growth rates should also be measured in the absence and in the presence of secondary nucleation, to determine if the nuclei are formed three dimensionally.

7. Impurities like Formal, (X), HCHO, and NaOH appear to adsorb strongly on the face (101). This indicates their possible incorporation into the growing crystal. However, in the absence of an adsorption isotherm the result is inconclusive. It is suggested, therefore, that to elucidate the mechanism of impurity effect, adsorption isotherms should be determined for several impurities on the three crystallographic faces.

CHAPTER 10

APPENDIX

10.1 Experimental Techniques

10.1.1 Secondary Nucleation

The polishing of the cell S_1 prevented the formation of secondary nuclei up to a period of 15 hours for T = 60^{o}C and Δc = 4.00×10^{-2} (KgPe/Kg solution). However, the growth rates obtained were of the order of 10^{-6} cm/min due to the presence of the impurity (X). The extraction of (X) increased the growth rates by two orders of magnitude and it was found almost impossible to prevent secondary nucleation for more than a few minutes at this increased growth rate in the glass cell G_1 or the metal cell S_2. The observed oscillating growth rates necessitated the prolonged duration of an experiment in order to obtain a representative growth rate, and therefore it was required to seek some method of eliminating secondary nucleation for longer periods. Although the complete prevention of the formation of any secondary nucleus for an indefinite period was found impossible in this work, the development of several techniques made it possible to perform an experiment without growing the undesired nuclei for a satisfactory period.

The Pe solutions prepared in a beaker were filtered hot through 0.1 μm membrane filters to attempt to eliminate microscopic particles which could provide active sites for heterogeneous nucleation. The cell temperature was initially at least 10^{o}C above the working temperature when solution was transferred from the filtering flask

into the cell. The most difficult task was found to be the prevention of initial breeding during the insertion of the seed crystal into the cell solution. A considerable amount of secondary nuclei was obtained when the seed was at room temperature before insertion. The extreme brittleness of Pe crystals and their poor resistence to mechanical and thermal shock had already been appreciated by Rogers[84]. The removal of (X) in the present work was found to increase the sensitivity and it was required to keep the seed crystal at not less than the same temperature as the solution.

Initially the mounted seed crystal was heated along with its support rod by a hot air blower to a temperature of 80°C before insertion into the cell. Unfortunately this also resulted in thermal shock causing fracture on insertion. Various seed temperatures were then tried without any success. It was then decided to immerse the mounted seed and the rod into Pe solutions of varying concentrations below the working concentration, at various temperatures and for varying periods of time. The aim was firstly to remove any small nuclei which might have grown over the seed crystals during the seed preparation, and secondly to coat the seed surface with a layer of solution. However, still no significant improvement was achieved. Finally it was decided to use distilled water at various temperatures instead of Pe solutions. A temperature of distilled water 5-10°C above the working temperature proved to be the most successful in preventing the initial breeding of secondary nuclei for the required duration of the experiment. However, at the highest growth rates (of the order of 10^{-3} cm/min) experiments could not be performed for as long a duration as at low growth rates due to other kinds of breeding.

However this technique was used throughout the experimental work for the initial curing of seed crystals.

10.1.2 Preparation of Seed Crystals

The preliminary experiments indicated that the linear growth rate of Pe crystals in pure solutions was very strongly influenced by the imperfection of seed crystals. This necessitated the investigation of several techniques in order to achieve the production of crystal seeds of consistent quality. All the Pe used was carefully purified by the hydrolysis and extraction of the commercial material and attempts were first made to obtain the seed crystal by the classical techniques.

In the first attempt saturated solutions were nucleated by slow cooling and stirring in closed containers. The cooling rate achieved was not uniform and the crystals obtained were of poor quality and unsuitable for microscopic work. Secondly ground purified Pe was added to the supersaturated solutions of Pe which were stirred. The quality of the seed was still not much improved. Thirdly, attempts were made to grow crystals by self nucleation on a substrate (Epitaxial Growth). The earlier work on Epitaxial growth of seed crystals from solutions of hydrolysed Pe in test tubes had shown that tinned copper wire was the best substrate as far as the quality of the crystals was concerned. The minimum concentration difference requirement however, was found to be 8.00×10^{-2} at $60^{o}C$ for the growth of crystals within a reasonable duration of time. Experimental conditions were repeated with solutions of hydrolysed and extracted Pe at various supersaturations

and temperatures down to $\Delta c = 0.50 \times 10^{-2}$ (KgPe/Kg Solutions) and $30^{o}C$. Crystals of satisfactory quality could still not be obtained. At high supersaturation and temperatures masses of small crystals were obtained whereas at low temperatures and supersaturation a few crystals with exaggerated growth were obtained perhaps because of the proximity of the test tube walls.

Crystals of much better quality were finally obtained by crystallisation from stagnant solutions. The quality of the seeds obtained from this technique depended entirely upon the supersaturation achieved at the time of nucleation. Thus, high supersaturations usually led to a large number of small poorly formed crystals. At low values of supersaturation crystallisation frequently did not take place and when it did, only a few large good crystals were formed. Therefore, an intermediate supersaturation was chosen to obtain a satisfactory number of well formed crystals. The technique is described in section (5.5) and was followed throughout the experimental work for the preparation of seed crystals.

10.1.3 Mounting of Seed Crystals

The seed crystals used initially, for a part of the preliminary experiments (Exp. 1 - 30, section 6.3), were those which were grown from Pe solutions purified with hydrochloric acid and passed over molecular sieves. After the successful extraction of (X) with charcoal the seed crystals used throughout the experimental work were only those which were grown from Pe solutions purified with hydrochloric acid and charcoal. All such crystals had (001) and

(110) faces apart from the generally found faces (101) on crystals grown from the material containing (X). These crystals were mounted on one end of a "J" shaped glass rod with Tensol cement (a low molecular weight polymethyl methacrylate). The single crystals were so positioned that a face (101) was always as horizontal as possible. The continued observation of the oscillating growth rates even in the absence of secondary nucleation suggested that perhaps the polymer cement was slightly soluble or had a plasticizer which was leached out by Pe solution. Another glue, Durofix cement (a water resistent, nitrocellulose-based adhesive) was therefore tried. The rythmicity of crystal growth still persisted. It was thought that perhaps the presence of a plasticizer in both the above glues was responsible for this behaviour. A polystyrene contact cement was then used which was claimed by the manufacturer to be free of any plasticizer but even this technique failed to yield a steady-state growth.

Seed holders were then made from lengths of type 316 stainless steel rods 1.50 mm in diameter. One end of the holders was sharpened and the rod was heated to a temperature above the melting point of Pe(~ 260^{o}C). The sharp hot end was then plunged into the seed crystal at the appropriate point. Although this technique had been successfully employed by Botsaris and Denk[38], the melting point of Pe being much higher than that of Potash alum used by Botsaris and Denk and the Pe crystals being very brittle, thermal shocks always resulted in mechanical fracture making this technique unsuitable. To minimise the temperature difference between

the rod and the seed, the seed crystal was preheated to a temperature of 150^{o}C before bringing it in contact with the rod. The seed crystals were still found to be shattered and even in one or two cases when success was achieved initially during mounting, mechanical fracture occurred when the seed was inserted into the Pe solution. Molten lead was then used to form an intermediate layer between the sharpened end of the rod and the seed crystal but without success. Unsuccessful attempts were also made to drill Pe crystals.

Metal tweezers (drawing board pen) were also used to hold the seeds in the required position. Although, this proved to be a more successful technique than the previous ones it offered two main difficulties; firstly, all the attempts to prevent secondary nucleation, resulting from the breakage of tiny crystallites at the points where the two prongs held the seed, failed. Secondly, it was not found possible to mount the tweezers sufficiently rigidly for microscopic work.

Finally, a very simple technique was tried and was found to be the most successful of all in ensuring that the unsteady state growth rates were not due to any glue. Different shaped holes (circular, triangular and rectangular) were made in the end of the "J" shaped glass rod and washed seed crystals were rested on these holes without the use of any glue and the whole assembly was then lowered into the Pe solution. In each case it was found that the only time when the seed tends to fall is when it passes the liquid/air interface. Therefore, the crystal was gently held in place

during the lowering operation by resting another glass rod on top of it.

Experiments conducted with seeds mounted by this last technique still exhibited the continuous increasing and decreasing growth rates thereby confirming that this is a real crystallisation effect and not due to any impurity from the glue. Although the above technique was satisfactory for test experiments, it was decided not to use this technique of crystal mounting for actual growth tests because of the inhibition of the growth of those crystal faces which were touching the walls of the glass rods inside the holes. Such an inhibition of growth of some faces would not permit the close observation of the change in crystal habit. Therefore, throughout the rest of the experimental work Durofix cement was used as a glue for mounting seed crystals on glass rods.

10.2 Tables

TABLE 1

Reticular Densities of Pe crystals

Tetragonal bipyramid (class 4/mmm)

2nd order {h0l} $c_o/a_o = 1.4345$

Face	Reticular Density
{101}	1.000
{001}	0.873
{110}	0.860
{111}	0.613
{100}	0.609

TABLE 2

PRELIMINARY EXPERIMENTS WITHOUT IMPURITY ADDITION

Exp.	Solute	T (C^o)	$\Delta c \times 10^{+2}$ (KgPe/Kg Solution)	g(max) (cm/min)	g(min) (cm/min)	g(avg.1) (cm/min)	g(avg 2) (cm/min)
1	D	60	2.00	7.99×10^{-6}	-	-	-
2	D	60	2.00	3.25×10^{-6}	-	-	-
3	DH	60	2.00	3.75×10^{-5}	-	-	-
4	DH	60	2.00	2.72×10^{-5}	-	-	-
5	DH	60	2.00	2.25×10^{-5}	-	-	-
6	DHE(13X)C_1	60	2.00	1.29×10^{-5}	-	-	-
7	DHE(13X)C_1	60	2.00	2.78×10^{-5}	-	-	-
8	DHE(13X)C_2	60	2.00	3.78×10^{-5}	-	-	-
9	DHE(13X)C_2	60	2.00	1.88×10^{-5}	-	-	-
10	DHE(13X)C_3	60	2.00	3.52×10^{-5}	-	-	-
11	DHE(13X)B_3	60	2.00	2.46×10^{-5}	-	-	-
12	DHE(13X)B_6	60	4.00	4.12×10^{-5}	-	-	-

cont'd

TABLE 2 continued...

Exp	Solute	T (C^o)	$\Delta c \times 10^{+2}$ (Kg/Pe/Kg solution)	g(max) (cm/min)	g(min) (cm/min)	g(avg.1) (cm/min)	g(avg.2) (cm/min)
13	DHE(13X)B_3	60	4.00	5.38×10^{-5}	-	-	-
14	DHE(4A)C_3	60	4.00	6.12×10^{-5}	-	-	-
15	DHE(5A)C_3	60	4.00	6.37×10^{-5}	-	-	-
16	DHE(NK)B_1	60	2.00	2.52×10^{-3}	-	-	-
17	DHE(NK)B_1	60	1.00	7.81×10^{-4}	-	-	-
18	DHE(NK)B_1	60	1.00	4.82×10^{-4}	-	-	-
19	DHE(NK)B_1	60	1.00	6.02×10^{-4}	-	-	-
20	DHE(NK)B_1	60	0.30	2.15×10^{-4}	-	-	-
21	DHE(NK)B_1	40	2.00	1.80×10^{-3}	-	-	-
22	DHE(NK)B_1	30	2.00	4.62×10^{-4}	7.35×10^{-5}	8.95×10^{-5}	1.33×10^{-4}
23	DHE(NK)B_1	30	2.00	4.52×10^{-4}	7.50×10^{-5}	1.10×10^{-4}	1.82×10^{-4}
24	DHE(NK)B_1	30	2.00	3.15×10^{-4}	9.12×10^{-5}	2.17×10^{-4}	2.50×10^{-4}

cont'd

TABLE 2 continued...

Exp	Solute	T (C^o)	$\Delta c \times 10^{+2}$ (Kg/Pe/Kg solution)	g(max) (cm/min)	g(min) (cm/min)	g(avg.1) (cm/min)	g(avg.2) (cm/min)
25	DHE(SX1)B_1	30	2.00	3.33×10^{-4}	9.33×10^{-5}	2.38×10^{-4}	2.26×10^{-4}
26	DHE(SX1)B_2	30	2.00	5.77×10^{-4}	3.13×10^{-4}	4.21×10^{-4}	4.27×10^{-4}
27	DHE(SX1)B_3	30	2.00	5.33×10^{-4}	3.45×10^{-4}	4.32×10^{-4}	4.28×10^{-4}
28	DHE(SX1)B_4	30	2.00	6.04×10^{-4}	2.95×10^{-4}	4.80×10^{-4}	4.15×10^{-4}
29	DHE(SX1)B_6	30	2.00	6.78×10^{-4}	3.58×10^{-4}	4.29×10^{-4}	4.78×10^{-4}
30	DHE(SX1)B_3	30	2.00	5.33×10^{-4}	3.25×10^{-4}	4.48×10^{-4}	4.80×10^{-4}
31	DHE(SX1)B_3	30	2.00	5.66×10^{-4}	3.37×10^{-4}	4.03×10^{-4}	3.88×10^{-4}
32	DH	30	2.00	1.58×10^{-5}	-	-	-

TABLE 3

PRELIMINARY EXPERIMENTS WITH IMPURITY ADDITION

Exp	Solute	Cell	Impurity	Glue	g(max) (cm/min)	g(min) (cm/min)	g(avg.1) (cm/min)	g(avg.2) (cm/min)
33	DH	S_2	Charcoal	No glue	2.05×10^{-5}	-	-	-
34	DHE(SX1)B_3	S_2	-	-	6.25×10^{-4}	2.48×10^{-4}	4.75×10^{-4}	4.32×10^{-4}
35	DHE(SX1)B_3	S_2	Water containing (X)	No glue	5.32×10^{-5}	-	-	-
36	DHE(SX1)B_3	S_2	Deionized Water	No glue	6.82×10^{-4}	3.25×10^{-4}	4.13×10^{-4}	4.33×10^{-4}
37	DHE(SX1)B_3	S_2	" "	No glue	6.35×10^{-4}	2.75×10^{-4}	4.50×10^{-4}	3.73×10^{-4}
38	DHE(SX1)B_3	G_1	-	Durofix	6.25×10^{-4}	2.95×10^{-4}	4.75×10^{-4}	4.50×10^{-4}
39	DHE(SX1)B_3	G_1	-	Polystyrene Cement	5.54×10^{-4}	2.75×10^{-4}	4.33×10^{-4}	4.75×10^{-4}
40	DHE(SX1)B_3	S_2	Perspex Cement	Perspex Cement	5.85×10^{-4}	3.13×10^{-4}	4.53×10^{-4}	4.50×10^{-4}
41	DHE(SX1)B_3	S_2	Durofix	Perspex	6.88×10^{-4}	3.21×10^{-4}	4.63×10^{-4}	4.23×10^{-4}
42	DHE(SX1)B_3	G_1	Durofix	Durofix	6.33×10^{-4}	3.15×10^{-4}	4.72×10^{-4}	4.79×10^{-4}

cont'd

TABLE 3 continued...

Exp	Solute	Cell	Impurity	Glue	g(max) (cm/min)	g(min) (cm/min)	g(avg.1) (cm/min)	g(avg.2) (cm/min)
43	DHE(SX1)B_3	S_2	Polystyrene	Polysterene	$8.25x10^{-4}$	$4.28x10^{-4}$	$5.53x10^{-4}$	$6.13x10^{-4}$
44	DHE(SX1)B_3	G_1	None	No glue	$6.13x10^{-4}$	$3.37x10^{-4}$	$4.95x10^{-4}$	$5.33x10^{-4}$
45	DHE(SX1)B_3	S_2	None	No glue	$5.35x10^{-4}$	$1.53x10^{-4}$	$3.25x10^{-4}$	$4.17x10^{-4}$
46	DHE(SX1)B_3	S_2	Araldite	Durofix	$6.75x10^{-4}$	$2.86x10^{-4}$	$4.37x10^{-4}$	$4.95x10^{-4}$
47	DHE(SX1)B_3	G_1	Neoprene	Durofix	$8.38x10^{-4}$	$3.88x10^{-4}$	$5.11x10^{-4}$	$5.65x10^{-4}$
48	DHE(SX1)B_3	G_1	Araldite	Durofix	$6.81x10^{-4}$	$2.77x10^{-4}$	$4.32x10^{-4}$	$4.62x10^{-4}$
49	DHE(SX1)B_3	S_2	Neoprene	Durofix	$6.26x10^{-4}$	$3.12x10^{-4}$	$4.82x10^{-4}$	$4.50x10^{-4}$
50	DHE(SX1)B_3	G_2	None	No glue	$7.13x10^{-4}$	$3.75x10^{-4}$	$4.73x10^{-4}$	$4.93x10^{-4}$
51	DHE(SX1)B_3	G_2	None	No glue	$6.50x10^{-4}$	$3.28x10^{-4}$	$4.55x10^{-4}$	$5.03x10^{-4}$
52	DHE(SX1)B_3	G_2	None	Durofix	$6.71x10^{-4}$	$3.33x10^{-4}$	$4.45x10^{-4}$	$4.83x10^{-4}$
53	DHE(SX1)B_3	S_2	None	Durofix	$6.81x10^{-4}$	$3.38x10^{-4}$	$4.12x10^{-4}$	$4.98x10^{-4}$

TABLE 4

Linear Growth Rate without Impurity at 50°C ($c^* = 13.64 \times 10^{-2}$ KgPe/Kg solution)

Total Growth time = Time for the secondary nucleation ($t_{s.n.}$)

Exp No.	$\Delta c \times 10^{+2}$ (KgPe/Kg Solution)	Total Growth Time (min)	g(min) (cm/min)	g(max) (cm/min)	g(avg.1) (cm/min)	g(avg.2) (cm/min)
54	2.36	32	6.82×10^{-4}	1.28×10^{-3}	1.06×10^{-3}	9.53×10^{-4}
55		31	8.08×10^{-4}	2.11×10^{-3}	1.10×10^{-3}	1.05×10^{-3}
56		22	7.10×10^{-4}	2.00×10^{-3}	1.10×10^{-3}	9.60×10^{-4}
	Average of various g		7.30×10^{-4}	1.79×10^{-3}	1.08×10^{-3}	9.87×10^{-4}
57	1.86	26	5.62×10^{-4}	1.91×10^{-3}	8.25×10^{-4}	8.85×10^{-4}
58		36	6.78×10^{-4}	1.39×10^{-3}	7.65×10^{-4}	8.10×10^{-4}
59		40	5.50×10^{-4}	1.20×10^{-3}	7.85×10^{-4}	7.80×10^{-4}
	Average of various g		5.96×10^{-4}	1.50×10^{-3}	7.91×10^{-4}	8.27×10^{-4}
60	1.36	48	3.94×10^{-4}	1.10×10^{-3}	6.25×10^{-4}	6.22×10^{-4}
61		40	3.86×10^{-4}	1.19×10^{-3}	7.20×10^{-4}	6.92×10^{-4}
62		80	4.26×10^{-4}	6.40×10^{-4}	6.22×10^{-4}	5.38×10^{-4}
	Average of various g		3.96×10^{-4}	9.80×10^{-4}	6.56×10^{-4}	6.14×10^{-4}

CONT"D

TABLE 4 continued...

Exp No.	$\Delta c \times 10^{+2}$ (KgPe/Kg Solution)	Total Growth Time (min)	g(min) (cm/min)	g(max) (cm/min)	g(avg.1) (cm/min)	g(avg.2) (cm/min)
63	0.86	76	2.56×10^{-4}	5.61×10^{-4}	3.08×10^{-4}	3.58×10^{-4}
64		110	2.64×10^{-4}	3.48×10^{-4}	3.26×10^{-4}	3.12×10^{-4}
65		104	1.36×10^{-4}	3.40×10^{-4}	3.18×10^{-4}	2.16×10^{-4}
	Average of various g		2.19×10^{-4}	4.16×10^{-4}	3.17×10^{-4}	2.95×10^{-4}
66	0.50	150	7.82×10^{-5}	1.19×10^{-4}	1.15×10^{-4}	1.04×10^{-4}
67		120	1.92×10^{-4}	5.90×10^{-4}	2.12×10^{-4}	2.27×10^{-4}
	Average of various g		3.51×10^{-5}	3.54×10^{-4}	1.63×10^{-4}	1.65×10^{-4}
68	0.25	(300) No nucl^{n}.	2.11×10^{-5}	2.98×10^{-5}	5.84×10^{-5}	2.25×10^{-5}
69		223	9.60×10^{-5}	1.37×10^{-4}	7.36×10^{-5}	9.75×10^{-5}
	Average of various g		5.85×10^{-5}	8.34×10^{-5}	6.60×10^{-5}	6.00×10^{-5}

TABLE 5

Linear Growth Rate without Impurity at 40°C ($c^* = 10.30 \times 10^{-2}$ KgPe/Kg solution)

Total Growth Time = Time for the secondary nucleation ($t_{s.n.}$)

Exp No.	$\Delta c \times 10^{+2}$ (KgPe/Kg Solution)	Total Growth Time (min)	g(min) (cm/min)	g(max) (cm/min)	g(avg.1) (cm/min)	g(avg.2) (cm/min)
70	2.60	40	1.02×10^{-3}	1.21×10^{-3}	1.11×10^{-3}	9.20×10^{-4}
71		34	6.98×10^{-4}	1.18×10^{-3}	1.14×10^{-3}	9.19×10^{-4}
72		26	7.93×10^{-4}	1.47×10^{-3}	1.13×10^{-3}	1.11×10^{-3}
	Average of various g		8.37×10^{-4}	1.28×10^{-3}	1.13×10^{-3}	9.83×10^{-4}
73	2.10	37	7.10×10^{-4}	1.19×10^{-3}	1.11×10^{-3}	9.58×10^{-4}
74		50	6.14×10^{-4}	1.92×10^{-3}	6.23×10^{-4}	6.23×10^{-4}
75		45	3.83×10^{-4}	1.59×10^{-3}	6.25×10^{-4}	6.26×10^{-4}
	Average of various g		5.69×10^{-4}	1.56×10^{-3}	7.86×10^{-4}	7.36×10^{-4}
76	1.60	120	2.74×10^{-4}	4.80×10^{-4}	3.74×10^{-4}	3.08×10^{-4}
77		115	3.33×10^{-4}	3.66×10^{-4}	3.54×10^{-4}	3.54×10^{-4}
78		87	2.44×10^{-4}	5.15×10^{-4}	3.58×10^{-4}	3.54×10^{-4}
	Average of various g		2.83×10^{-4}	4.53×10^{-4}	3.62×10^{-4}	3.38×10^{-4}

cont'd

TABLE 5 continued...

Exp No.	$\Delta c \times 10^{+2}$ (KgPe/Kg Solution)	Total Growth Time (min)	g(min) (cm/min)	g(max) (cm/min)	g(avg.1) (cm/min)	g(avg.2) (cm/min)
79	1.10	110	2.06×10^{-4}	3.08×10^{-4}	2.18×10^{-4}	2.55×10^{-4}
80		124	1.84×10^{-4}	3.82×10^{-4}	1.86×10^{-4}	2.38×10^{-4}
81		165	1.65×10^{-4}	1.92×10^{-4}	1.77×10^{-4}	1.77×10^{-4}
	Average of various g		1.85×10^{-4}	2.94×10^{-4}	1.93×10^{-4}	2.23×10^{-4}
82	0.60	142	0.86×10^{-4}	1.41×10^{-4}	1.38×10^{-4}	1.15×10^{-4}
83		110	1.99×10^{-4}	2.44×10^{-4}	2.02×10^{-4}	2.13×10^{-4}
84		170	1.42×10^{-4}	2.16×10^{-4}	1.77×10^{-4}	1.74×10^{-4}
	Average of various g		1.42×10^{-4}	2.00×10^{-4}	1.72×10^{-4}	1.67×10^{-4}
85	0.25	No nucl^{n}. (300)	-	-	4.97×10^{-5}	4.98×10^{-5}
86		210	-	-	1.11×10^{-4}	1.11×10^{-4}
	Average of various g		-	-	8.03×10^{-5}	8.04×10^{-5}

TABLE 6

Linear Growth Rate without Impurity at $30^{o}C$ ($c^* = 7.62 \times 10^{-2}$ KgPe/Kg solution)

Total Growth Time = Time for the secondary nucleation ($t_{s.n.}$)

Exp No.	$\Delta c \times 10^{+2}$ (KgPe/Kg Solution)	Total Growth Time (min)	g(min) (cm/min)	g(max) (cm/min)	g(avg.1) (cm/min)	g(avg.2) (cm/min)
87	2.58	(80)	4.95×10^{-4}	8.08×10^{-4}	5.80×10^{-4}	5.88×10^{-4}
88		44	6.81×10^{-4}	1.16×10^{-3}	6.85×10^{-4}	8.53×10^{-4}
89		60	5.29×10^{-4}	1.03×10^{-3}	6.05×10^{-4}	6.57×10^{-4}
	Average of various g		5.68×10^{-4}	9.99×10^{-4}	6.23×10^{-4}	7.66×10^{-4}
90	2.08	100	3.16×10^{-4}	5.30×10^{-4}	4.20×10^{-4}	4.25×10^{-4}
91		95	3.04×10^{-4}	5.30×10^{-4}	4.36×10^{-4}	4.22×10^{-4}
92		90	3.48×10^{-4}	8.52×10^{-4}	4.06×10^{-4}	4.76×10^{-4}
	Average of various g		3.22×10^{-4}	6.37×10^{-4}	4.21×10^{-4}	4.41×10^{-4}
93	1.58	85	2.52×10^{-4}	4.34×10^{-4}	2.81×10^{-4}	2.88×10^{-4}
94		(300) No nucl^{n}.	2.33×10^{-4}	3.48×10^{-4}	2.53×10^{-4}	2.89×10^{-4}
95		(335) No nucl^{n}.	2.17×10^{-4}	4.34×10^{-4}	2.32×10^{-4}	2.65×10^{-4}
	Average of various g		2.34×10^{-4}	4.05×10^{-4}	2.67×10^{-4}	2.80×10^{-4}

cont'd

TABLE 6 continued...

Exp No.	$\Delta c \times 10^{+2}$ (KgPe/Kg Solution)	Total Growth Time (min)	g(min) (cm/min)	g(max) (cm/min)	g(avg.1) (cm/min)	g(avg.2) (cm/min)
96	1.08	$(2880)_n$ No nucl^n.	8.85×10^{-5}	1.44×10^{-4}	1.40×10^{-4}	1.09×10^{-4}
97		$(359)_n$ No nucl^n.	1.09×10^{-4}	1.53×10^{-4}	1.46×10^{-4}	1.45×10^{-4}
98		$(223)_n$ No nucl^n.	9.95×10^{-5}	1.52×10^{-4}	1.36×10^{-4}	1.51×10^{-4}
	Average of various g		9.89×10^{-5}	1.49×10^{-4}	1.40×10^{-4}	1.35×10^{-4}
99	0.58	$(302)_n$ No nucl^n.	8.35×10^{-5}	1.36×10^{-4}	8.48×10^{-5}	9.07×10^{-5}
100		$(200)_n$ No nucl^n.	5.91×10^{-5}	1.19×10^{-4}	1.14×10^{-4}	9.52×10^{-5}
101		$(315)_n$ No nucl^n.	6.40×10^{-5}	9.85×10^{-5}	9.15×10^{-5}	8.58×10^{-5}
	Average of various g		6.89×10^{-5}	1.18×10^{-4}	9.68×10^{-5}	9.06×10^{-5}
102	0.25	$(300)_n$ No nucl^n.	9.85×10^{-6}	8.42×10^{-5}	5.56×10^{-5}	6.40×10^{-5}
103		$(300)_n$ No nucl^n.	1.56×10^{-5}	5.32×10^{-5}	2.13×10^{-5}	1.07×10^{-5}
—	Average of various g		1.27×10^{-5}	6.87×10^{-5}	3.84×10^{-5}	3.73×10^{-5}

TABLE 7

Linear Growth Rates without Impurity at 20°C ($c^* = 5.52 \times 10^{-2}$ KgPe/Kg solution)

Total Growth Time = Time for the secondary nucleation ($t_{s.n.}$)

Exp No.	$\Delta c \times 10^{+2}$ (KgPe/Kg Solution)	Total Growth Time (min)	g(min) (cm/min)	g(max) (cm/min)	g(avg.1) (cm/min)	g(avg.2) (cm/min)
104	2.53	(76)	2.98×10^{-4}	5.97×10^{-4}	5.13×10^{-4}	4.22×10^{-4}
105		(66)	4.04×10^{-4}	5.91×10^{-4}	5.25×10^{-4}	4.71×10^{-4}
106		(76)	4.51×10^{-4}	7.67×10^{-4}	4.92×10^{-4}	5.63×10^{-4}
	Average of various g		3.84×10^{-4}	6.52×10^{-4}	5.10×10^{-4}	4.85×10^{-4}
107	2.03	(86)	2.52×10^{-4}	9.55×10^{-4}	3.82×10^{-4}	3.76×10^{-4}
108		(118)	1.91×10^{-4}	3.42×10^{-4}	3.08×10^{-4}	2.66×10^{-4}
109		(139)	1.83×10^{-4}	3.84×10^{-4}	2.46×10^{-4}	2.55×10^{-4}
	Average of various g		2.09×10^{-4}	5.60×10^{-4}	3.12×10^{-4}	2.99×10^{-4}

cont'd

TABLE 7 continued...

Exp No.	$\Delta c \times 10^{+2}$ (KgPe/Kg Solution)	Total Growth Time (min)	g(min) (cm/min)	g(max) (cm/min)	g(avg.1) (cm/min)	g(avg.2) (cm/min)
110	1.53	(130)	2.02×10^{-4}	6.13×10^{-4}	2.13×10^{-4}	2.70×10^{-4}
111		(100)	1.92×10^{-4}	4.26×10^{-4}	2.07×10^{-4}	2.29×10^{-4}
112		(126)	9.56×10^{-5}	1.99×10^{-4}	1.94×10^{-4}	1.45×10^{-4}
	Average of various	g	1.63×10^{-4}	4.13×10^{-4}	2.05×10^{-4}	2.14×10^{-4}
113	1.03	$(416)_n$ No nucl.	0.48×10^{-4}	0.87×10^{-4}	0.86×10^{-4}	0.57×10^{-4}
114		$(286)_n$ No nucl.	1.01×10^{-4}	6.04×10^{-4}	1.06×10^{-4}	1.47×10^{-4}
115		$(202)_n$ No nucl.	0.83x10	2.16×10^{-4}	1.03×10^{-4}	1.18×10^{-4}
	Average of various	g	0.77×10^{-4}	3.02×10^{-4}	0.99×10^{-4}	1.07×10^{-4}
116	0.53	$(1200)_n$ No nucl.	g(max) first reading equals 4.80×10^{-5}			
			Later the growth rate sharply decreases $\sim 10^{-8}$ cm/min			
117		$(430)_n$ No nucl.	Continuous dissolution			
118			"			

TABLE 8

Linear Growth Rates without Impurity at 10°C ($c^* = 3.91 \times 10^{-2}$ KgPe/Kg solution)

Total Growth Time = Time for the secondary nucleation ($t_{s.n.}$)

Exp No.	$\Delta c \times 10^{+2}$ (KgPe/Kg Solution)	Total Growth Time (min)	g(min) (cm/min)	g(max) (cm/min)	g(avg.1) (cm/min)	g(avg.2) (cm/min)
119	2.07	(106)	2.17×10^{-4}	3.97×10^{-4}	2.23×10^{-4}	2.48×10^{-4}
120		(118)	2.28×10^{-4}	4.27×10^{-4}	2.28×10^{-4}	2.68×10^{-4}
121		(115)	2.20×10^{-4}	5.42×10^{-4}	2.40×10^{-4}	2.70×10^{-4}
	Average of various R		2.22×10^{-4}	4.55×10^{-4}	2.30×10^{-4}	2.82×10^{-4}
124	1.57	(140)	9.55×10^{-5}	2.52×10^{-4}	1.00×10^{-4}	1.35×10^{-4}
125		(235) No nucl^{n}.	5.18×10^{-5}	1.26×10^{-4}	8.75×10^{-5}	7.67×10^{-5}
126		(165)	9.62×10^{-5}	5.12×10^{-4}	1.69×10^{-4}	1.83×10^{-4}
	Average of various R		8.11×10^{-5}	2.96×10^{-4}	1.19×10^{-4}	1.32×10^{-4}

cont'd

TABLE 8 continued...

Exp No.	$\Delta c \times 10^{+2}$ (KgPe/Kg Solution)	Total Growth Time (min)	g(min) (cm/min)	g(max) (cm/min)	g(avg.1) (cm/min)	g(avg.2) (cm/min)
127	1.07	(198) $_{\text{No nucl}^n}$.	4.18×10^{-5}	2.07×10^{-4}	7.24×10^{-5}	7.24×10^{-5}
128		(370) $_{\text{No nucl}^n}$.	6.85×10^{-5}	2.40×10^{-4}	8.20×10^{-5}	1.04×10^{-4}
129		(370) $_{\text{No nucl}^n}$.	3.46×10^{-5}	1.49×10^{-4}	6.32×10^{-5}	5.18×10^{-5}
	Average of various R		4.83×10^{-5}	1.98×10^{-4}	7.25×10^{-5}	7.60×10^{-5}
130	0.57	(1390) $_{\text{No nucl}^n}$.	2.63×10^{-5}	8.52×10^{-5}	3.84×10^{-5}	3.68×10^{-5}
131		(1390) $_{\text{No nucl}^n}$.	9.95×10^{-5}	7.95×10^{-5}	2.72×10^{-5}	3.22×10^{-5}
132		(1500) $_{\text{No nucl}^n}$.	1.80×10^{-5}	7.40×10^{-5}	1.90×10^{-5}	2.65×10^{-5}
	Average of various R		1.84×10^{-5}	7.69×10^{-5}	2.82×10^{-5}	3.18×10^{-5}

TABLE 9

Linear Growth Rate with di-Pe as Impurity $T = 30^{o}C$, $\Delta c = 2.23 \times 10^{-2}$ (KgPe/Kg solution)

Total Growth time = Time for secondary nucleation ($t_{s.n.}$)

Exp No.	ci x 10^{+2} (Kg di-Pe/Kg Solution)	Total Growth Time (min)	g(min) (cm/min)	g(max) (cm/min)	g(avg.1) (cm/min)	g(avg.2) (cm/min)
133	0.05	41	5.03×10^{-4}	1.06×10^{-3}	5.62×10^{-4}	6.32×10^{-4}
134		100	2.89×10^{-4}	8.10×10^{-4}	3.84×10^{-4}	3.75×10^{-4}
	Average of various g		3.96×10^{-4}	9.35×10^{-4}	4.73×10^{-4}	5.03×10^{-4}
135	0.10	47	5.20×10^{-4}	2.00×10^{-3}	8.20×10^{-4}	7.98×10^{-4}
136a		65	4.95×10^{-4}	2.00×10^{-3}	6.50×10^{-4}	6.72×10^{-4}
136b		62	4.60×10^{-4}	1.40×10^{-3}	6.45×10^{-4}	6.85×10^{-4}
	Average of various g		4.91×10^{-4}	1.80×10^{-3}	7.05×10^{-4}	7.18×10^{-4}
137	0.13	38	5.40×10^{-4}	1.08×10^{-3}	8.20×10^{-4}	8.75×10^{-4}
138		55	5.90×10^{-4}	2.90×10^{-3}	7.00×10^{-4}	7.58×10^{-4}
	Average of various g		5.65×10^{-4}	1.98×10^{-3}	7.60×10^{-4}	8.16×10^{-4}

cont'd

TABLE 9 continued...

Exp No.	$c_i \times 10^{+2}$ (Kg di-Pe/Kg Solution)	Total Growth Time (min)	g(min) (cm/min)	g(max) (cm/min)	g(avg.1) (cm/min)	g(avg.2) (cm/min)
139	0.15	47	6.50×10^{-4}	4.00×10^{-3}	7.20×10^{-4}	8.00×10^{-4}
140		49	6.00×10^{-4}	9.00×10^{-4}	8.80×10^{-4}	8.68×10^{-4}
141		1480	g not measured			
	Average of various g		6.25×10^{-4}	2.45×10^{-3}	8.00×10^{-4}	8.34×10^{-4}
142	0.20	51	4.50×10^{-4}	2.48×10^{-3}	7.93×10^{-4}	8.43×10^{-4}
143		80	5.49×10^{-4}	9.61×10^{-4}	6.21×10^{-4}	6.21×10^{-4}
	Average of various g		4.99×10^{-4}	1.67×10^{-3}	7.07×10^{-4}	7.32×10^{-4}
144	0.27	112	2.36×10^{-4}	6.68×10^{-4}	5.86×10^{-4}	4.67×10^{-4}
145		61	3.53×10^{-4}	1.91×10^{-3}	7.62×10^{-4}	6.50×10^{-4}
146		83	2.26×10^{-4}	1.46×10^{-3}	4.80×10^{-4}	4.89×10^{-4}
	Average of various g		2.71×10^{-4}	1.35×10^{-3}	6.09×10^{-4}	5.35×10^{-4}

cont'd

TABLE 9 continued...

Exp No.	$c_i \times 10^{+2}$ (Kg di-Pe/Kg Solution)	Total Growth Time (min)	g(min) (cm/min)	g(max) (cm/min)	g(avg.1) (cm/min)	g(avg.2) (cm/min)
147	0. 50	136	1.77×10^{-4}	3.40×10^{-4}	3.41×10^{-4}	2.78×10^{-4}
148		126	3.20×10^{-4}	9.05×10^{-4}	4.84×10^{-4}	4.60×10^{-4}
149		85	2.81×10^{-4}	7.95×10^{-4}	3.16×10^{-4}	4.26×10^{-4}
	Average of various g		2.59×10^{-4}	6.80×10^{-4}	3.80×10^{-4}	3.88×10^{-4}
150	0.65	110	2.65×10^{-4}	1.36×10^{-3}	3.76×10^{-4}	4.20×10^{-4}
151		97	3.65×10^{-4}	4.64×10^{-4}	3.92×10^{-4}	4.12×10^{-4}
	Average for various g		3.15×10^{-4}	9.12×10^{-4}	3.84×10^{-4}	4.16×10^{-4}
152	0.75	118	3.02×10^{-4}	1.00×10^{-3}	3.84×10^{-4}	3.20×10^{-4}
153		105	2.84×10^{-4}	8.80×10^{-4}	3.66×10^{-4}	3.50×10^{-4}
154		75	3.17×10^{-4}	7.85×10^{-4}	4.50×10^{-4}	4.80×10^{-4}
155			g not measured			
	Average of various g		3.01×10^{-4}	8.88×10^{-4}	4.00×10^{-4}	3.83×10^{-4}

TABLE 10

Linear Growth Rate with di-Pe as Impurity $T = 30^{o}C$, $\Delta c = 2.00 \times 10^{-2}$ (KgPe/Kg solution)

Total Growth Time = Time for the secondary nucleation ($t_{s.n.}$)

Exp No.	$c_i \times 10^{+2}$ (Kg di-Pe/Kg Solution)	Total Growth Time (min)	g(min) (cm/min)	g(max) (cm/min)	g(avg.1) (cm/min)	g(avg.2) (cm/min)
156	0.15	104	2.20×10^{-4}	5.12×10^{-4}	4.27×10^{-4}	3.68×10^{-4}
157		75	2.38×10^{-4}	6.00×10^{-4}	3.15×10^{-4}	3.25×10^{-4}
	Average of various g		2.29×10^{-4}	5.56×10^{-4}	3.71×10^{-4}	3.46×10^{-4}
158	0.30	245	2.70×10^{-4}	6.40×10^{-4}	4.61×10^{-4}	4.28×10^{-4}
159		No nucl^{n}. 65	2.81×10^{-4}	6.98×10^{-4}	3.40×10^{-4}	3.63×10^{-4}
	Average of various g		2.75×10^{-4}	6.69×10^{-4}	4.00×10^{-4}	3.95×10^{-4}
160	0.35	72	3.84×10^{-4}	9.02×10^{-4}	5.12×10^{-4}	5.38×10^{-4}
161		68	3.00×10^{-4}	9.02×10^{-4}	3.49×10^{-4}	3.97×10^{-4}
	Average of various g		3.42×10^{-4}	9.02×10^{-4}	4.31×10^{-4}	4.67×10^{-4}

cont'd

TABLE 10 continued...

Exp No.	ci x 10^{+2} (Kg di-Pe/Kg Solution)	Total Growth Time (min)	g(min) (cm/min)	g(max) (cm/min)	g(avg.1) (cm/min)	g(avg.2) (cm/min)
162	0.40	80	3.70×10^{-4}	1.00×10^{-3}	4.70×10^{-4}	4.76×10^{-6}
163		110	3.90×10^{-4}	7.90×10^{-4}	4.31×10^{-4}	4.76×10^{-4}
	Average of various g		3.80×10^{-4}	8.95×10^{-4}	4.51×10^{-4}	4.76×10^{-4}
164	0.45	90	2.74×10^{-4}	5.90×10^{-4}	4.98×10^{-4}	4.30×10^{-4}
165		75	3.81×10^{-4}	9.17×10^{-4}	3.02×10^{-4}	3.39×10^{-4}
	Average of various g		3.27×10^{-4}	7.53×10^{-4}	4.00×10^{-4}	3.84×10^{-4}
166	0.50	90	2.00×10^{-4}	6.40×10^{-4}	4.98×10^{-4}	4.03×10^{-4}
167		110	2.38×10^{-4}	7.00×10^{-4}	2.62×10^{-4}	2.84×10^{-4}
	Average of various g		2.19×10^{-4}	6.70×10^{-4}	3.80×10^{-4}	3.43×10^{-4}
168	0.75	172	2.20×10^{-4}	5.00×10^{-4}	2.95×10^{-4}	2.78×10^{-4}
169		113	2.70×10^{-4}	4.75×10^{-4}	3.55×10^{-4}	3.88×10^{-4}
	Average of various g		2.45×10^{-4}	4.87×10^{-4}	3.25×10^{-4}	3.33×10^{-4}

TABLE 11

Linear Growth Rate with di-Pe as Impurity $T = 30^{o}C$, $\Delta c = 1.73 \times 10^{-2}$ (KgPe/Kg solution)

Total Growth Time = Time for secondary nucleation ($t_{s.n.}$)

Exp No.	ci x 10^{+2} (Kg di-Pe/Kg Solution)	Total Growth Time (min)	g(min) (cm/min)	g(max) (cm/min)	g(avg.1) (cm/min)	g(avg.2) (cm/min)
170	0.15	115	2.80×10^{-4}	6.00×10^{-4}	2.95×10^{-4}	3.05×10^{-4}
171		210	1.15×10^{-4}	5.20×10^{-4}	2.65×10^{-4}	2.06×10^{-4}
	Average of various g		1.97×10^{-4}	5.60×10^{-4}	2.80×10^{-4}	2.55×10^{-4}
172	0.30	150	8.00×10^{-5}	3.12×10^{-4}	2.10×10^{-4}	1.95×10^{-4}
173		120	9.25×10^{-5}	5.00×10^{-4}	2.70×10^{-4}	2.68×10^{-4}
	Average of various g		8.62×10^{-5}	4.06×10^{-4}	2.40×10^{-4}	2.31×10^{-4}
174	0.50	92	9.25×10^{-5}	4.12×10^{-4}	2.20×10^{-4}	2.53×10^{-4}
175		160	6.58×10^{-5}	2.95×10^{-4}	1.80×10^{-4}	1.78×10^{-4}
	Average of various g		7.91×10^{-5}	3.53×10^{-4}	2.00×10^{-4}	2.15×10^{-4}

cont'd

TABLE 11 continued...

Exp No.	ci x 10^{+2} (Kg di-Pe/Kg Solution)	Total Growth Time (min)	g(min) (cm/min)	g(max) (cm/min)	g(avg.1) (cm/min)	g(avg.2) (cm/min)
176	0.65	300 No nucl^{n}.	5.00×10^{-5}	2.56×10^{-4}	2.00×10^{-4}	1.28×10^{-4}
177		226	5.90×10^{-5}	3.00×10^{-4}	1.10×10^{-4}	1.05×10^{-4}
	Average of various g		5.45×10^{-5}	2.78×10^{-4}	1.55×10^{-4}	1.16×10^{-4}
178	0.75	210	8.55×10^{-5}	6.38×10^{-4}	1.23×10^{-4}	1.46×10^{-4}
179		165	9.60×10^{-5}	1.79×10^{-4}	1.80×10^{-4}	1.54×10^{-4}
	Average of various g		9.07×10^{-5}	4.08×10^{-4}	1.51×10^{-4}	1.50×10^{-4}

TABLE 12

Linear Growth Rate with di-Pe as Impurity $T = 30^{o}C$, $\Delta c = 1.23 \times 10^{-2}$ (KgPe/Kg solution)

Total Growth Time = Time for the secondary nucleation ($t_{s.n.}$)

Exp No.	ci x 10^{+2} (Kg di-Pe/Kg Solution)	Total Growth Time (min)	g(min) (cm/min)	g(max) (cm/min)	g(avg.1) (cm/min)	g(avg.2) (cm/min)
180	0.10	221	1.60×10^{-4}	7.53×10^{-4}	1.80×10^{-4}	9.86×10^{-5}
181a		225 (no $nucl^{n}$)	0.96×10^{-4}	6.80×10^{-4}	1.30×10^{-4}	1.06×10^{-4}
181b		342 (no $nucl^{n}$)	1.35×10^{-4}	8.00×10^{-4}	1.97×10^{-4}	8.84×10^{-5}
	Average of various g		1.30×10^{-4}	7.44×10^{-4}	1.69×10^{-4}	9.76×10^{-5}
182	0.27	212	8.75×10^{-5}	2.03×10^{-4}	1.20×10^{-4}	1.20×10^{-4}
183		155	1.45×10^{-4}	5.68×10^{-4}	1.72×10^{-4}	2.05×10^{-4}
184		189	7.65×10^{-5}	1.98×10^{-4}	1.05×10^{-4}	1.20×10^{-4}
	Average of various g		1.03×10^{-4}	3.23×10^{-4}	1.32×10^{-4}	1.48×10^{-4}

cont'd

TABLE 12 continued...

Exp No.	$c_i \times 10^{+2}$ (Kg di-Pe/Kg Solution)	Total Growth Time (min)	g(min) (cm/min)	g(max) (cm/min)	g(avg.1) (cm/min)	g(avg.2) (cm/min)
185	0.50	170 No nucl^{n}.	0.58×10^{-4}	2.19×10^{-4}	0.85×10^{-4}	0.88×10^{-4}
186		179 No nucl^{n}.	0.72×10^{-4}	3.67×10^{-4}	0.98×10^{-4}	1.02×10^{-4}
187		200	0.75×10^{-4}	1.79×10^{-4}	1.23×10^{-4}	1.29×10^{-4}
	Average of various g		0.68×10^{-4}	2.55×10^{-4}	1.02×10^{-4}	1.06×10^{-4}
188	0.65	142	0.96×10^{-4}	3.20×10^{-4}	1.38×10^{-4}	1.50×10^{-4}
189		300 No nucl^{n}.	0.60×10^{-4}	1.00×10^{-4}	0.90×10^{-4}	1.05×10^{-4}
190		300 No nucl^{n}.	0.62×10^{-4}	1.92×10^{-4}	0.92×10^{-4}	1.02×10^{-4}
	Average of various g		0.73×10^{-4}	2.06×10^{-4}	1.06×10^{-4}	1.19×10^{-4}
191	0.75	175	0.84×10^{-4}	1.53×10^{-4}	1.07×10^{-4}	1.30×10^{-4}
192		300 No nucl^{n}.	0.58×10^{-4}	2.80×10^{-4}	1.20×10^{-4}	1.15×10^{-4}
193		300 No nucl^{n}.	0.64×10^{-4}	1.93×10^{-4}	0.88×10^{-4}	1.15×10^{-4}
	Average of various g		0.68×10^{-4}	2.08×10^{-4}	1.05×10^{-4}	1.20×10^{-4}

TABLE 13

Linear Growth Rate with di-Pe as Impurity $T = 40^{o}C$, $\Delta c = 2.23 \times 10^{-2}$ (KgPe/Kg solution)

Total Growth Time = Time for the secondary nucleation ($t_{s.n.}$)

Exp No.	ci x 10^{+2} (Kg di-Pe/Kg Solution)	Total Growth Time (min)	g(min) (cm/min)	g(max) (cm/min)	g(avg.1) (cm/min)	g(avg.2) (cm/min)
194	0.05	39	6.40×10^{-4}	1.50×10^{-3}	9.60×10^{-4}	9.75×10^{-4}
195		27	6.00×10^{-4}	1.41×10^{-3}	8.38×10^{-4}	8.74×10^{-4}
	Average of various g		6.20×10^{-4}	1.45×10^{-3}	8.99×10^{-4}	9.24×10^{-4}
196	0.10	24	7.38×10^{-4}	1.80×10^{-3}	9.20×10^{-4}	9.79×10^{-4}
197		28	6.98×10^{-4}	1.54×10^{-3}	1.06×10^{-3}	1.03×10^{-3}
	Average of various g		7.18×10^{-4}	1.67×10^{-3}	9.80×10^{-4}	1.00×10^{-3}

cont'd

TABLE 13 continued...

Exp No.	ci x 10^{+2} (Kg di-Pe/Kg Solution)	Total Growth Time (min)	g(min) (cm/min)	g(max) (cm/min)	g(avg.1) (cm/min)	g(avg.2) (cm/min)
198	0.15	43	6.00×10^{-4}	1.60×10^{-3}	8.58×10^{-4}	8.85×10^{-4}
199		24	6.82×10^{-4}	1.47×10^{-3}	1.02×10^{-3}	9.92×10^{-4}
	Average of various g		6.41×10^{-4}	1.53×10^{-3}	9.40×10^{-4}	9.38×10^{-4}
200	0.75	75	3.20×10^{-4}	9.00×10^{-4}	5.50×10^{-4}	5.04×10^{-4}
201		44	3.40×10^{-4}	9.68×10^{-4}	7.08×10^{-4}	5.48×10^{-4}
	Average of various g		3.30×10^{-4}	9.34×10^{-4}	6.19×10^{-4}	5.26×10^{-4}

TABLE 14

Linear Growth Rate with di-Pe as Impurity $T = 40^{o}C$, $\Delta c = 1.23 \times 10^{-2}$ (KgPe/Kg solution)

Total Growth Time = Time for the secondary nucleation ($t_{s.n.}$)

Exp No.	ci x 10^{+2} (Kg di-Pe/Kg Solution)	Total Growth Time (min)	g(min) (cm/min)	g(max) (cm/min)	g(avg.1) (cm/min)	g(avg.2) (cm/min)
202	0.10	198	1.40×10^{-4}	2.95×10^{-4}	2.00×10^{-4}	1.93×10^{-4}
203		104	1.49×10^{-4}	3.00×10^{-4}	2.40×10^{-4}	2.27×10^{-4}
	Average of various g		1.45×10^{-4}	2.97×10^{-4}	2.20×10^{-4}	2.10×10^{-4}
204	0.20	222	1.10×10^{-4}	2.05×10^{-4}	1.75×10^{-4}	1.66×10^{-4}
205		205	1.33×10^{-4}	2.80×10^{-4}	2.25×10^{-4}	1.91×10^{-4}
	Average of various g		1.21×10^{-4}	2.42×10^{-4}	2.00×10^{-4}	1.78×10^{-4}
206	0.35	300 No nucl^{n}.	8.99×10^{-5}	2.20×10^{-4}	1.27×10^{-4}	1.38×10^{-4}
207		155	1.27×10^{-4}	2.60×10^{-4}	2.14×10^{-4}	2.40×10^{-4}
	Average of various g		1.08×10^{-4}	2.40×10^{-4}	1.70×10^{-4}	1.89×10^{-4}

cont'd

TABLE 14 continued...

Exp No.	ci x 10^{+2} (Kg di-Pe/Kg Solution)	Total Growth Time (min)	g(min) (cm/min)	g(max) (cm/min)	g(avg.1) (cm/min)	g(avg.2) (cm/min)
208	0.50	135	2.25×10^{-5}	3.0×10^{-4}	1.58×10^{-4}	1.68×10^{-4}
209		300 No nucln.	7.0×10^{-5}	9.85×10^{-4}	1.00×10^{-4}	1.28×10^{-4}
	Average of various g		4.62×10^{-5}	6.42×10^{-4}	1.29×10^{-4}	1.48×10^{-4}
210	0.75	235	8.38×10^{-5}	1.88×10^{-4}	0.99×10^{-4}	1.52×10^{-4}
211		127	1.15×10^{-4}	2.60×10^{-4}	1.59×10^{-4}	1.78×10^{-4}
	Average of various g		9.94×10^{-5}	2.24×10^{-4}	1.29×10^{-4}	1.65×10^{-4}

TABLE 15

Linear Growth Rate with Formal as Impurity $T = 30^{o}C$, $\Delta c = 2.23 \times 10^{-2}$ (KgPe/Kg solution)

No secondary nucleation

Exp No.	$c_{if} \times 10^{+2}$ (Kg Formal/ Kg solution)	Total Growth Time (min)	g(min) (cm/min)	g(max) (cm/min)	g(avg.1) (cm/min)	g(avg.2) (cm/min)
214	0.025	300	2.34×10^{-4}	5.32×10^{-4}	2.45×10	2.48×10^{-4}
215		300	1.60×10^{-4}	9.03×10^{-4}	3.14×10^{-4}	2.86×10^{-4}
	Average of various g		1.97×10^{-4}	7.17×10^{-4}	2.79×10^{-4}	2.67×10^{-4}
216	0.05	600	6.63×10^{-5}	2.84×10^{-4}	2.59×10^{-4}	2.43×10^{-4}
217		1440	1.69×10^{-5}	1.28×10^{-4}	1.19×10^{-4}	9.15×10^{-5}
	Average of various g		4.16×10^{-5}	2.06×10^{-4}	1.89×10^{-4}	1.67×10^{-4}
218	0.0752	2160	3.80×10^{-5}	8.20×10^{-5}	7.25×10^{-5}	6.90×10^{-5}
219		2160	9.00×10^{-6}	4.50×10^{-5}	3.55×10^{-5}	3.80×10^{-5}
	Average of various g		2.35×10^{-5}	6.35×10^{-5}	5.40×10^{-5}	5.35×10^{-5}

cont'd

TABLE 15 continued...

Exp No.	$c_{if} \times 10^{+2}$ (Kg Formal/ Kg solution)	Total Growth Time (min)	g(min) (cm/min)	g(max) (cm/min)	g(avg.1) (cm/min)	g(avg.2) (cm/min)
220	0.100	1380	continuous dissolution for 23 h.			
221		1380	Growth continuously decreasing from 7.12×10^{-5} to 1.42×10^{-5} after 23 h.			
222	0.127	1140	Only 1 reading after 295 min. (i.e. g max = 1.30×10^{-5} cm/min). No growth after that for the measured 19 h.			
223	0.153	2880	Only 1 reading at a g max = 6.00×10^{-6} (cm/min) No growth after that.			

TABLE 16

Linear Growth Rate with Formal as Impurity $T = 30^{\circ}C$, $\Delta c = 1.23 \times 10^{-2}$ (KgPe/Kg solution)

No secondary nucleation

Exp No.	$c_{if} \times 10^{+2}$ (Kg Formal/Kg solution)	Total Growth Time (min)	g(min) (cm/min)	g(max) (cm/min)	g(avg.1) (cm/min)	g(avg.2) (cm/min)
224	0.00664	407	1.06×10^{-4}	2.74×10^{-4}	1.50×10^{-4}	1.45×10^{-4}
225		300	0.61×10^{-4}	1.99×10^{-4}	0.94×10^{-4}	0.98×10^{-4}
	Average of various g		0.88×10^{-4}	2.36×10^{-4}	1.22×10^{-4}	1.21×10^{-4}
226	0.00887	1812	5.97×10^{-5}	1.10×10^{-4}	9.96×10^{-5}	9.66×10^{-5}
227		1790	8.43×10^{-5}	1.28×10^{-4}	1.20×10^{-4}	1.16×10^{-4}
	Average of various g		7.20×10^{-5}	1.19×10^{-4}	1.10×10^{-4}	1.07×10^{-4}
228	0.0222	1300	Growth rate continuously decreasing g(max) = 2.56×10^{-5} cm/min.			
229		1320	Continuous dissolution			
230	0.045	2040	g(max) = 0.98×10^{-5} cm/min, then continuously decreasing for 24 h; g(max) = 1.28×10^{-5} cm/min.			
231		2760	Continuous dissolution after that.			

TABLE 17

Linear Growth Rate with Formal as Impurity $T = 40^{o}C$, $\Delta c = 4.00 \times 10^{-2}$ (KgPe/Kg solution)

Total Growth Time = Time for secondary nucleation ($t_{s.n}$)

Exp No.	cif x 10^{+2} (Kg Formal/Kg solution)	Total Growth Time (min)	g(min) (cm/min)	g(max) (cm/min)	g(avg.1) (cm/min)	g(avg.2) (cm/min)
232	0.072	25	1.56×10^{-3}	2.35×10^{-3}	2.35×10^{-3}	2.05×10^{-3}
233		20	1.99×10^{-3}	2.57×10^{-3}	2.17×10^{-3}	2.05×10^{-3}
	Average of various g		1.77×10^{-3}	2.46×10^{-3}	2.26×10^{-3}	2.05×10^{-3}
234	0.145	19	0.95×10^{-3}	3.07×10^{-3}	1.79×10^{-3}	2.20×10^{-3}
235		15	1.59×10^{-3}	4.76×10^{-3}	2.50×10^{-3}	2.41×10^{-3}
	Average of various g		1.27×10^{-3}	3.91×10^{-3}	2.14×10^{-3}	2.30×10^{-3}
236	0.182	93	6.40×10^{-4}	1.10×10^{-3}	8.85×10^{-4}	8.45×10^{-4}
237	0.217	1200 No $nucl^{n}$.	g(max) = 3.20×10^{-4} later decrease			
238		1200 No $nucl^{n}$.	g(max) = 1.45×10^{-5} later decrease			

TABLE 18

Linear Growth Rate with Formal as Impurity $\dot{g}$ = 40°C, $\Delta c = 3.00 \times 10^{-2}$ (KgPe/Kg solution)

Total Growth Time = Time for secondary nucleation ($t_{s.n.}$)

Exp No.	$cif \times 10^{+2}$ (Kg Formal/Kg Solution)	Total Growth Time (min)	g(min) (cm/min)	g(max) (cm/min)	g(avg.1) (cm/min)	g(avg.2) (cm/min)
239	0.067	34	7.94×10^{-4}	1.91×10^{-3}	1.32×10^{-3}	1.25×10^{-3}
240	0.135	97	1.02×10^{-4}	4.80×10^{-4}	3.20×10^{-4}	3.17×10^{-4}
241	0.169	1800 No nucl^{n}.	1.85×10^{-4} later continuously decreasing			

Experiments for Gas Chromatographic Analyses

Exp.No.	$cif \times 10^{+2}$ (Kg Formal/Kg solution)	Total time of growth (min)	g(avg.2) (cm/min)
242	0.0752	7200 min	2.50×10^{-5}
243	0.00887	2160	7.75×10^{-5}

TABLE 19

Linear Growth Rates with Miscellaneous Impurities Added. $T = 30^{o}C, \Delta c = 2.23 \times 10^{-2}$ (KgPe/Kg solution)

Total Growth Time = Time for the secondary nucleation ($t_{s.n.}$)

Exp No.	Impurity	$c_i \times 10^{+2}$ (Kg Impurity/ Kg solution)	Total Growth Time (min)	g(min) (cm/min)	g(max) (cm/min)	g(avg.1) (cm/min)	g(avg.2) (cm/min)
244	NaCL	0.10	76	2.64×10^{-4}	7.93×10^{-4}	5.62×10^{-4}	4.28×10^{-4}
245			61	3.84×10^{-4}	7.32×10^{-4}	4.38×10^{-4}	4.50×10^{-4}
246			85	2.33×10^{-4}	5.95×10^{-4}	5.30×10^{-4}	4.48×10^{-4}
		Average of various g		2.93×10^{-4}	7.06×10^{-4}	5.10×10^{-4}	4.42×10^{-4}
247		1.00	35	3.84×10^{-4}	6.97×10^{-4}	4.80×10^{-4}	5.01×10^{-4}
248			62.	3.67×10^{-4}	9.23×10^{-4}	5.30×10^{-4}	5.78×10^{-4}
249			45	3.08×10^{-4}	5.78×10^{-4}	5.62×10^{-4}	4.64×10^{-4}
		Average of various g		3.53×10^{-4}	7.32×10^{-4}	5.24×10^{-4}	5.14×10^{-4}
250	NaOH	1.00	158	1.17×10^{-4}	2.31×10^{-4}	1.99×10^{-4}	1.93×10^{-4}
251	(solution)		103	9.26×10^{-5}	1.92×10^{-4}	1.84×10^{-4}	1.50×10^{-4}
252			127	1.24×10^{-4}	2.33×10^{-4}	1.73×10^{-4}	1.87×10^{-4}
		Average of various g		1.11×10^{-4}	2.15×10^{-4}	1.85×10^{-4}	1.76×10^{-4}

cont'd

TABLE 19 continued...

Exp No.	Impurity	$C_i \times 10^{+2}$ (Kg Impurity/ Kg solution)	Total Growth Time (min)	g(min) (cm/min)	g(max) (cm/min)	g(avg.1) (cm/min)	g(avg.2) (cm/min)
253	NaOH	1.00	106	1.10×10^{-4}	1.90×10^{-4}	1.87×10^{-4}	1.64×10^{-4}
254	(Pellets)		(120) No nucl^{n}.	1.44×10^{-4}	3.20×10^{-4}	1.83×10^{-4}	1.81×10^{-4}
		Average of various g		1.27×10^{-4}	1.70×10^{-4}	1.85×10^{-4}	1.72×10^{-4}
255		2.13	Continuous dissolution for 3 HRs.				
256			No growth at all				
257	HCL	0.10	38	3.40×10^{-4}	7.93×10^{-4}	5.32×10^{-4}	5.11×10^{-4}
258			75	3.67×10^{-4}	7.33×10^{-4}	4.76×10^{-4}	4.86×10^{-4}
259			51	6.88×10^{-4}	1.10×10^{-3}	6.97×10^{-4}	8.18×10^{-4}
		Average of various g		4.65×10^{-4}	8.75×10^{-4}	5.68×10^{-4}	6.05×10^{-4}

cont'd

TABLE 19 continued...

Exp No.	Impurity	$c_i \times 10^{+2}$ (Kg Impurity/ Kg solution)	Total Growth Time (min)	g(min) (cm/min)	g(max) (cm/min)	g(avg.1) (cm/min)	g(avg.2) (cm/min)
260	HCL	1.00	25	4.76×10^{-4}	8.67×10^{-4}	7.34×10^{-4}	6.77×10^{-4}
261			38	5.29×10^{-4}	7.33×10^{-4}	6.80×10^{-4}	6.63×10^{-4}
262			85	6.05×10^{-4}	9.95×10^{-4}	6.33×10^{-4}	6.62×10^{-4}
		Average of various g		5.36×10^{-4}	8.65×10^{-4}	6.82×10^{-4}	6.67×10^{-4}
263	Polysa-	0.001	27	3.82×10^{-4}	7.34×10^{-4}	4.55×10^{-7}	5.00×10^{-4}
264	charide		88	2.38×10^{-4}	6.37×10^{-4}	3.82×10^{-4}	3.67×10^{-4}
265	Sulphate		107	2.74×10^{-4}	7.68×10^{-4}	3.84×10^{-4}	3.92×10^{-4}
		Average of various g		2.98×10^{-4}	7.13×10^{-4}	4.07×10^{-4}	4.19×10^{-4}
266		0.100	78	2.27×10^{-4}	7.93×10^{-4}	3.53×10^{-4}	3.64×10^{-4}
267			113	2.13×10^{-4}	3.93×10^{-4}	2.98×10^{-4}	2.95×10^{-4}
268			95	2.17×10^{-4}	7.34×10^{-4}	3.97×10^{-4}	3.70×10^{-4}
		Average of various g		2.19×10^{-4}	6.40×10^{-4}	3.49×10^{-4}	3.43×10^{-4}

cont'd

TABLE 19 continued...

Exp No.	Impurity	$c_i \times 10^{+2}$ (Kg Impurity / Kg solution)	Total Growth Time (min)	g(min) (cm/min)	g(max) (cm/min)	g(avg.1) (cm/min)	g(avg.2) (cm/min)
269	Methanol	1.00	72	1.59×10^{-4}	7.34×10^{-4}	6.82×10^{-4}	4.46×10^{-4}
270			63	2.99×10^{-4}	8.68×10^{-4}	5.62×10^{-4}	4.75×10^{-4}
271			35	4.27×10^{-4}	6.57×10^{-4}	4.52×10^{-4}	4.84×10^{-4}
		Average of various g		2.95×10^{-4}	7.53×10^{-4}	5.65×10^{-4}	4.68×10^{-4}
272		5.00	75	4.64×10^{-4}	6.40×10^{-4}	4.65×10^{-4}	4.88×10^{-4}
273			125	3.97×10^{-4}	7.93×10^{-4}	5.95×10^{-4}	5.78×10^{-4}
274			117	3.07×10^{-4}	8.67×10^{-4}	4.54×10^{-4}	4.61×10^{-4}
		Average of various g		3.89×10^{-4}	7.66×10^{-4}	5.05×10^{-4}	5.09×10^{-4}
275	Non-idet	0.10	128	2.51×10^{-4}	4.34×10^{-4}	3.18×10^{-4}	3.14×10^{-4}
276	(P-40)		159	2.75×10^{-4}	3.48×10^{-4}	3.06×10^{-4}	3.06×10^{-4}
277			283	2.12×10^{-4}	4.34×10^{-4}	2.88×10^{-4}	3.00×10^{-4}
		Average of various g		2.46×10^{-4}	4.05×10^{-4}	3.04×10^{-4}	3.06×10^{-4}
		0.75	Solution too opaque to be used for the observation of a single crystal.				

TABLE 19 continued...

Exp No.	Impurity	$c_i \times 10^{+2}$ (Kg Impurity/ Kg solution)	Total Growth Time (min)	g(min) (cm/min)	g(max) (cm/min)	g(avg.1) (cm/min)	g(avg.2) (cm/min)
278	White	Saturated	117	1.77×10^{-4}	3.41×10^{-4}	3.18×10^{-4}	2.54×10^{-4}
279	Spirit	Amount	131	2.07×10^{-4}	2.98×10^{-4}	2.73×10^{-4}	2.61×10^{-4}
280			102	2.90×10^{-4}	4.52×10^{-4}	2.96×10^{-4}	3.22×10^{-4}
		Average of various g		2.24×10^{-4}	3.63×10^{-4}	2.95×10^{-4}	2.79×10^{-4}

cont'd

TABLE 19 continued...

Exp No.	Impurity	Impurity concentration	Total Growth Time (min)	g(min) (cm/min)	g(max) (cm/min)	g(avg.1) (cm/min)	g(avg.2) (cm/min)
281	Silco-lapse 5000	1 ppm	51	4.76×10^{-4}	5.95×10^{-4}	5.30×10^{-4}	5.15×10^{-4}
282			33	2.98×10^{-4}	5.62×10^{-4}	5.30×10^{-4}	4.66×10^{-4}
283			78	4.52×10^{-4}	9.60×10^{-4}	4.52×10^{-4}	5.52×10^{-4}
		Average of various g		4.08×10^{-4}	7.06×10^{-4}	5.04×10^{-4}	5.17×10^{-4}
284		10 ppm	55	2.98×10^{-4}	9.65×10^{-4}	4.76×10^{-4}	4.47×10^{-4}
285			87	4.38×10^{-4}	8.53×10^{-4}	4.66×10^{-4}	4.78×10^{-4}
286			128	2.98×10^{-4}	6.37×10^{-4}	4.54×10^{-4}	4.16×10^{-4}
		Average of various g		3.44×10^{-4}	8.18×10^{-4}	4.72×10^{-4}	4.47×10^{-4}
287		80 ppm	93	3.97×10^{-4}	7.93×10^{-4}	5.02×10^{-4}	4.98×10^{-4}
288			75	4.80×10^{-4}	8.52×10^{-4}	5.48×10^{-4}	5.73×10^{-4}
289			123	3.82×10^{-4}	8.68×10^{-4}	5.31×10^{-4}	5.18×10^{-4}
		Average of various g		4.19×10^{-4}	8.37×10^{-4}	5.27×10^{-4}	5.29×10^{-4}

con't

TABLE 19 continued...

Exp No.	Impurity	Impurity concentration	Total Growth Time (min)	g(min) (cm/min)	g(max) (cm/min)	g(avg.1) (cm/min)	g(avg.2) (cm/min)
290	Silco-lapse 437	10 ppm	91	4.66×10^{-4}	1.40×10^{-3}	4.80×10^{-4}	5.88×10^{-4}
291			85	3.74×10^{-4}	7.45×10^{-4}	4.52×10^{-4}	4.44×10^{-4}
292			156	2.27×10^{-4}	6.82×10^{-4}	4.54×10^{-4}	4.11×10^{-4}
		Average of various g		3.56×10^{-4}	9.42×10^{-4}	4.62×10^{-4}	4.81×10^{-4}
293		100 ppm	76	3.54×10^{-4}	6.98×10^{-4}	3.93×10^{-4}	4.11×10^{-4}
294			63	4.81×10^{-4}	7.93×10^{-4}	5.95×10^{-4}	5.02×10^{-4}
295			82	3.41×10^{-4}	5.98×10^{-4}	4.34×10^{-4}	4.26×10^{-4}
		Average of various g		3.92×10^{-4}	6.96×10^{-4}	4.74×10^{-4}	4.46×10^{-4}

cont'd

TABLE 19 continued...

Exp No.	Impurity	$c_i \times 10^{+2}$ (Kg Impurity / (Kg solution)	$t_{s.n.}$ (min)	g(min) (cm/min)	g(max) (cm/min)	g(avg.1) (cm/min)	g(avg.2) (cm/min)
296	$Ca(OH)_2$	Saturated	93	4.92×10^{-4}	8.75×10^{-4}	5.90×10^{-4}	6.25×10^{-4}
297			65	3.33×10^{-4}	6.72×10^{-4}	4.54×10^{-4}	4.83×10^{-4}
		Average of various g		4.12×10^{-4}	7.73×10^{-4}	5.22×10^{-4}	5.54×10^{-4}
298	HCHO	1.00	No nucl^{n}.	2.69×10^{-5}	4.59×10^{-5}	3.98×10^{-5}	3.67×10^{-5}
299			No nucl^{n}.	4.65×10^{-5}	1.28×10^{-4}	5.48×10^{-5}	5.82×10^{-5}
		Average of various g		3.67×10^{-5}	8.69×10^{-5}	4.73×10^{-5}	4.74×10^{-5}
300	Low viscosity Oil	2.00	5.50	4.52×10^{-4}	9.13×10^{-4}	4.65×10^{-4}	5.22×10^{-4}
301	High viscosity Oil	0.33	8.50	3.84×10^{-4}	7.68×10^{-4}	5.68×10	5.58×10^{-4}
302	T.W.I.	100 ppm	56.00	3.34×10^{-4}	9.60×10^{-4}	4.52×10^{-4}	4.03×10^{-4}
303	Topanol O	0.10	69.00	4.68×10^{-4}	1.12×10^{-3}	5.12×10^{-4}	5.56×10^{-4}
304	Passage of CO_2 in hydrolysed solution.	-	No nucl^{n}.	-	2.02×10^{-5}	-	-
305	H_2O_2 in hydrolysed solution	1.00	No nucl^{n}.	-	1.65×10^{-5}	-	-

TABLE 19 continued...

Exp. No.	Impurity	ci x 10^{+2} (Kg Impurity/ KG solution)	Total Growth Time (min)	g(min) (cm/min)	g(max) (cm/min)	g(avg.1) (cm/min)	g(avg.2) (cm/min)
306	1,1,1, Trimethylol-ethane	1.00	(300) No $nucl^{n}$.	0.76×10^{-4}	2.23×10^{-4}	1.53×10^{-4}	1.47×10^{-4}
307	D-Erythrose	1.00	66	4.05×10^{-4}	7.50×10^{-4}	4.98×10^{-4}	5.32×10^{-4}
308	Meso-Erythritol	1.00	47	4.65×10^{-4}	8.73×10^{-4}	5.17×10^{-4}	4.83×10^{-4}

TABLE 20

The effects of Miscellaneous Impurities at T = $30^{o}C$ and $\Delta c = 2.23 \times 10^{-2}$ (Kg Pe/Kg solution)

Growth rate of pure Pe at $30^{o}C$ and $\Delta c = 2.23 \times 10^{-2}$ (Kg Pe/Kg solution) $= 5.10 \times 10^{-4}$ (cm/min)

Impurity	ci x 10^{+2} (Kg Impurity/ Kg solution)		Growth Rate gi x 10^{+4}, (cm/min)	gi/g
NaCl	0.10	(1,000 ppm)	5.10	1.000
	1.00	(10,000 ppm)	5.24	1.028
NaOH	1.00(Solutions)		1.85	0.364
	1.00		1.85	0.364
	2.23	(22,300 ppm)	Complete inhibition of growth	
HCL	0.10		5.68	1.125
	1.00		6.82	1.342
Methanol	1.00		5.65	1.100
	5.00	(50,000 ppm)	5.05	0.991
Nonidet	0.10		3.04	0.597
	0.75	(7,500 ppm)	Too opaque to be used	
Polysach-aride	0.001	(10 ppm)	4.07	0.796
Sulphate	0.100		3.49	0.685
White Spirit	Saturated mount		2.95	0.578
$Ca(OH)_2$	Saturated		5.22	1.023

cont'd

TABLE 20 continued...

Impurity	ci x 10^{+2} (Kg Impurity/ Kg solution)		Growth Rate gi x 10^{+4} (cm/min)	gi/g
H_2O_2	1.00 (added in hydrolysed solutions)		< 10^{-5}	
HCHO	1.00		0.473	0.0928
Passage of CO_2 gas through the hydrolysed solution			< 10^{-5}	
Silcolapse 5000		(1 ppm)	5.04	0.990
		(10 ppm)	4.72	0.926
		(80 ppm)	5.27	1.032
		(100 ppm)	Too opaque	
Silcolapse 437		(10 ppm)	4.62	0.906
		(100 ppm)	4.74	0.930
Low viscosity oil	2.00	(20,000 ppm)	4.65	0.912
High viscosity oil	0.33	(3,300 ppm)	5.68	1.115
W.T.I.oil		(100 ppm)	4.52	0.886
Topanol 0	0.10	(1,000 ppm)	5.12	1.003
1,1,1,tri-methylol-ethane	1.00		1.53	0.33
D-Erythrose	1.00		4.98	0.978
Meso-Erythritol	1.00		5.17	1.002

10.3 Subsidiary Calculations

10.3.1 Surface Free Energy

From thermodynamics $\rho_c = \frac{\sigma V_c}{RTX}$ (3)

Cabrera and Vermilyea[42] have suggested that the growth of a crystal face ceases when $\rho_x \leq 2\rho_c$

Therefore $\rho_c \simeq \rho_{x/2} = f(c_f)_s$ (68)

where $(c_f)_s$ is the concentration of Formal at the crystal surface and equals to (moles of Formal/moles of Pe) surface.

Assuming that the molar concentration of Formal at the crystal surface equals that in the bulk of the solution

$$(c_f)_s = (c_f)_b = \left(\frac{\text{moles of Formal}}{\text{moles of Pe}}\right)_{\text{bulk}} \quad (69)$$

let the numbers of Pe moles/cm^2 at the crystal surface = n

Then the number of Formal moles/cm^2 = $n(c_f)_s = n(c_f)_b$

Assuming a cubic symmetry for Formal moles distribution at the crystal surface

$$n(c_f)_b = 1/(\rho_x)^2 \quad (70)$$

$$\rho_x = [n(c_f)_b]^{-\frac{1}{2}} \quad (71)$$

$$\rho_c = \rho_{x/2} = [4\,n(c_f)_b]^{-\frac{1}{2}} \quad (72)$$

Area per Pe molecule on the (101) face $= a_o(a_o^2 + c_o^2)^{\frac{1}{2}}/2$ (73)

$$= \frac{6.083 \pm 10.63}{2} \; {}^{o}A^2$$

where a_o and c_o are crystal lattice parameters.

Since there are two Pe molecules per unit cell

$$n = \frac{2 \times 10^{16}}{6.083 \times 10.62} = 3.09 \times 10^{14} \text{ mol/cm}^2$$

From (3) $$\sigma = \frac{RT \times \rho_c}{V_c} \qquad (74)$$

The method used to calculate σ has been shown in the following paragraph for concentrations of Formal at which no growth was observed.

1. $T = 30^{o}C$; $\Delta c = 2.23 \times 10^{-2}$ KgPe/Kg Solution; $(c_{if})_b = 0.135 \times 10^{-2}$ (Kg Formal/Kg Solution)

Assuming a linear relationship between increase in solubility and Formal concentration

$$c^* = (7.62 + 0.26)10^{-2} = 7.88 \times 10^{-2} \text{ KgPe/Kg Solution}$$

where the increase in solubility due to Formal = 0.26×10^{-2} KgPe/Kg Solution

$$c = (7.88 + 2.23)10^{-2} = 10.11 \times 10^{-2} \text{ KgPe/Kg Solution}$$

$$(c_f)_b = 6.42 \times 10^{-3} \text{ mol Formal/mol Pe}$$

$$X = 2.23 \times 10^{-2}/7.88 \times 10^{-2} = 0.284$$

$$\rho_c = \{4(3.09 \times 10^{14})(6.42 \times 10^{-3})\}^{-\frac{1}{2}} = 3.55 \times 10^{-7} \text{ (cm)}$$

$$V_c = 136/1.396 = 97.50 (\text{cm}^3)(\text{mol})^{-1}$$

$$R = 8.3144 \times 10^{7} \quad (\text{ergs})(\text{mol})^{-1}(\text{K})^{-1}$$

$$T = 303 \quad \text{K}$$

Substituting these values in equation (74)

$$\sigma = 26.10 \text{ ergs/cm}^2$$

The rest of the values are shown below:

T (^oC)	Δc (KgPe/Kg Solution)	$(c_{if})_b$ (Kg Formal/Kg Solution)	σ (ergs/cm^2)
30	2.23×10^{-2}	0.135×10^{-2}	26.10
30	1.23×10^{-2}	0.025×10^{-2}	32.20
40	4.00×10^{-2}	0.214×10^{-2}	26.10
40	3.00×10^{-2}	0.164×10^{-2}	34.40

10.3.2 Growth rate for a purely Diffusion-Controlled process

Applying Ficks law to the Three dimensional diffusion of solute to a Pe crystal

$$g = \mathbf{Z}D\mathbf{N}\Delta c/L\mathbf{M} \qquad (67)$$

where L = Distance between two diametrically opposite identical faces (cm)

The diffusivity was calculated from Spalding's equation[102] as follows:

$$(Sc)_{20^oC} = \{140(M)^{0.397}\} + 0.20\ \{140(M)^{0.397}\}$$

$$= 1176$$

where M = Molecular weight of the solute

Also $(Sc)_{50^oC} / (Sc)_{20^oC} = 0.28$

$$(Sc)_{50^oC} = 328$$

(i) At $20^{o}C$ $\quad Sc = 1176$

$\rho = 1 \ g/cm^3$

$\mu = \frac{2.50}{2.42} \times 10^{-3} = 1.03 \times 10^{-3} \ g/cmS$

$D = 1.03 \times 10^{-3}/1176 = 0.88 \times 10^{-5} \ cm^2/S$

$\Delta c = 0.50/1.10 \quad g/100 \ cm^3$

$$g = \frac{(2)(0.88\times10^{-5})(0.50)(60)(1.10)}{(0.20)(1.396)(1.10)} = 0.207 \times 10^{-4} \ cm/min$$

(ii) At $T = 50^{o}C$

$(Sc)_{50} = 328$

$\mu = (1.33/2.42)(1/100) = 5.50 \times 10^{-3} \ g/cmS$

$D = 1.67 \times 10^{-5} \ cm^2/S$

$$g = \frac{(2)(1.67\times10^{-5})(0.50)(60)(1.10)}{(0.2)(1.396)(1.10)}$$

$= 0.393 \times 10^{-4} \ cm/min$

T (^{o}C)	Δc ($g/100 \ cm^3$)	g (cm/min)
20	0.50	0.207×10^{-4}
50	0.50	0.393×10^{-3}

10.4 NOMENCLATURE

Symbol		Unit
A	Surface Area of a crystal face	m^2
BCF	Abbr. for Burton, Cabrera and Frank.	-
BDM	Abbr. for Birth and Spread Model	-
c	Concentration of solute in solution	Kg solute/ Kg solution
c*	Equilibrium concentration of solute in solution	Kg solute/ Kg solution
c_i	Impurity concentration in solution	Kg Impurity/ Kg solution
c_{if}	Formal concentration in solution	Kg Formal/ Kg solution
c_s^*	Equilibrium solute concentration on the crystal surface	Molecules/m^2
d	Surface density of adsorption of impurities	Molecules/m^2
di-Pe (or Di-Pe)	Abbr. for Di-Pentaerythritol	-
D	Diffusivity constant in solution	m^2/s
D_s	Diffusivity constant on the crystal surface	m^2/s
f	Vibration frequency molecule adsorbed on the crystal surface	s^{-1}
g	Linear growth rate of a crystal face	m/s or cm/min
GC	Abbr. for Gas chromatography	-
h	Monomolecular step height, or Unit lattice spacing	m
H	Density of Pentaerythritol solution	Kg/m^3
I	Rate of formation of TDN per unit area	$1/m^2s$
ICG	Abbr. for Impurity concentration gradient	-
J_i	Impurity flux to the crystal surface	molecules/m^2S

Symbol		Unit
K	Boltzman constant (or the abbr. for kil o) (or the absolute temperature)	ergs/ molecule
L	Distance between two opposite identical crystallographic faces	m
MNTDN	Abbr. for Mono-Nuclear Two-Dimensional Nucleation	-
n_D	Refractive index of Pe solution	-
n_o	Concentration of adsorbed molecules on the crystal surface	molecules/m^2
Pe	Abbr. for Pentaerythritol	-
PNTDN	Abbr. for Poly-Nuclear Two-Dimenaional Nucleation	-
R	Gas constant	ergs/mol K
S	Supersaturation ratio ($c/_{c^*}$)	
SDM	Abbr. for Surface Diffusion Model	-
t	Time	S or min
T	Temperature	^oC or K
TDN	Abbr. for Two-Dimensional nucleation	-
TMS	Abbr.for Trimethyl silizane	-
v	Velocity of a step across a crystal surface	m/s
v_ρ	Velocity of a step with radius of curvature ρ	m/s
v_∞	Velocity of a straight step in the absence of an impurity (v_ρ for $\rho \to \infty$)	m/s
v_i	Step velocity in the presence of an impurity i	m/s
V_c	Molar volume of solute	m^3/mol
V_m	Volume of a molecule in the crystal	m^3/molecule
W	Energy of formation of a kink in a step	ergs/m^2
W_o	Energy of evaporation	ergs/m^2

Symbol		Unit
x_1	Mass fraction of Pe	-
x_o	Mean distance between kinks along a step	m
x_s	Mean displacement of molecules adsorbed on a crystal surface	m
X	Supersaturation (defined as $\Delta c/c^*$)	-
X_c	Critical supersaturation in the presence of impurities	-
y_o	Distance between radially successive steps of the spiral	m

Greek Symbols

Δ_c	Concentration difference ($c-c^*$)	kg Pe/kg solution
δ	Thickness of a boundary layer around a crystal surface	m
ω	Apparent angular velocity of a spiral	Radians/s
π	Ratio of circumference to diameter of a circle	-
ρ	Radius of curvature of advancing step	m
ρ_c	Radius critical size Two-Dimensional nucleus	m
ρ_x	Distance between impurity molecules	m
σ	Surface free energy per unit area	$ergs/m^2$
γ	Edge energy of a nucleus per molecule	erg/molecule
ν_i	Flow rate of a step with impurity	m/s
ν_o	Flow rate of a step without impurity	m/s

Subscript

b	Bulk of the solution
s	Surface of the crystal

10.5 BIBLIOGRAPHY

1. Gibbs, J.W., "Collected Works", Vol.1, Longmans Green, London, (1928).

2. Curie, P., Bull.Soc.Fr.Miner., 8, 145 (1885).

3. Wullf, G., Z. Kristallogr. 34, 449 (1901).

4. Marc, R., and Ritzel, A., Z.Phys.Chem. 76, 584 (1911).

5. Frank, F.C.,"Growth and Perfection of Crystals", Doremus, Roberts, and Turnbull, eds., John Wiley and Sons Inc., 411(1958)

6. Noyes, A.A., and Whitney, W.R., J.Am.Chem.Soc., 19, 930 (1897).

7. Nernst, W., Z.Phys.Chem., 47, 52 (1904).

8. Berthoud, A., J.Chem.Phys., 10, 624 (1912).

9. Valeton, J.J.P., Z.Kristalloger. 59, 135 (1923).

10. Miers, H.A., Phil.Trans., A-202, 492 (1904).

11. Marc, R., Z.Phy.Chem., 61, 385 (1908).

12. Smythe, B.M., Aust.J.Chem. 20, 1087 (1967).

13. Kossel, W., in FALKENHAGEN, Quantemtheorie und Chemie, Leipzig, (1928).

14. Stranski, I.N., Z.Phys.Chem., 136, 259 (1928).

15. Frank, F.C., Burton, W.K., and Cabrera, N., Phil.Trans.Roy.Soc., London, A-243, 299 (1951).

16. Ohara, Makoto, "Kinetic Theories of Crystal Growth with Emphasis on Solution Growth",
D.Sc.Thesis, Chem.Eng.Dept., M.I.T. (1970).

17. Canning, T.F., and Randolph, A.D.,
A.I. Chem.E.J., 13, 5 (1967).

18. Yamamoto, T., "Scientific Papers of the Institute of Physical and Chemical Research", Tokyo, 35, 246 (1939).

19. Sheftal', N.N., "Vestn.Mosk.Univ",
Ser.IV, 21, (6), 28 (1966).

20. Petrov, T.J., "Growing Crystals from Solutions",
Consultant Bureau, New York. (1969).

21. Vermilyea, D.A., J.Chem.Phys. 27, 814 (1957).

22. Volmer, M., Z.Phys.Chem., 102, 267 (1922).

23. Brandes, H., Z.Phys.Chem., 126, 196 (1927).

24. Bunn, C.W., Disc. Faraday Soc., (5), 132 (1949).

25. Berg, W.F., Proc.Roy.Soc.London A-164 79 (1938).

26. Frank, F.C., Disc.Faraday Soc., (5), 49 (1949).

27. Frenkel, J.Phys., U.S.S.R., 9, 392 (1945).

28. Bennema, P., Phys.Stat.Sol. 17, 563 (1966).

29. Beck, W.F., "Effects of Surface Active Agents on Adipic Acid Crystals grown from Aqueous Solutions",
D.Sc.Thesis, Chem.Eng.Dept.; M.I.T. (1964).

30. Cartier, R., Pindzola, D., and Bruins, P.F., Ind. Eng.Chem., 51, 1409 (1959).

31. Chernov, A.A., Soviet Physics Uspekhi, 4, (1), 116 (1961).

32. Bytena, I.M., "Growth of Crystals", Consultant Bureau, New York, Shubnikov, A.V., and Sheftal', eds., Vol.3, 213 (1962).

33. Bennema, P., J.Crystal Growth, 5, 29 (1969).

34. Liu, C.Y., Tsuei, H.S., and Youngquist, G.R., Chem.Eng.Progr., Symp.Series, 67, (110), 44 (1971).

35. Liu, Sung-Tsuen, Nancollas, G.H., J.Crystal Growth. 6, 281 (1970).

36. Levina, I.M.,and Belyustin, A.V., Soviet Phys. - Crystg., 14, (6), 954 (1970).

37. Nielson, A.E., "Kinetics of Precipitation", Pergamon Press, New York. (1964).

38. Bennema, P., Kern, R., and Simons, B., Phys.Stat.Sol., 19, 211 (1967).

39. Botsaris, G.D., and Denk, E.G., Ind.Eng.Chem.Fundam., 9, (2), 276 (1970).

40. Lefever, R.A., "Preparation and Properties of Solid State Materials", Marcel Dekker, Inc., New York. (1971).

41. Humphreys-Owen, S.P.F., Disc. Faraday Soc., (5), 144 (1949).

42. Cabrera, N., and Vermilyea, D.A., "Growth and Perfection of Crystals", Doremus, Robert and Turnbull, eds., John Wiley, New York. 393 (1958).

43. Dukova, E.D., and Gavrilenko, E.,
Soviet Phys.- Crystg., 14, 736 (1970).

44. Strickland-Constable, R.F., "Kinetics and Mechanism of
Crystallisation", Academic Press, London, (1968).

45. Lal, D.P., Mason, R.A., and Strickland-Constable, R.F.,
J. Crystal Growth, 5, 1 (1969).

46. Garabedian, H., and Strickland-Constable, R.F.,
J. Crystal Growth, 13/14, 506 (1972).

47. Ibid. 12, 53 (1972).

48. Denk, E.G., and Botsaris, G.D.,
J. Crystal Growth, 15, 57 (1972).

49. Ibid. 13/14, 493 (1972).

50. Botsaris, G.D., Denk, E.G., and Chua, J.O.,
Chem.Eng.Progr. (Symp. Series), (118), (1972).

51. Shor, S.M., and Larson, M.A.,
Chem.Eng.Progr. (Symp. Series), 67, (110), 32 (1971).

52. Belyustin, A.V., and Rogacheva, E.D., "Growth of Crystals",
Vol.4, Shubnikov and Sheftal', eds.,
Consultant Bureau, New York, 3 (1966).

53. Mussard, F., and Goldsztaub, S.,
J. Crystal Growth, 13/14 445 (1972).

54. Ovsienko, D.E., and Alfintsev, G.A.,
"Crystallisation Processes", Sirota, Gorskii, and
Varikash, eds., Consultant Bureau, New York, 25 (1966).

55. Trevius, E.B., Soviet Phys-Crystg., 15, (5), 950 (1970).

56. Buckley, H.E., "Crystal Growth", John Wiley, New York, (1951).

57. Frank, F.C., Disc. Faraday Soc., (5), 189 (1949).

58. Morris, I.B., and Strickland-Constable, R.F.,
Trans. Faraday Soc., 50, 1378 (1954).

59. Kirtisinghe, D., and Strickland-Constable, R.F., Nature, 204
465 (1964).

60. Kirtisinghe, D., Morris, P.J., and Strickland-Constable, R.F.,
"Crystal Growth", Frank, Mullin, and Peiser, eds.,
North Holland, Amsterdam, 771 (1968).

61. Walton, A.G., "The Formation and Properties of Precipitates",
Interscience, 53 (1967).

62. Lemmlein, G.G., and Dukova, E.D.,
Soviet Phys - Crystalg. 1, 84 (1956).

63. Bunn, C.W., and Emmett, H.,
Disc. Faraday Soc., (5), 119 (1949).

64. White, E.T., and Wright, P.G.,
Chem.Eng.Progr. (Symp. Series), 67, (110) 81 (1971).

65. Dukova, E.D., and Lemmlein, G.G.,
Soviet Phys.- Crystg., 1, 375 (1956).

66. Kasatkin, A.P., Soviet Phys.- Crystg., 9, 239 (1964-65).

67. Kasatkin, A.P., Soviet Phys.- Crystg., 10, (4), 459 (1966).

68. Booth, A.H., and Buckley, H.E.
Can. J. Chem., 33, 1162 (1955).

69. Petrov, T.G., "Growth of Crystals", Consultant Bureau, New York, Shubnikov and Sheftal', eds., Vol.3., 107 (1962).

70. Denbigh, K.G., and White, E.T., Nature, 199, 799 (1963).

71. Brooks, R., Hortons, A.T., and Torgesen, J.L., J. Crystal Growth, 2, (5), 279 (1968).

72. Cabrera, N., and Coleman, R.V., "The Art and Science of Growing Crystals", Gilman, J.J., ed., John Wiley, London, (1963).

73. Troost, S., J. Crystal Growth, 3-4, 340 (1968).

74. Sears, G.W., "Growth and Perfection of Crystals", Doremus, Roberts and Turnbull, eds., John Wiley and Sons Inc., 441 (1958).

75. Smythe, B.M., Sugar Tech.Review, 1, (3), 191 (1971).

76. Khamskii, E.V., "Crystallisation from Solutions", Consultant Bureau, London, (1969).

77. Slavnova, E.N., Gordeeva, N.V., and Sitnik, T.K., Soviet Phys.- Crystg., 13, (3), 401 (1968).

78. Dunning, W.J., Jackson, R.W., Mead, D.G., Colloq. Int.Nat.Centre.Rech.Sci., Nancy, 152, 303 (1965).

79. Mullin, J.W., "Crystallisation", Butterworth, London, (1972).

80. Creasy, D.E., and Rogers, J.F., Paper presented in BACG Annual Meeting, London. (1972).

81. Wyckoff, R.W.G., "Crystal Structures", Interscience, 5, (1966).

82. Wells, A.F., Phil.Mag., 37, 184 (1946).

83. Frevel, L.K., et.al.,
Ind.Eng.Chem. (Analy.), 18, 83(1946).

84. Rogers, J.F.,
Ph.D. Thesis, University of Aston in Birmingham. (1969).

85. Thomas, J.M., and Evans, J.R.N.,
Solid State Communications, 9, (13), 1163 (1971).

86. Kuznetsova, L.I., and Gavrilova, I.V.,
"Growth of Crystals", Consultant Bureau, New York, 3, 203 (1962).

87. Whetstone, J., Research Supplement, 2-4, 194 (1949).

88. Berlow, E., Barth, R.H., and Snow, J.E.,
"The Pentaerythritol", A.C.S. Monograph No.136,
Reihold, New York, (1958).

89. Rogers, J.F., Farazmand, and Creasy, D.E., To be published.

90. Wyler, J.A., and Warnett, E.A., (Trojan Powder Company),
U.S. Patent (2,299,048), (1942).

91 Llewellyn, F.J., et.al.,
J.Chem.Soc., 140, 883 (1937).

92. Cook, E.G.,
Paint Manufacture, 18, 125 (1948).

93. Bradley, R.S., and Cotson, S.,
J.Chem.Soc., 1984 (1953).

94. Nitta, I., Seki, S., and Suzuki, K.,
Bull.Chem.Soc. (Jap.), 2463 (1951).

95. Suchanec, R., Anal.Chem. 37, (11), 1361 (1965).

96. Simons, T. Private Communication.

97. Bankier, K.J., "Epitaxial Growth", M.Sc. Dissertation University of Aston in Birmingham, (1972).

98. Wacks, R., M.Sc Dissertation, University of Aston in Birmingham, (1970).

99. U.S.A. Patent 936082, Sept. (1963).

100. Van der Merwe, J.H., Disc. Faraday Soc., 4-6, 201 (1948-49).

101. Farazmand, H., "Crystallisation Properties of Pentaerythritol", M.Phil.Thesis, University of Aston in Birmingham,to be published (1973).

102. Spalding, D.B., "Convective Mass Transfer", Edward Arnold, London, (1963).

103. Michaels, A.S., and Tausch, F.W,Jnr., J.Phys.Chem., 65, 1730 (1961).

104. Elgi, P.H., and Zerfoss, S., Disc. Faraday Soc., (5), 61 (1949).